Biochemical and Biophysical Research Communications 464 (2015) 787–793

Contents lists available at ScienceDirect

Biochemical and Biophysical Research Communications

journal homepage: www.elsevier.com/locate/ybbrc

Mitochondrial ATP synthasome: Expression and structural interaction of its components

Hana Nůsková [a, b], Tomáš Mráček [a], Tereza Mikulová [a], Marek Vrbacký [a], Nikola Kovářová [a], Jana Kovalčíková [a], Petr Pecina [a], Josef Houštěk [a, *]

[a] Department of Bioenergetics, Institute of Physiology of the Czech Academy of Sciences, Vídeňská 1083, 14220 Prague, Czech Republic
[b] Charles University in Prague, First Faculty of Medicine, Kateřinská 32, 12108 Prague, Czech Republic

ARTICLE INFO

Article history:
Received 26 June 2015
Accepted 7 July 2015
Available online 10 July 2015

Keywords:
Mitochondria
Oxidative phosphorylation
Supercomplexes
ATP synthasome

ABSTRACT

Mitochondrial ATP synthase, ADP/ATP translocase (ANT), and inorganic phosphate carrier (PiC) are supposed to form a supercomplex called ATP synthasome. Our protein and transcript analysis of rat tissues indicates that the expression of ANT and PiC is transcriptionally controlled in accordance with the biogenesis of ATP synthase. In contrast, the content of ANT and PiC is increased in ATP synthase deficient patients' fibroblasts, likely due to a post-transcriptional adaptive mechanism. A structural analysis of rat heart mitochondria by immunoprecipitation, blue native/SDS electrophoresis, immunodetection and MS analysis revealed the presence of ATP synthasome. However, the majority of PiC and especially ANT did not associate with ATP synthase, suggesting that most of PiC, ANT and ATP synthase exist as separate entities.

1. Introduction

The complexes of respiratory chain in the inner mitochondrial membrane form higher structural entities – supercomplexes [1]. Similarly, the key component of the oxidative phosphorylation (OXPHOS) system, F_1F_o-ATP synthase, can associate into more complex structures, such as dimers and higher oligomers [2].

ATP synthase was reported to participate in a range of other supramolecular structures, most importantly ATP synthasome, which is suggested to be composed of ATP synthase, ADP/ATP translocase (ANT), and inorganic phosphate carrier (PiC). Together, they would form a single catalytic unit responsible for ATP production [3]. Since the original reports [4,5], it was also found in bovine heart mitochondria [2,6,7] as well as in the protozoan *Leishmania* [8], suggesting that ATP synthasome is an evolutionary conserved structure, albeit with questionable functional significance [5].

ANT and PiC belong to the mitochondrial carrier family of hydrophobic proteins encoded by the *SLC25* genes [9]. In rodents, three genes coding for tissue-specific ANT isoforms have been described whereas four genes have been identified in humans – *SLC25A4* (ANT1, a heart-type isoform), *SLC25A5* (ANT2, a liver-type isoform), *SLC25A6* (ANT3, expressed in highly proliferative cells, present only as a pseudogene in rodents), and *SLC25A31* (ANT4, testes-specific isoform) [11]. In the case of PiC, two isoforms PiC-A (a heart-type isoform) and PiC-B (a liver-type isoform) originate from alternative splicing of a single transcript (*SLC25A3*) [10].

While the existence of ATP synthasome is mostly accepted, little is known about its relative abundance in comparison with free forms of its constituents, stoichiometry or regulation of its biogenesis. Therefore, we set to clarify two major objectives: to examine whether the total content of the carriers (ANT and PiC) is affected by the content and function of ATP synthase and to better describe the structural associations between ATP synthasome components.

2. Materials and methods

2.1. Animals

Adult (3–4 months old) and newborn (3–5 days old) Wistar rats were killed in CO_2 narcosis. All procedures were performed in accordance with EU Directive 2010/63/EU for animal experiments. Mitochondria from rat tissues (heart, liver, kidney, brain, skeletal

Abbreviations: ANT, ADP/ATP translocase; PiC, inorganic phosphate carrier; BAT, brown adipose tissue; DDM, n-dodecyl β-D-maltoside.

* Corresponding author.
E-mail address: houstek@biomed.cas.cz (J. Houštěk).

http://dx.doi.org/10.1016/j.bbrc.2015.07.034
0006-291X/

muscle, brown adipose tissue) were isolated by differential centrifugation [12,13].

2.2. Cell cultures

All human samples were obtained on the basis of written informed consent and handled in accordance with the Code of Ethics of the World Medical Association. Primary fibroblast cultures derived from skin biopsies of 3 healthy individuals, 7 patients with an isolated ATP synthase defect due to the homozygous nucleotide substitution 317-2A>G in the gene *TMEM70* [14], a patient with a mutation in the gene *ATP5E* coding for the subunit F_1-ε [15], and a patient harboring a mutation in the mitochondrial gene *MT-ATP6* coding for the subunit F_o-a [16,17] were cultivated under standard conditions [15]. Further patients' characteristics have been described previously [14–19]. Fibroblast mitochondria were isolated by hypotonic shock cell disruption [15].

2.3. RNA extraction and gene expression analysis

The total RNA was isolated using Trizol (Life Technologies) and reverse-transcribed with the SCRIPT cDNA Synthesis Kit (Jena Bioscience). cDNA was used as a template for the quantitative PCR performed on the ViiA 7 instrument (Life Technologies) with the 5x HOT FIREPol Probe qPCR Mix (Solis Biodyne) and predesigned TaqMan gene expression assays (Life Technologies; Supplementary Table S1).

2.4. Electrophoreses and immunoblotting

The separation of proteins with the tricine SDS-PAGE [20] was performed on 10% polyacrylamide minigels (MiniProtean III, Bio-Rad) [13]. The blue native electrophoresis (BN-PAGE) [21] was performed on 4–13 or 4–8 % gradient gels [13]. The BN gels were stained by the ATPase in-gel activity assay [22] to identify ATP synthase. The visualized bands of ATP synthase monomer and dimer were excised, incubated in 1% SDS +1% 2-mercaptoethanol and subjected to SDS-PAGE (16%) for 2D resolution under denaturing conditions.

The gels from both BN-PAGE and SDS-PAGE were blotted onto a PVDF membrane (Immobilon-FL, Merck Millipore) [13]. For the list of used primary antibodies see Supplementary Table S2. Fluorescent signals of secondary antibodies labelled with Alexa Fluor 680 (Life Technologies) or IRDye 800 (Rockland) were recorded with the infrared Odyssey Imager (Li-Cor) and quantified using the Aida 3.21 software (Raytest).

2.5. MS analysis

Protein bands from the BN gels containing ATP synthase were identified by the ATPase in-gel assay run in parallel [22], excised and processed by in-gel trypsin digestion [23]. The setup of LC-MS/MS analysis on the maXis UHR-TOF (Bruker) has been described previously [24].

2.6. Immunoprecipitation

For the co-immunoprecipitation analysis with the ATP Synthase Immunocapture Kit (Abcam), rat heart mitochondria were solubilized with 1% Triton X-100 [13] and 30,000 *g* supernatants were subjected to immunoprecipitation according to the manufacturer's protocol. Co-immunoprecipitated proteins were eluted with 0.2 M glycine (pH 2.5), neutralized with 1 M Tris-base, separated with SDS-PAGE (10%) and identified on Western blots. As a negative control, proteins captured non-specifically onto protein G-agarose beads were investigated.

3. Results

3.1. Expression of mitochondrial carriers ANT and PiC in rat

To gain insight into the physiological regulation of the biogenesis of ATP synthasome constituents, we analyzed the expression of ATP synthase subunits, ANT, and PiC at the protein and transcript level in 6 adult (heart, skeletal muscle, brain, brown adipose tissue (BAT), kidney, and liver) and 3 newborn (heart, BAT, and liver) rat tissues.

We used antibodies reacting with all PiC or ANT isoforms [25] and an antibody to subunit F_1-α as a proxy for the ATP synthase content (Fig. 1A). The ATP synthase content was highest in mitochondria from the tissues with high energetic demands – heart and skeletal muscle, lower in kidney and liver and lowest in thermogenic BAT (~30% of heart), where the down-regulated expression of subunit F_o-c limits the ATP synthase biogenesis [26]. The tissue-specific distribution of ANT and PiC was analogous to that of ATP synthase.

At the transcript level, the expression of two structural subunits of ATP synthase (*ATP5A1* and *ATP5G1* coding for F_1-α and F_o-c, respectively), all three isoforms of ANT (ANT1 – *SLC25A4*, ANT2 – *SLC25A5*, ANT4 – *SLC25A31*) and PiC (*SLC25A3*) correlated with protein profiles (Fig. 1B–D). As anticipated, the *ATP5G1* transcript level was lowest in BAT. With respect to the ANT genes, we observed the expected tissue profiles with heart and skeletal muscle expressing ANT1, liver expressing ANT2, and brain and BAT displaying a mixed profile. The *SLC25A31* transcript was hardly detectable in the analyzed tissues (not shown), in agreement with its primarily testicular expression [27]. The *SLC25A3* transcript levels paralleled the distribution of PiC across the tissues.

3.2. Expression of ANT and PiC in human fibroblasts with an ATP synthase deficiency

To find out whether PiC and ANT can be affected by an altered function of ATP synthase, we used two types of patient fibroblasts: (i) cells with a pronounced decrease in the content of ATP synthase due to a mutation in *TMEM70* or *ATP5E* and (ii) cells with a mtDNA mutation in the *MT-ATP6* gene, characterized by a normal amount of ATP synthase that lost the ability to synthesize ATP. The protein content of ANT and PiC was not only preserved, but mostly increased, regardless of the different genetic origin or clinical and biochemical manifestation of ATP synthase dysfunction (Fig. 2A). Accordingly, the ATP synthase dysfunctions were associated with an up to 7-fold increase in the ratio between the carriers and ATP synthase (Fig. 2B).

3.3. ATP synthasome – immunoprecipitation

By co-immunoprecipitation, we found ATP synthase associated with the mitochondrial carriers ANT and PiC (Fig. 3A). While this association was specific and not caused by non-specific binding to empty beads, the enrichment of ATP synthase subunits in the immunoprecipitate contrasted with the low signal of co-immunoprecipitated carriers, especially ANT. This suggests that only a minority of ANT and PiC interact with ATP synthase, or that the interactions are weak and readily dissociate. Either way, there have to exist two forms of ATP synthase, i.e. the free ATP synthase and the ATP synthasome supercomplex.

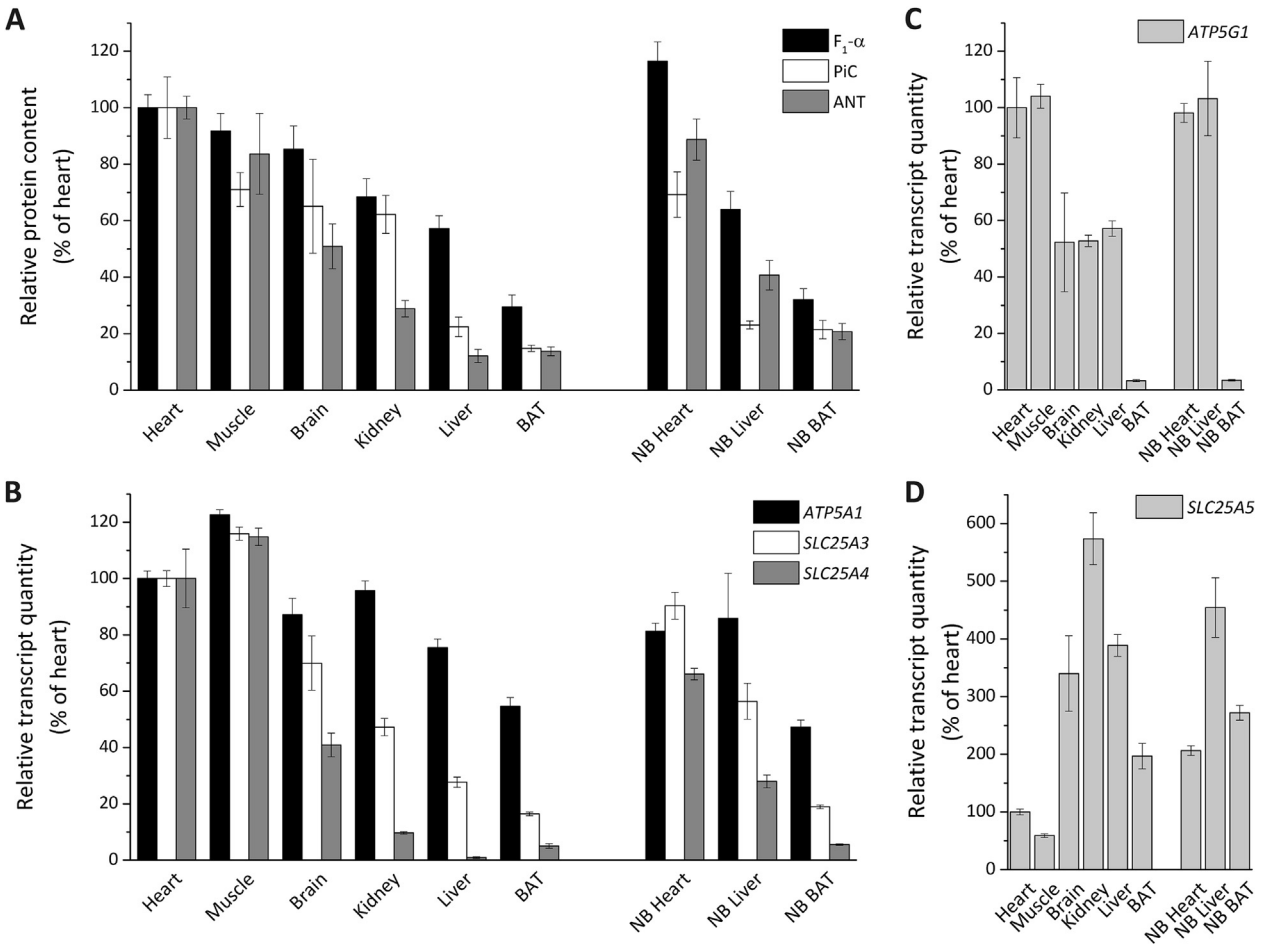

Fig. 1. The protein and transcript levels of ATP synthase and mitochondrial carriers ANT and PiC in rat tissues. (**A**) Isolated mitochondria were analyzed on Western blots (25 μg protein per lane). The signal of F_1-α, ANT, and PiC was normalized to the signal of SDHA. The values, expressed as a percentage of the heart value, are mean ± SEM (n = 4). (**B, C, D**) RT-qPCR quantification of *ATP5A1*, *ATP5G1*, *SLC25A3*, *SLC25A4*, *SLC25A5*, and *SDHA* encoding the subunits F_1-α and F_o-c of ATP synthase, PiC, ANT1, ANT2, and SDHA (used for data normalization), respectively, in adult and newborn (NB) rat tissues.

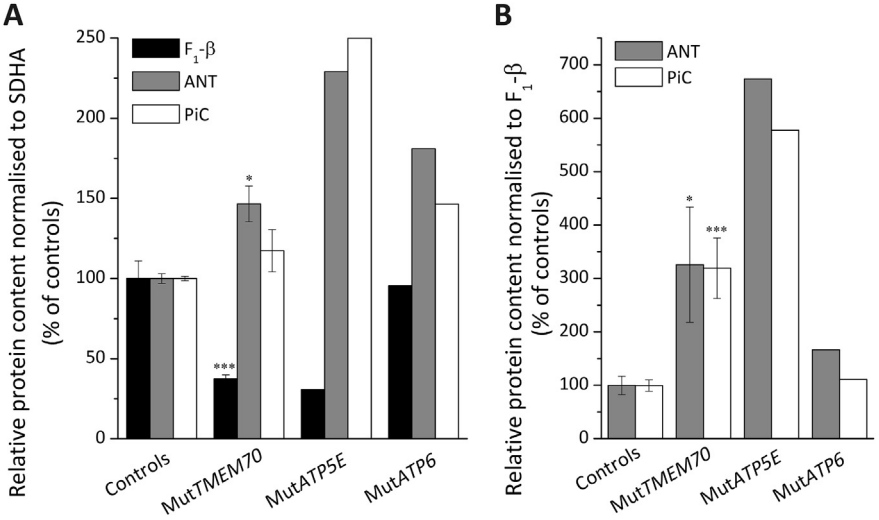

Fig. 2. The content of ATP synthase, ANT and PiC in human fibroblasts with ATP synthase deficiencies. The protein content of F_1-β subunit of ATP synthase, ANT and PiC was analyzed in mitochondria from human fibroblasts of healthy controls, patients with the mutated *TMEM70* (mut*TMEM70*), *ATP5E* (mut*ATP5E*), and *MT-ATP6* (mut*ATP6*) on Western blots (20 μg protein per lane). (**A**) The signal of specific antibodies was normalized to SDHA. (**B**) The signal for ANT and PiC was normalized to F_1-β. The values are mean from 3 experiments. The results of 3 controls and 7 patients of mut*TMEM70* are pooled for statistical analysis (***$p < 0.001$, *$p < 0.05$), mut*ATP5E* and mut*ATP6* samples represent multiple cultures of one patient each.

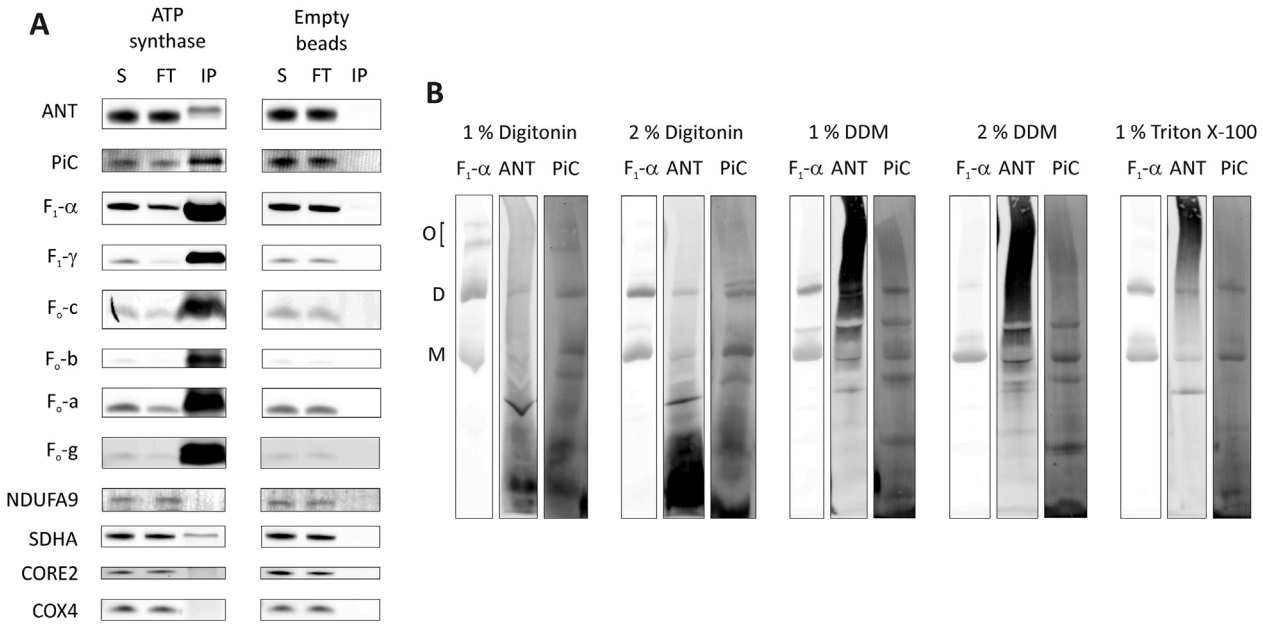

Fig. 3. Characterization of ATP synthasome by means of immunoprecipitation and BNE. (**A**) Rat heart mitochondria solubilized with 1% Triton X-100 (1 g detergent per 1 g protein) were used to perform immunoprecipitation using the ATP synthase capture kit (MS501, Abcam). The immunoprecipitates (IP) as well as input solubilizates (S), and flow-through material (FT) are shown on Western blots. As a negative control, empty protein G-coupled agarose beads were examined. (**B**) Rat heart mitochondria solubilized as indicated were analyzed by BN-PAGE (30 μg protein per lane; 4–13 % gradient). On Western blots, antibodies specific to ATP synthase (F_1-α), ANT, and PiC were used. The ATP synthase monomer (M), dimer (D) and higher oligomers (O) are indicated. The corresponding detergent to protein ratios are 1:1 and 2:1 for 1% and 2% detergents, respectively.

3.4. ATP synthasome – analysis of BN gel regions with the ATPase activity

To examine the supramolecular organization of mitochondrial ATP-synthesizing apparatus, rat heart mitochondria were solubilized with mild detergents (digitonin, DDM, and Triton X-100) and separated by BN-PAGE (Fig. 3B). Under all the different conditions that resolved ATP synthase in varying oligomerization states, we observed co-localization with PiC and ANT. However, the vast majority of PiC and ANT was present in other regions of the gel, indicating that the majority of PiC and ANT do not associate with ATP synthase. To better evaluate their interactions, we excised regions of BN gels that were stained for the ATPase activity and separated them with SDS-PAGE (Fig. 4A**).** Similar proportions among PiC, ANT, and ATP synthase were found in the monomers, irrespective of the detergent used. The detection of ANT in the dimers varied and was very weak upon digitonin solubilization. MS analysis confirmed all the components of ATP synthasome associated into a supercomplex – several ATP synthase subunits and different isoforms of ANT and PiC were detected in the regions of ATP synthase monomer and dimer, even in the digitonin solubilizates (Table 1).

In all experiments, we observed a significant difference between the total signal of PiC and especially ANT and its portion co-localizing with ATP synthase. To estimate the fraction of ANT and PiC present in ATP synthasome, we quantitatively compared solubilized mitochondria (1% Triton X-100) with excised monomers of ATP synthase (Fig. 4B and C). In the gel region containing the ATP synthase monomer and representing ≥85% of all ATP synthase present, we found only 3% of the signal for ANT and 16% for PiC, compared to the original mitochondria and normalized to the ATP synthase subunit F_1-α. Normalization to other ATP synthase subunits (F_1-γ, F_o-a) revealed similar or even smaller portions of both carriers associated with ATP synthase, confirming that most of PiC and especially of ANT was present as separate entities, not associated with ATP synthase.

4. Discussion

The presence of mitochondrial ATP synthasome has been reported in several species [2–8], but without further insight into the regulation of its biogenesis. Therefore, we focused on co-expression analysis of PiC, ANT, and ATP synthase and structural investigation of the purported ATP synthasome.

First, we investigated tissue-specific differences at the transcript and protein level of ATP synthase subunits, ANT, and PiC (Fig. 1). Our results indicated that the protein levels of ANT and PiC are controlled in accordance with the ATP synthase content. Indeed, expression of many OXPHOS proteins is transcriptionally regulated and shares common regulatory pathways [28], although the control of some genes may still be independent, such as distinct regulation of *ATP5A1* and *ATP5G1* in BAT [26] or tissue-specific up-regulation of ANT2 expression by thyroid hormones in rat heart and liver [29]. To observe possible developmental features of ANT and PiC expression, we also compared three tissues from newborn rats. While BAT did not show any major developmental changes, the neonatal heart was characterized by a decreased content of ANT and PiC. Furthermore, a reduction in the *SLC25A4* transcript was accompanied by an increase in *SLC25A5*, reflecting that the fetal and neonatal heart depends predominantly on anaerobic glycolysis whereas the mature adult heart is almost exclusively aerobic [30]. Apparently, the protein content of ATP synthase rises faster than that of ANT and PiC in heart after the birth.

A distinct type of regulation of ATP synthasome constituents appears to be associated with the pathophysiological conditions. In all of the studied fibroblasts from ATP synthase deficient patients (Fig. 2), the protein levels of ANT and PiC remained normal or even raised. In these cells, we have previously described an adaptive increase in the respiratory chain complexes III and IV that was not accompanied by any changes in transcript levels of individual ANT and PiC isoforms [19]. Thus, while the physiological regulation of ATP synthasome components likely occurs at the transcriptional level, the observed adaptive responses are regulated post-

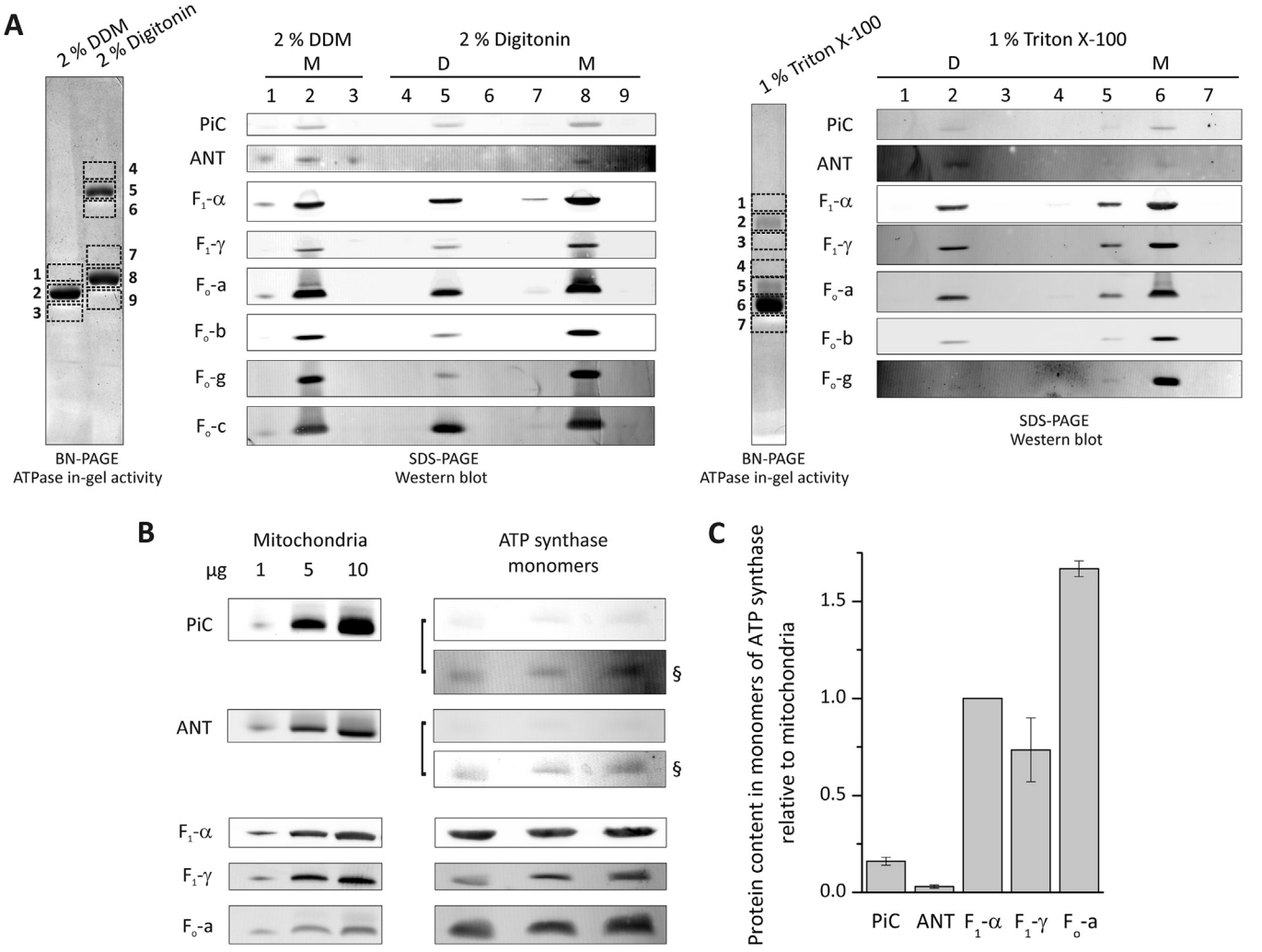

Fig. 4. Analysis of BNE excised ATPase bands in the second dimension. (**A**) Rat heart mitochondria were solubilized with mild detergents as indicated and resolved in the first dimension using BN-PAGE (30 µg protein per lane; 4–8 % gradient). The bands of ATP synthase monomers (M) and dimers (D) as well as adjoining gel pieces were excised and resolved on SDS-PAGE (16%). (**B**) The protein composition of ATP synthase monomers solubilized with 1% Triton X-100 (50 µg protein per lane; 4–8 % gradient) was compared to the input mitochondria. The antibody signals in mitochondria and excised ATP synthase monomers are shown at the same detection sensitivity. In the case of PiC and ANT, a higher sensitivity is also shown (§). (**C**) Calibration curves were constructed for dose response of each antibody, based on the signal in mitochondria. The antibody signals were normalized to the respective signal of the antibody against F_1-α and all the signals in the monomers were expressed relatively at the theoretical unit quantity. The values are mean ± SEM, n = 3.

transcriptionally, possibly at the level of protein stability. This would be similar to OXPHOS complexes whose observed compensatory up-regulation also occurred at the post-transcriptional level [19].

In the second part of our study, we examined the structural association of ATP synthase, ANT, and PiC. While it was likely observed already in the 1970's [31], the so-called ATP synthasome was first reported only decades later, when all its components co-localized in vesicles of mitochondrial cristae membrane from rat liver [4,5]. Since then, the interaction of ATP synthase and ANT has been described in bovine heart while separating digitonin-solubilized mitochondria on clear native [6] or blue native gels [2].

We found ANT and PiC in the ATP synthase immunoprecipitate from rat heart mitochondria (Fig. 3A), where we also detected a signal of SDHA that was much stronger than in empty beads, and hence represented a true interaction between succinate dehydrogenase and ATP synthase. Such an interaction has been described previously as a part of a putative mitochondrial ATP-sensitive K^+ (mitoK_{ATP}) channel [32,33].

Subsequently, we used BN-PAGE for a more detailed investigation into the stability and quantity of ATP synthasome. As detergents, we chose digitonin, DDM and Triton X-100, which effectively solubilize the intact and active ATP synthase [4] and also yield stable ANT preparations [34]. A well-documented problem with ANT is smearing on BN-PAGE (Fig. 3B), due to its high pI and hydrophobicity [6,35] an also its high abundance [36]. Therefore, we analyzed the excised gel pieces containing monomers and dimers of ATP synthase by Western blotting and LC-MS/MS and found them to contain most of the ATP synthase subunits, ANT1, ANT2, and PiC (Fig. 4A, Table 1). The subunits of ATP synthase that were not detected by LC-MS/MS represent highly hydrophobic parts of the F_o domain, and their absence rather reflects the limits of MS approach than the actual lack of these proteins. Interestingly, we detected ATP synthasome upon solubilization with 2% DDM, arguing for rather stable interactions between the ATP synthasome constituents. ATP synthasome may also be detected by the complexome profiling studies that represent another approach aimed at detection of novel mitochondrial supercomplexes. While one study on DDM-solubilized HEK293 mitochondria observed this supercomplex [28], another study on digitonin-solubilized rat heart mitochondria failed to detect any such association [37].

Table 1
MS analysis of ATP synthase bands from blue native gels. Excised monomers (M) and dimers (D) of ATP synthase solubilized with 1% detergents and resolved on 4–8 % BN-PAGE were analyzed by LC-MS/MS. The detected proteins (black dots; empty dots represent detected proteins with a score too low to be reported as a valid detection; n.d. – not detected) are indicated in the overview of proteins relevant to the ATP synthasome supercomplex. For complete datasheets see Supplementary Table S3.

Gene	Protein	MW (kDa)	Digitonin		DDM		Triton X-100	
			M	D	M	D	M	D
SLC25A3	PiC	39.6	●	●	●	●	●	●
SLC25A4	ANT1	33.0	●	●	●	●	●	●
SLC25A5	ANT2	32.9	●	●	●	●	●	●
ATP5A1	F_1-α	59.8	●	●	●	●	●	●
ATP5B	F_1-β	56.4	●	●	●	●	●	●
ATP5C1	F_1-γ	30.2	●	●	●	●	●	●
ATP5D	F_1-δ	17.6	●	●	●	●	●	●
ATP5E	F_1-ε	5.8	○	○	○	○	●	○
ATP5G1	F_o-c	14.2	n.d.	n.d.	n.d.	n.d.	n.d.	n.d.
MT-ATP6	F_o-a	25.1	n.d.	n.d.	n.d.	n.d.	●	n.d.
ATP5O	OSCP	23.4	●	●	●	●	●	●
ATP5F1	F_o-b	28.9	●	●	●	●	●	●
ATP5H	F_o-d	18.8	●	●	●	●	●	●
ATP5I	F_o-e	8.3	●	●	●	●	●	●
ATP5J2	F_o-f	10.5	●	●	●	●	●	●
ATP5L	F_o-g	11.4	●	●	●	●	●	●
ATP5J2	F_o-F6	12.5	n.d.	n.d.	n.d.	n.d.	n.d.	n.d.
MT-ATP8	A6L	7.6	●	●	●	●	●	●
ATPIF1	IF1	12.2	n.d.	n.d.	n.d.	n.d.	n.d.	n.d.
USMG5	DAPIT	6.4	●	●	●	●	●	●
C14ORF2	MLQ	6.8	n.d.	n.d.	n.d.	○	n.d.	○

When we tried to quantify ANT and PiC associated with ATP synthase in comparison to their total mitochondrial content, we confirmed that a large portion of PiC and especially of ANT was not organized into ATP synthasome (Fig. 4B and C). Indeed, this is also in agreement with our immunoprecipitation data, where the observed recovery for PiC and ANT was 4.2 and 14.9 times lower, respectively, than that of ATP synthase. This may well reflect differences in the protein content of ATP synthase, ANT, and PiC: ANT is estimated to represent ~10% of all mitochondrial proteins [36] and the molar ratio between ANT and PiC is ~4:1 [38]. Indeed, we found approximately 16% of the total PiC and 3% of the total ANT to be incorporated into ATP synthasome, which is in line with the ATP synthasome components proposed stoichiometry of 1:1:1 [5]. As the carriers are likely present in molar excess to ATP synthase [38], it may not be surprising that most of the ANT and PiC proteins are detected in a free form. However, we cannot make clear-cut conclusions regarding the presence of free ATP synthase. If we take into account the ratio between ANT and cytochrome *c* oxidase in mitochondria (2.5:1 – likely being similar to the ratio between ANT and ATP synthase) [38] and our ratio between the free and ATP synthasome-bound ANT (33:1), it can be expected that also ATP synthase exists predominantly in the free form.

In conclusion, we have demonstrated that ATP synthasome is present in rat heart mitochondria and that its constituents likely share common transcriptional regulation. However, its components do not mutually depend on one another and a large portion of the carriers was found out of the association with ATP synthase. Given the relative minority of the proteins present as the ATP synthasome supercomplex, its physiological role in tighter coupling of the whole ATP production machinery remains questionable.

Acknowledgements

This work was financially supported by the Czech Science Foundation (P303/12/1363), the Ministry of Education, Youth, and Sports of the Czech Republic (RVO: 67985823, ERC CZ: LL1204) and the Grant Agency of the Charles University in Prague (1160214). Funders had no role in the study design, writing of the report or decision to publish. The proteomics facility of the Institute of Physiology CAS is acknowledged for performing LC-MS/MS analyses.

Appendix A. Supplementary data

Supplementary data related to this article can be found at http://dx.doi.org/10.1016/j.bbrc.2015.07.034.

Transparency document

Transparency document related to this article can be found online at http://dx.doi.org/10.1016/j.bbrc.2015.07.034.

References

[1] G. Lenaz, M.L. Genova, Structural and functional organization of the mitochondrial respiratory chain: a dynamic super-assembly, Int. J. Biochem. Cell Biol. 41 (2009) 1750–1772.
[2] H. Seelert, N.A. Dencher, ATP synthase superassemblies in animals and plants: two or more are better, Biochim. Biophys. Acta 1807 (2011) 1185–1197.
[3] B. Clemencon, Yeast mitochondrial interactosome model: metabolon membrane proteins complex involved in the channeling of ADP/ATP, Int. J. Mol. Sci. 13 (2012) 1858–1885.
[4] Y.H. Ko, M. Delannoy, J. Hullihen, et al., Mitochondrial ATP synthasome. Cristae-enriched membranes and a multiwell detergent screening assay yield dispersed single complexes containing the ATP synthase and carriers for Pi and ADP/ATP, J. Biol. Chem. 278 (2003) 12305–12309.
[5] C. Chen, Y. Ko, M. Delannoy, et al., Mitochondrial ATP synthasome: three-dimensional structure by electron microscopy of the ATP synthase in complex formation with carriers for Pi and ADP/ATP, J. Biol. Chem. 279 (2004) 31761–31768.
[6] I. Wittig, H. Schagger, Structural organization of mitochondrial ATP synthase, Biochim. Biophys. Acta 1777 (2008) 592–598.
[7] J. Murray, M.F. Marusich, R.A. Capaldi, et al., Focused proteomics: monoclonal antibody-based isolation of the oxidative phosphorylation machinery and detection of phosphoproteins using a fluorescent phosphoprotein gel stain, Electrophoresis 25 (2004) 2520–2525.
[8] S. Detke, R. Elsabrouty, Identification of a mitochondrial ATP synthase-adenine nucleotide translocator complex in Leishmania, Acta Trop. 105 (2008) 16–20.
[9] F. Palmieri, C.L. Pierri, A. De Grassi, et al., Evolution, structure and function of mitochondrial carriers: a review with new insights, Plant J. 66 (2011) 161–181.
[10] G. Fiermonte, V. Dolce, F. Palmieri, Expression in Escherichia coli, functional characterization, and tissue distribution of isoforms A and B of the phosphate carrier from bovine mitochondria, J. Biol. Chem. 273 (1998) 22782–22787.
[11] C. Dahout-Gonzalez, H. Nury, V. Trezeguet, et al., Molecular, functional, and pathological aspects of the mitochondrial ADP/ATP carrier, Physiol. Bethesda 21 (2006) 242–249.
[12] T. Mracek, A. Pecinova, M. Vrbacky, et al., High efficiency of ROS production by glycerophosphate dehydrogenase in mammalian mitochondria, Arch. Biochem. Biophys. 481 (2009) 30–36.
[13] A. Pecinova, Z. Drahota, H. Nuskova, et al., Evaluation of basic mitochondrial functions using rat tissue homogenates, Mitochondrion 11 (2011) 722–728.
[14] A. Cizkova, V. Stranecky, J.A. Mayr, et al., TMEM70 mutations cause isolated ATP synthase deficiency and neonatal mitochondrial encephalocardiomyopathy, Nat. Genet. 40 (2008) 1288–1290.
[15] J.A. Mayr, V. Havlickova, F. Zimmermann, et al., Mitochondrial ATP synthase deficiency due to a mutation in the ATP5E gene for the F1 epsilon subunit, Hum. Mol. Genet. 19 (2010) 3430–3439.
[16] P. Jesina, M. Tesarova, D. Fornuskova, et al., Diminished synthesis of subunit a (ATP6) and altered function of ATP synthase and cytochrome c oxidase due to the mtDNA 2 bp microdeletion of TA at positions 9205 and 9206, Biochem. J. 383 (2004) 561–571.
[17] K. Hejzlarova, V. Kaplanova, H. Nuskova, et al., Alteration of structure and function of ATP synthase and cytochrome c oxidase by lack of Fo-a and Cox3 subunits caused by mitochondrial DNA 9205delTA mutation, Biochem. J. 466 (2015) 601–611.
[18] T. Honzik, M. Tesarova, J.A. Mayr, et al., Mitochondrial encephalocardiomyopathy with early neonatal onset due to TMEM70 mutation, Arch. Dis. Child. 95 (2010) 296–301.
[19] V. Havlickova Karbanova, A. Cizkova Vrbacka, K. Hejzlarova, et al., Compensatory upregulation of respiratory chain complexes III and IV in isolated deficiency of ATP synthase due to TMEM70 mutation, Biochim. Biophys. Acta 1817 (2012) 1037–1043.
[20] H. Schagger, Tricine-SDS-PAGE, Nat. Protoc. 1 (2006) 16–22.

[21] I. Wittig, H.P. Braun, H. Schagger, Blue native PAGE, Nat. Protoc. 1 (2006) 418–428.
[22] I. Wittig, R. Carrozzo, F.M. Santorelli, et al., Functional assays in high-resolution clear native gels to quantify mitochondrial complexes in human biopsies and cell lines, Electrophoresis 28 (2007) 3811–3820.
[23] A. Shevchenko, H. Tomas, J. Havlis, et al., In-gel digestion for mass spectrometric characterization of proteins and proteomes, Nat. Protoc. 1 (2006) 2856–2860.
[24] M. Jagr, A. Eckhardt, S. Pataridis, et al., Comprehensive proteomic analysis of human dentin, Eur. J. Oral Sci. 120 (2012) 259–268.
[25] J. Kolarov, S. Kuzela, V. Krempasky, et al., ADP, ATP translocator protein of rat heart, liver and hepatoma mitochondria exhibits immunological cross-reactivity, FEBS Lett. 96 (1978) 373–376.
[26] T.V. Kramarova, I.G. Shabalina, U. Andersson, et al., Mitochondrial ATP synthase levels in brown adipose tissue are governed by the c-Fo subunit P1 isoform, FASEB J. 22 (2008) 55–63.
[27] J.V. Brower, N. Rodic, T. Seki, et al., Evolutionarily conserved mammalian adenine nucleotide translocase 4 is essential for spermatogenesis, J. Biol. Chem. 282 (2007) 29658–29666.
[28] H.J. Wessels, R.O. Vogel, R.N. Lightowlers, et al., Analysis of 953 Human Proteins from a Mitochondrial HEK293 Fraction by Complexome Profiling, PLoS ONE 8 (2013) e68340.
[29] K. Dummler, S. Muller, H.J. Seitz, Regulation of adenine nucleotide translocase and glycerol 3-phosphate dehydrogenase expression by thyroid hormones in different rat tissues, Biochem. J. 317 (Pt 3) (1996) 913–918.
[30] A. Bass, M. Stejskalova, A. Stieglerova, et al., Ontogenetic development of energy-supplying enzymes in rat and guinea-pig heart, Physiol. Res. 50 (2001) 237–245.
[31] Y.M. Galante, S.Y. Wong, Y. Hatefi, Composition of complex V of the mitochondrial oxidative phosphorylation system, J. Biol. Chem. 254 (1979) 12372–12378.
[32] H. Ardehali, Z. Chen, Y. Ko, et al., Multiprotein complex containing succinate dehydrogenase confers mitochondrial ATP-sensitive K+ channel activity, Proc. Natl. Acad. Sci. U. S. A. 101 (2004) 11880–11885.
[33] N. Kovarova, T. Mracek, H. Nuskova, et al., High molecular weight forms of mammalian respiratory chain complex II, PLoS ONE 8 (2013) e71869.
[34] M. Klingenberg, H. Aquila, P. Riccio, Isolation of functional membrane proteins related to or identical with the ADP, ATP carrier of mitochondria, Methods Enzym. 56 (1979) 407–414.
[35] B. Meyer, I. Wittig, E. Trifilieff, et al., Identification of two proteins associated with mammalian ATP synthase, Mol. Cell Proteomics 6 (2007) 1690–1699.
[36] D.H. Boxer, The location of the major polypeptide of the ox heart mitochondrial inner membrane, FEBS Lett. 59 (1975) 149–152.
[37] H. Heide, L. Bleier, M. Steger, et al., Complexome profiling identifies TMEM126B as a component of the mitochondrial complex I assembly complex, Cell Metab. 16 (2012) 538–549.
[38] M. Klingenberg, The ADP and ATP transport in mitochondria and its carrier, Biochim. Biophys. Acta 1778 (2008) 1978–2021.

OPEN ACCESS Freely available online

PLOS ONE

High Molecular Weight Forms of Mammalian Respiratory Chain Complex II

Nikola Kovářová[1☯], Tomáš Mráček[1☯], Hana Nůsková[1], Eliška Holzerová[1], Marek Vrbacký[1], Petr Pecina[1], Kateřina Hejzlarová[1], Katarína Kľučková[2], Jakub Rohlena[2], Jiri Neuzil[2,3], Josef Houštěk[1*]

1 Department of Bioenergetics, Institute of Physiology Academy of Sciences of the Czech Republic, Prague, Czech Republic, **2** Laboratory of Molecular Therapy, Institute of Biotechnology Academy of Sciences of the Czech Republic, Prague, Czech Republic, **3** Apoptosis Research Group, School of Medical Science and Griffith Health Institute, Griffith University, Southport, Queensland, Australia

Abstract

Mitochondrial respiratory chain is organised into supramolecular structures that can be preserved in mild detergent solubilisates and resolved by native electrophoretic systems. Supercomplexes of respiratory complexes I, III and IV as well as multimeric forms of ATP synthase are well established. However, the involvement of complex II, linking respiratory chain with tricarboxylic acid cycle, in mitochondrial supercomplexes is questionable. Here we show that digitonin-solubilised complex II quantitatively forms high molecular weight structures (CII_{hmw}) that can be resolved by clear native electrophoresis. CII_{hmw} structures are enzymatically active and differ in electrophoretic mobility between tissues (500 – over 1000 kDa) and cultured cells (400–670 kDa). While their formation is unaffected by isolated defects in other respiratory chain complexes, they are destabilised in mtDNA-depleted, rho0 cells. Molecular interactions responsible for the assembly of CII_{hmw} are rather weak with the complexes being more stable in tissues than in cultured cells. While electrophoretic studies and immunoprecipitation experiments of CII_{hmw} do not indicate specific interactions with the respiratory chain complexes I, III or IV or enzymes of the tricarboxylic acid cycle, they point out to a specific interaction between CII and ATP synthase.

Citation: Kovářová N, Mráček T, Nůsková H, Holzerová E, Vrbacký M, et al. (2013) High Molecular Weight Forms of Mammalian Respiratory Chain Complex II. PLoS ONE 8(8): e71869. doi:10.1371/journal.pone.0071869

Editor: Nagendra Yadava, UMASS-Amherst/Tufts University School of Medicine, United States of America

Received May 14, 2013; **Accepted** July 10, 2013; **Published** August 13, 2013

Funding: This work was supported by the Grant Agency of the Czech Republic (P303/10/P227, P301/10/1937), Ministry of Education, Youth and Sports of the Czech Republic (ERC CZ LL1204 and RVO: 67985823) and Ministry of Health of the Czech Republic (NT12370-5). The funders had no role in study design, data collection and analysis, decision to publish, or preparation of the manuscript.

Competing interests: The authors have declared that no competing interests exist.

* E-mail: houstek@biomed.cas.cz

☯ These authors contributed equally to this work.

Introduction

The mitochondrial oxidative phosphorylation system (OXPHOS) is the main source of energy in mammals. This metabolic pathway is localised in the inner mitochondrial membrane (IMM) and includes the respiratory chain complexes I, II, III and IV (CI, CII, CIII, CIV), ATP synthase (complex V, CV), plus the mobile electron transporters coenzyme Q (CoQ) and cytochrome *c*. Energy released by oxidation of NADH and $FADH_2$ is utilised for proton transport across the membrane to establish proton gradient. The resulting electrochemical potential ($\Delta\mu_H^+$) is then utilised as a driving force for phosphorylation of ADP by ATP synthase.

CII (succinate: ubiquinone oxidoreductase; EC 1.3.5.1), catalyses electron transfer from succinate (via $FADH_2$) to CoQ and thus represents important crossroads of cellular metabolism, interconnecting the tricarboxylic acid (TCA) cycle and the respiratory chain [1]. It consists of 4 nuclear encoded subunits. The hydrophilic head of CII is formed by the SDHA subunit with covalently bound FAD and the SDHB subunit, which contains three Fe–S centres. The SDHC and SDHD subunits form the hydrophobic membrane anchor and are the site of cytochrome *b* binding [2].

Mutations in genes coding for any of the CII subunits are associated with severe neuroendocrine tumours such as paraganglioma and phaeochromocytoma [3–5] as well as other tumour types, including gastrointestinal stromal tumours [6] or renal tumours [7]. Conversely, the CII subunits also function as tumour suppressors and represent one of the potential molecular targets of anti-cancer drugs [8], whose mechanisms of action could lead to apoptosis of cancer cells through the inhibition of CII and a consequent metabolic collapse.

In comparison with other respiratory chain complexes, the assembly of CII has not yet been fully characterised. Up to now, two evolutionarily conserved assembly factors for CII have been described; SDHAF1 was discovered as disease-

causing gene in a case of infantile leukoencephalopathy presenting with a decrease in the CII content and activity [9]. The LYR motif in the protein structure suggests its role in the metabolism of the Fe–S centres [10]. The second assembly factor, SDH5, is a soluble mitochondrial matrix protein, which is most likely required for insertion of FAD into the SDHA subunit [11].

Recent studies indicate that the organisation of the OXPHOS complexes in the inner mitochondrial membrane (IMM) is characterised by non-stochastic protein–protein interactions. Individual complexes specifically interact with each other to create supramolecular structures referred to as supercomplexes (SCs). SCs behave as individual functional units, enabling substrate channelling [12]; more effective electron transport should prevent electron leak and reactive oxygen species generation [13]. Besides the kinetic advantage, SCs stabilise OXPHOS complexes and help to establish the IMM ultrastructure [14].

To date, the presence of CII in SCs is still a matter of debate. In yeast and mammalian mitochondria, the interaction of CI, III, IV and V within different types of SCs has been proven using native electrophoretic techniques in combination with mild detergents and/or the Coomassie Blue G (CBG) dye [15,16]. However, the presence of CII in such structures has only been reported by Acín-Peréz et al. [17], who described the existence of a large respirasome comprising all OXPHOS complexes including CII in mammalian cells. On the other hand, CII has been detected as a structural component of the mitochondrial ATP-sensitive K^+ channel (mitoK_{ATP}) [18]. Such structures do indeed represent higher molecular forms of CII, but their structural and physiological importance remains to be investigated.

CII as the only membrane bound component of the TCA cycle could also form complexes with other TCA cycle proteins, e.g. with its functional neighbours fumarase and succinyl CoA lyase. Different studies indicate the existence of a TCA cycle metabolon and possible supramolecular organisation of various parts of the TCA cycle [19,20], but these may be significantly more labile than the well described respiratory chain SCs.

In the present study we demonstrate the existence of high molecular weight forms of CII (CII_{hmw}), i.e. SCs containing CII, using mitochondrial membrane solubilisation with mild non-ionic detergents followed by electrophoretic analysis. These complexes are rather labile, and the presence of n-dodecyl-β-D-maltoside or CBG during the electrophoretic separation causes their dissociation to individual units. CII_{hmw} structures differ in their electrophoretic migration between mammalian cells and tissues, and their formation depends on the presence of the functional respiratory chain. Our experiments also clearly indicate the association of CII with CV.

Materials and Methods

Cell lines

The following cell lines were used in experiments: control human fibroblasts and fibroblasts from patients with isolated deficiency of CI (an unknown mutation), CIV (the *SURF1* mutation, described in [21,22]), CV (the *TMEM70* mutation described in [23]), human rho0 (ρ^0) cells (mtDNA-depleted 143B TK^- osteosarcoma cells [24]), human embryonic kidney cells HEK293, primary mouse (derived from the C57/Bl6 strain) and rat (derived from the SHR strain) fibroblasts. All cell lines were grown in the high-glucose DMEM medium (Lonza) supplemented with 10% (v/v) foetal bovine serum (Sigma) at 37 °C in 5% CO_2 atmosphere. Cells were harvested using 0.05% trypsin and 0.02% EDTA and stored as pellets at -80 °C.

Isolation of cell membranes and mitochondria from cells and tissues

Mitochondria from cultured cells were isolated after cell disruption by hypotonic shock as described [25]. In some experiments, membrane fractions from fibroblasts were prepared as described [26]. Human heart mitochondria and mitochondria from rat heart, liver and brown adipose tissues were isolated according to established procedures [27]. The protein concentration was measured by the Bradford method (BioRad).

Ethical aspects

All work involving human samples was carried out in accordance with the Declaration of Helsinki of the World Medical Association and was approved by the Ethics Committee of the Institute of Physiology, Academy of Sciences of the Czech Republic v.v.i. The written informed consent was obtained from patients or patients' parents.

All animal tissues were obtained on the basis of approval by the Expert Committee for Work with Animals of the Institute of Physiology, Academy of Sciences of the Czech Republic v.v.i. (Permit Number: 165/2010) and animal work was in accordance with the EU Directive 2010/63/EU for animal experiments.

Electrophoresis and western blot analysis

Isolated membranes or mitochondria were solubilised with digitonin (Sigma, 4 g/g protein) in an imidazole buffer (2 mM aminohexanoic acid, 1 mM EDTA, 50 mM NaCl, 50 mM imidazole, pH 7.0) for 15 min at 0 °C and centrifuged for 20 min at 20 000 *g* [26]. Samples were prepared by adding 5% (v/v) glycerol and 0.005% (v/v) Ponceau S dye for clear native and high resolution clear native electrophoresis (CNE, hrCNE3), or 5% (v/v) glycerol and CBG dye (Serva Blue G 250, 1:8 ratio (w/w) to digitonin) for blue native electrophoresis (BNE). Separation of mitochondrial proteins was performed using CNE, BNE [26] and hrCNE3 [28] on 6–15% polyacrylamide gradient gels using the Mini-Protean apparatus (BioRad). For 2D separation by CNE/SDS PAGE, the gel after CNE was cut into stripes that were incubated in 1% SDS and 1% 2-mercaptoethanol for 1 h and then subjected to SDS PAGE on a 10% slab gel [29]. In case of 2D separation by CNE/CNE_{CBG}, gel stripes after CNE were incubated in 3% CBG in the CNE cathode buffer for 1 h and then subjected to CNE on 6–15% gradient gels.

For western blot immunodetection, the separated proteins were transferred to a PVDF membrane (Immobilon-P, Millipore) by semi-dry electrotransfer. The membranes were blocked with 5% (w/v) non-fat dried milk in TBS (150 mM NaCl, 10 mM Tris,

pH 7.5) for 1 h and incubated overnight at 4 °C with specific primary antibodies diluted in TBST (TBS with 0.1% Tween-20). Monoclonal or polyclonal primary antibodies to the following enzymes of OXPHOS or TCA cycle were used: SDHA (ab14715, Abcam), SDHB (ab14714, Abcam), Core1 (ab110252, Abcam), NDUFA9 (ab14713, Abcam), Cox4 (ab14744, ab110261, Abcam), citrate synthase (ab129095, Abcam), isocitrate dehydrogenase (α subunit, ab58641, Abcam), aconitase 2 (ab110321, Abcam), α subunit of CV [30], fumarase (M01, Abnova), succinyl-CoA synthetase (α subunit, 5557, Cell Signaling Technology) and malate dehydrogenase (8610, Cell Signaling Technology). The detection of the signals was performed with the secondary Alexa Fluor 680-labelled antibody (Life Technologies) using the Odyssey fluorescence scanner (LI-COR).

Enzyme in-gel activity staining

In-gel activity assays were performed after separation of the respiratory complexes using CNE. For CIV in-gel activity staining, we used a recently described protocol [21]. The in-gel activity assay of the CV ATP hydrolytic activity was performed as described [28]. The activity of CII was detected using the modified succinate: nitroblue tetrazolium reductase assay [28]. Briefly, gel slices from CNE were incubated for 1 h (for tissues) or overnight (for cells) at room temperature in the dark in the staining solution (200 mM Tris, pH 7.4), 10 mM EDTA, 1 mg/mL nitroblue tetrazolium, 80 µM phenazine methosulfate, 2 mM KCN, 1.5 µg/mL rotenone and 30 mM succinate).

Immunoprecipitation

For co-immunoprecipitation analysis we used a rabbit polyclonal antibody against the F_1 part of ATP synthase (reacting with the ATP synthase subunits α, γ, and predominantly β, generated in our laboratory) or a mouse monoclonal antibody against the SDHA subunit of CII (ab14715, Abcam). The antibodies were immobilised on CNBr-activated agarose matrix (Sigma). Agarose beads with the bound antibody were equilibrated in PBS (140 mM NaCl, 5 mM KCl, 8 mM Na_2HPO_4, 1.5 mM KH $_2PO_4$, pH 7.2 -7.3) supplemented with 0.2% protease inhibitor cocktail (PIC, Sigma). For storage at 4 °C, they were dissolved in PBS+PIC supplemented with 0.025% thimerosal (Sigma). Solubilisation of rat heart mitochondria and human fibroblasts was performed with digitonin (2 g/g protein) in PBS+PIC. The solubilisates were mixed with the antibody-conjugated agarose beads and diluted with PBS+PIC supplemented with the same digitonin concentration as for sample solubilisation. The mixture was incubated overnight at 4 °C on a rotating mixer. The beads were then washed three times with PBS+PIC+digitonin (the same concentration as for sample solubilisation), PBS+PIC +digitonin (ten times diluted), and finally with PBS+PIC. All the washing steps included incubation for 5 min at 4 °C on a rotating mixer and centrifugation at 1000 *g* for 1 min at room temperature. The pelleted beads were combined with a small volume of the 2x SDS sample lysis buffer and incubated at 65 °C for 15 min. After a brief centrifugation, the supernatant with the released co-immunoprecipitated proteins was subjected to SDS PAGE and western blot analysis using specific antibodies (described in section 2.4.).

Results

High molecular weight forms of CII

The mammalian CII consists of four subunits, SDHA, SDHB, SDHC and SDHD, with the approximate molecular weight (MW) of 70, 30, 18 and 17 kDa, respectively. Digitonin-solubilised CII from mitochondria of human fibroblasts was resolved by BNE (in the presence of CBG) or hrCNE3 (in the presence of n-dodecyl-β-D-maltoside and deoxycholic acid in the cathode buffer) as a CII monomer of the expected mass of approximately 140 kDa (Figure 1A, B) which represented most of the CII signal. In addition, weaker bands smaller than 140 kDa and at approximately 200 kDa were also present; these could be CII sub-complexes and CII hetero-oligomers. When milder conditions of separation were applied using CNE, a completely different pattern of the CII signal was obtained, indicating the presence of its higher molecular weight forms (CII_{hmw}). As revealed by immunodetection with the SDHA antibody, the signal of CII was almost completely localised within the region of 400–670 kDa (Figure 1A). Similarly, the SDHB antibody (Figure 1B) or in-gel staining of CII (SDH) activity (Figure 1C) confirmed the presence of CII in the 400–670 kDa region. This was further demonstrated by 2D CNE/SDS PAGE analysis of the cells (Figure 2A), where the distributions of SDHA and SDHB in the second dimension gel indicate that the CII_{hmw} forms represent a complete and active CII, in accord with the profiles of CII activity in CNE. For comparison, we also analysed the CII profile in mitochondria isolated from rat heart and obtained similar results, except for the size of tissue CII_{hmw} on CNE gels, which increased to 500 – over 1000 kDa when detected either with the SDHA or SDHB antibodies (Figure 1D, E) or by the in-gel SDH activity staining (Figure 1F). This was also confirmed by 2D analysis (Figure 2B).

Further, we analysed the distribution profiles of other OXPHOS complexes on 2D blots with subunit-specific antibodies in an attempt to determine potential CII interaction partners within CII_{hmw}. As expected, a substantially different migration pattern was found in the case of CI (NDUFA9) while some CIII (Core1) signal overlapped with CII in heart, but not in fibroblasts (Figure 2A, B). The signal of CIV (Cox4) partially overlapped with that of CII_{hmw} (SDHA, SDHB), as shown by the distribution profiles below the western blot images. A similar overlap with the CII_{hmw} signal was found for CV (the α subunit), in particular in the case of fibroblasts (Figure 2A). This may reflect a coincidental co-migration of respective complexes because of the imprecise electrophoretic mobility inherent to the CNE system in the first dimension [31], but it can also indicate a possibility that CII_{hmw} include SCs of CII with CIII, CIV or CV.

CII_{hmw} differ between tissues and cells

When CNE analysis of digitonin-solubilised proteins was performed using fibroblasts and different immortalised/ malignant human or rodent cell lines (Figure 3A), an analogous

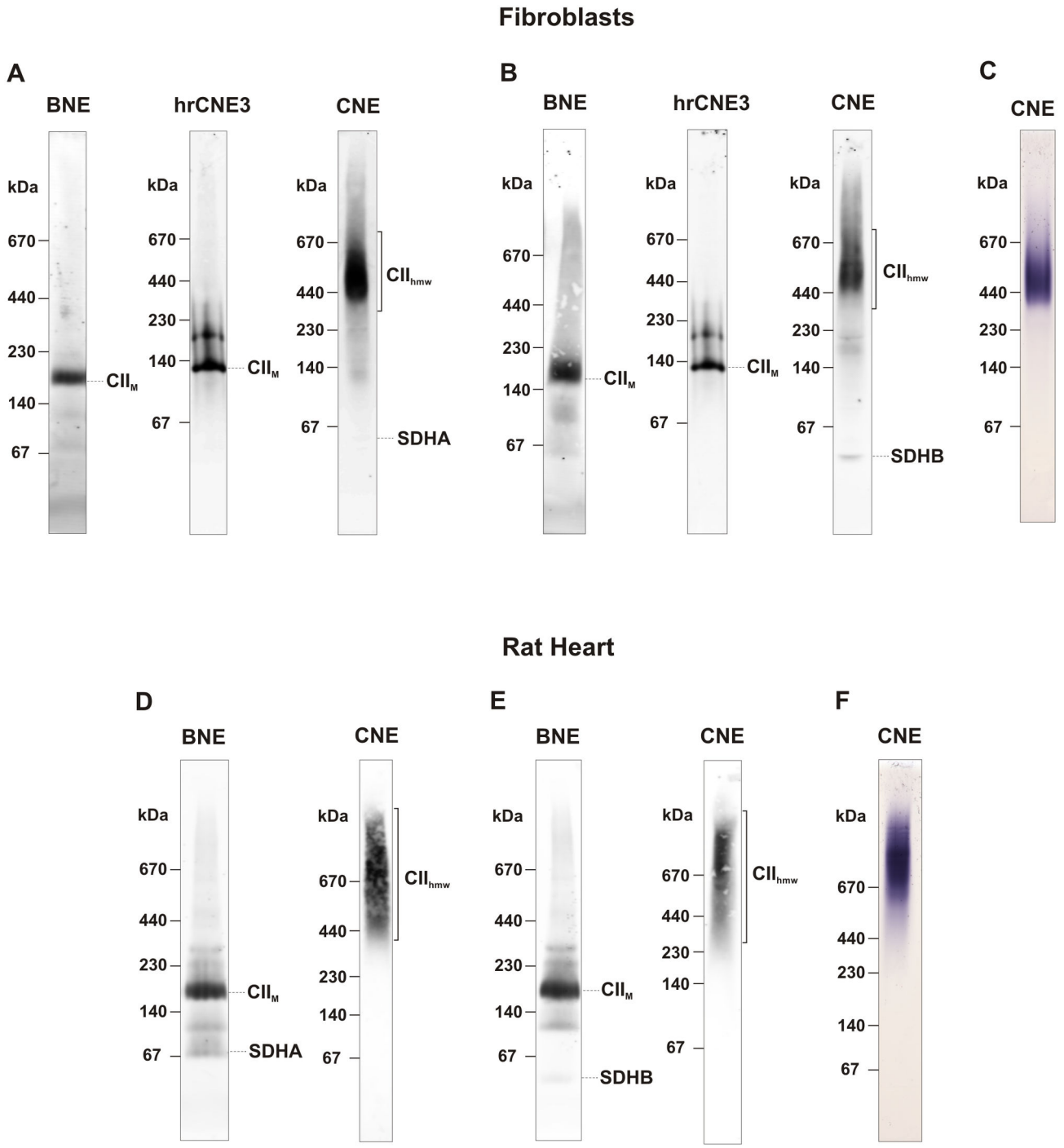

Figure 1. Higher molecular weight forms of complex II. Mitochondrial membrane proteins from control fibroblasts and rat heart were solubilised with digitonin (4 g/g protein), and 20 µg protein aliquots were separated using BNE, hrCNE3 and CNE. CII was immunodetected with the SDHA antibody (A, D) and SDHB antibody (B, E). In-gel activity staining of CII was performed in CNE gels (C, F). Migrations of higher molecular weight forms of CII (CII_{hmw}), CII monomer (CII_M), SDHA and SDHB subunits of CII are marked. The images are representative of three independent experiments.

doi: 10.1371/journal.pone.0071869.g001

CII_{hmw} pattern was obtained in all human, mouse and rat cells, indicating that most of CII is present as CII_{hmw}. Similarly, CII_{hmw} was found as a predominant form of CII in mitochondria of different human and rodent tissues (Figure 3B), suggesting that

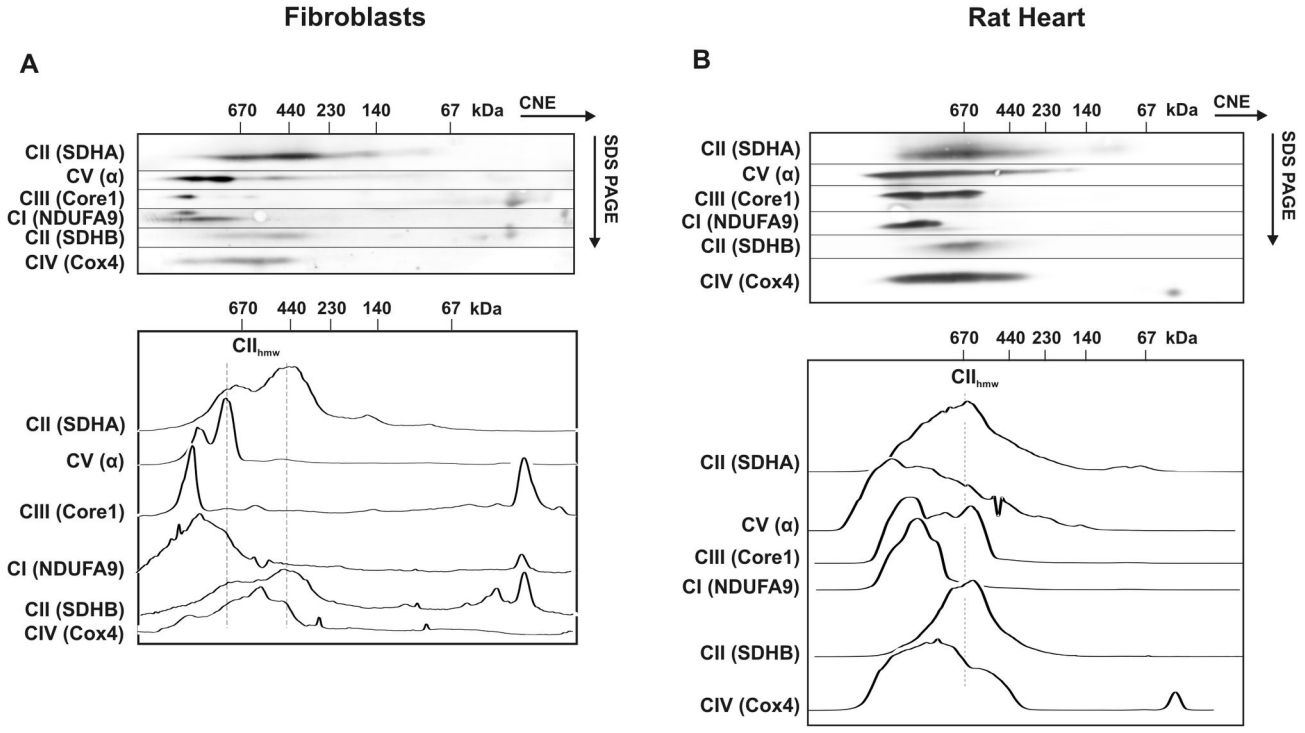

Figure 2. CNE/SDS PAGE analysis of OXPHOS proteins. Digitonin-solubilised proteins from human fibroblasts (A) and rat heart (B) mitochondria were separated by CNE in the first dimension (40 µg protein load) and by SDS PAGE in the second dimension. Subunits of the respiratory chain CI (NDUFA9), CII (SDHA, SDHB), CIII (Core1), CIV (Cox4) and CV (α) were immunodetected using specific antibodies. The dashed vertical lines in the distribution profiles below the western blots depict the main area of higher molecular weight forms of complex II (CII$_{hmw}$).

doi: 10.1371/journal.pone.0071869.g002

high molecular forms of CII are a universal property of mammalian respiratory chain. Nevertheless, the mobility of CII$_{hmw}$ in tissues was considerably different in comparison with cell lines. As shown in Figure 3B the main signal of the SDHA antibody in tissues was detected above 670 kDa, in the MW range of larger respiratory SCs (SDHB displayed an analogous distribution pattern, not shown). This was also observed on 2D CNE/SDS PAGE western blots (Figure 2B), where the signal of the CII SDHA and SDHB subunits was shifted to a higher MW. In contrast, other OXPHOS complexes were distributed comparably with the cultured cells (Figure 2A). Therefore, we performed in-gel activity staining of CII in CNE gels to confirm the detected antibody signals in the cells and tissues. Figure 3C, D reveals that CII$_{hmw}$ complexes were catalytically active and, indeed, differed between cells and tissues. In parallel, we performed in-gel CIV and CV activity staining to further analyse a possible co-migration or interaction with CII. In the case of cells, the dominant CIV activity signal could be ascribed to the CIV dimer (CIV$_D$) (Figure 3C), in the position corresponding to some of CII$_{hmw}$. The higher active CIV SCs did not co-migrate with the CII signal. Thus, the size of CII$_{hmw}$ in the cells more likely points to a mere co-migration of CII homo-/hetero-oligomers with CIV$_D$, rather than to a genuine specific interaction between the OXPHOS complexes.

Interestingly, the CIV activity signals were shifted to the higher MW in tissues and overlapped with the activity signal of CII$_{hmw}$ (see Figure 3D). The interaction of CII with CIV or other OXPHOS complexes in the MW range > 1 MDa thus cannot be excluded. The differences in the size of CII$_{hmw}$ when comparing cells and tissues could suggest the existence of two major functional forms of CII SCs. In cells, they may be present largely as CII homo-oligomers, while in tissues, CII may possibly form SCs with other OXPHOS complexes. In-gel activity of monomeric and homo-oligomeric CV did indicate co-migration or interaction with CII$_{hmw}$ in tissues but not in cells (Figure 3C, D).

CII$_{hmw}$ formation depends on other respiratory chain complexes

To learn more about possible interactions with other OXPHOS complexes, we performed CNE analysis of digitonin-solubilised mitochondria of human fibroblasts harbouring different types of OXPHOS defects that affect one or more respiratory chain complexes. We found that the selective deficiency of CIV (due to a *SURF1* mutation, Figure 4B) or CV (due to a *TMEM70* mutation, Figure 4C) did not affect the presence of CII$_{hmw}$ (Figure 4A). Similarly, the selective deficiency of CI (an unknown mutation) was without any effect

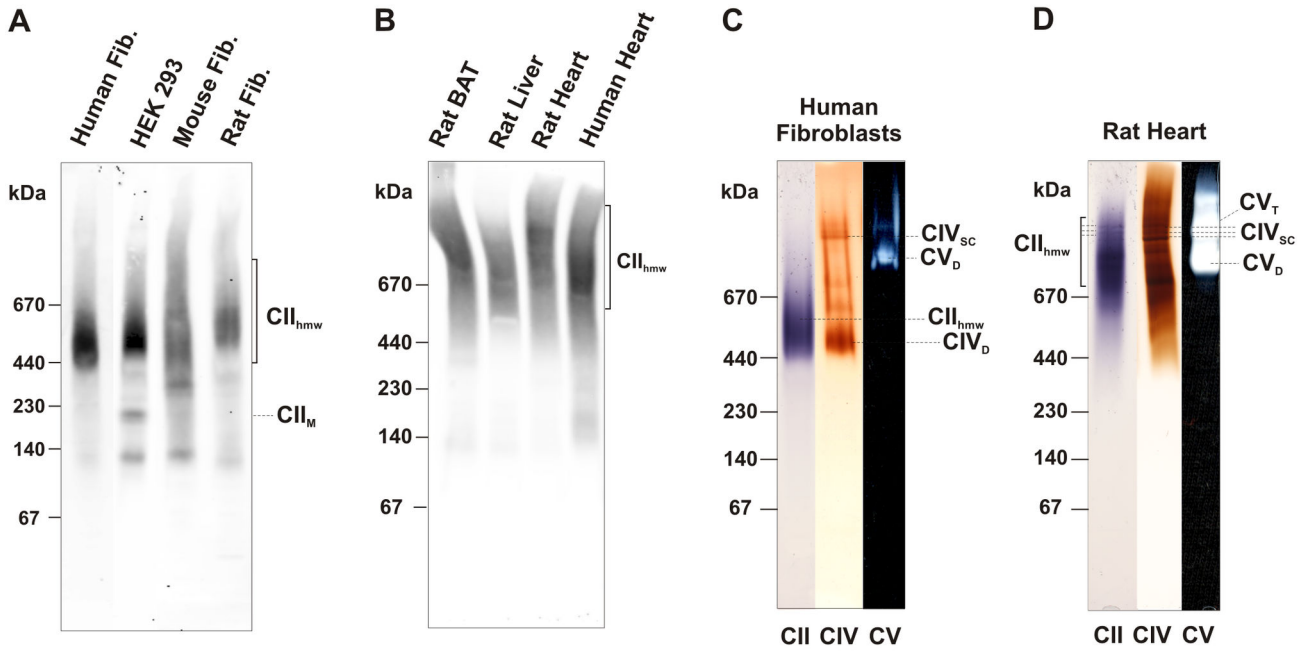

Figure 3. Comparison of CII$_{hmw}$ in cells and tissues by western blot and in-gel activity staining. Mitochondria from different human and rodent cells (A) and tissues (B) were solubilised with digitonin (4 g/g protein) and 20 µg protein aliquots were separated using CNE. CII was immunodetected with the SDHA antibody. The activities of CII (violet), CIV (brown) and CV (white) in CNE gels (protein load 50 µg for cells and 40 µg for tissues) are shown in human fibroblasts (C) and rat heart (D). The positions of higher molecular weight forms of CII (CII$_{hmw}$), CII monomer (CII$_M$), CIV dimer (CIV$_D$) and its supercomplexes (CIV$_{SC}$), CV dimer (CV$_D$) and tetramer (CV$_T$) are indicated in the figure. Rat BAT, rat brown adipose tissue.

doi: 10.1371/journal.pone.0071869.g003

on the CII$_{hmw}$ pattern. However, we obtained a different pattern in ρ^0 cells with depletion of mtDNA and thus lack of functional complexes I, III, IV and V [24]. Here, most of the CII$_{hmw}$ signal disappeared and CII was present as unassembled subunits or monomer. This demonstrates the requirement of fully assembled CII monomer for subsequent CII$_{hmw}$ formation, and also its dependence on the preserved integrity of a fully functional respiratory chain (Figure 4A).

CII$_{hmw}$ stability depends on very weak protein–protein interactions

The fact that CII$_{hmw}$ are retained in CNE gels but dissociate in BNE gels (Figure 1) points to their rather labile nature. To analyse these interactions in more detail, we used CNE as before but with the CBG dye added to the sample (Figure 5A). In this experiment, CII$_{hmw}$ dissociated into monomeric CII due to the presence of CBG, while other respiratory chain SCs (CIV shown as an example) remained unaffected, apart from the fact that they were better focused due to the negative charge introduced by CBG. We therefore performed 2D CNE/CNE$_{CBG}$ electrophoresis using CBG to treat the gel slice after the CNE separation in the first dimension (Figure 5 B–F). As shown by western blots with the antibodies to SDHA and SDHB, all CII$_{hmw}$ dissociated into CII monomers after exposure to CBG, that can bind to proteins due to its negative charge and thus interfered with weak non-covalent interactions. The main signal of CII from the first dimension can again be observed within the MW range of 400–670 kDa. On the contrary, the SCs of CI+III+IV were practically unaffected by CBG treatment (Figure 5E). Interestingly, the addition of CBG also partially affected oligomers of CV, which dissociated to lower molecular weight forms corresponding to the CV monomer and the F_1 sub-complex (Figure 5F).

To follow the potential differences between cultured cells and tissues, we examined the stability of CII$_{hmw}$ from rat heart mitochondria in the presence of CBG. While we detected a complete breakdown of CII$_{hmw}$ in the CNE gel after the addition of CBG to the sample (Figure 6A), most of the CII$_{hmw}$ was unaffected under 2D CNE/CNE$_{CBG}$ conditions. Based on good reproducibility of the experiments, we can conclude that CII$_{hmw}$ do have higher MW and are more stable in tissues than in cultured cells. This may indicate that CII has different interaction partners in tissues and cultured cells, and CII$_{hmw}$ thus ultimately represents several structurally and functionally different SCs. As in cultured cells, CIV and its SCs were unaffected (Figure 6A, 6D), while CV partially dissociated from its higher forms to the monomeric and the F_1 sub-complex forms (Figure 6E). The sensitivity of CII and CV to CBG indicates a similar type of mild interactions responsible for the formation of their respective higher molecular weight complexes.

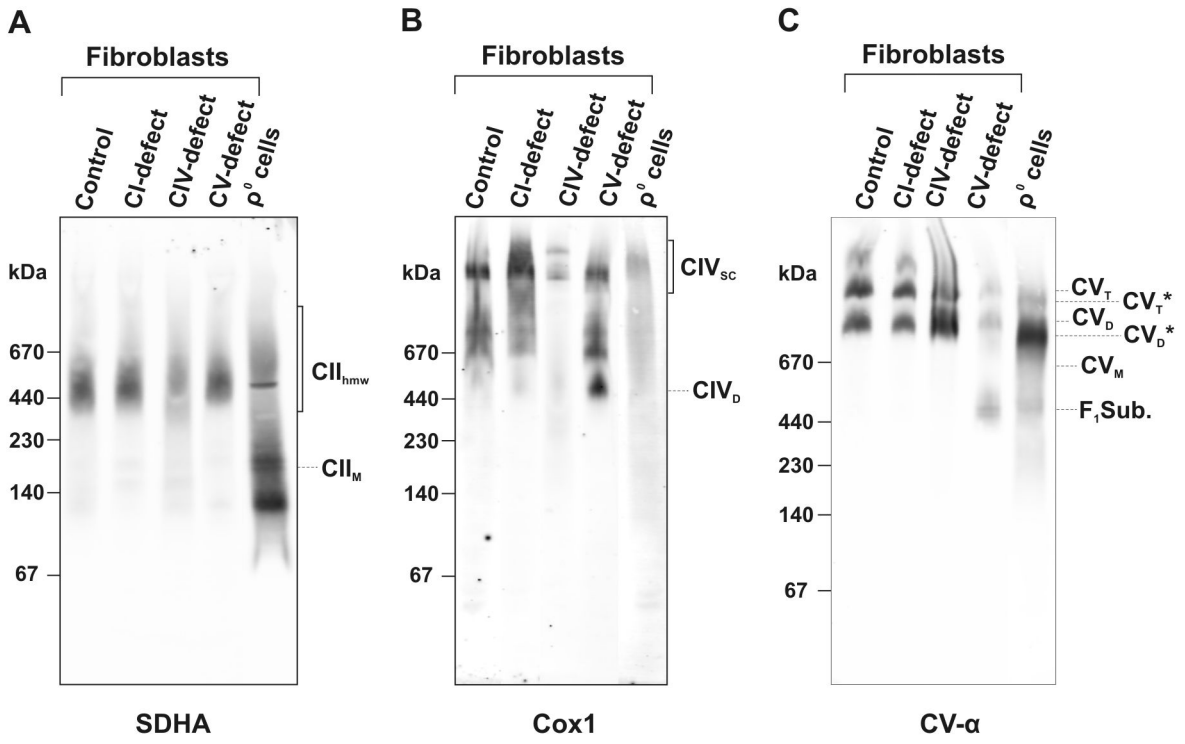

Figure 4. Presence of CII$_{hmw}$ in human fibroblasts with different types of OXPHOS defects and ρ^0 cells. Digitonin-solubilised mitochondrial complexes were analysed by CNE (20 µg protein load) and immunodetected using antibodies to individual subunits: (A) CII, SDHA; (B) CIV, Cox1; (C) CV, α subunit. Positions of the CII monomer (CII$_M$), high molecular weight forms of CII (CII$_{hmw}$), CIV dimer (CIV$_D$), supercomplexes of CIV (CIV$_{SC}$), F_1 subcomplex of CV (F $_1$Sub.), the monomer, dimer and tetramer of CV (CV$_M$, CV$_D$ and CV$_T$), and the dimer and tetramer of CV lacking the mtDNA-coded subunits (CV$_D$* and CV$_T$*) are marked.
doi: 10.1371/journal.pone.0071869.g004

CII co-immunoprecipitates with CV

To investigate possible interactions between CII and CV by a different approach, we immunoprecipitated CV from rat heart mitochondria (Figure 7A) using a highly specific rabbit polyclonal antibody (CV–F_1) to CV subunits α, β and γ. The antibody immobilised to agarose beads immunoprecipitated whole CV, as evidenced by the presence of both F_1 (α and γ) and F_o (a) subunits. The immunoprecipitate was free of CI, CIII and CIV subunits, but it contained a significant amount of the SDHA subunit of CII. Similarly, SDHA was co-immunoprecipitated using CV-F_1 antibody and solubilised fibroblasts (Figure 7B). In a cross-experiment, we immunoprecipitated CII from heart mitochondria using a highly specific monoclonal antibody against SDHA. The resulting immunoprecipitate contained CII as well as the whole CV as revealed by the presence of subunits from F_1 and F_o parts of CV (Figure 7A). In contrast, it was free of CI, CIII and CIV. Again, CV was also co-immunoprecipitated using SDHA antibody and solubilised fibroblasts (Figure 7B). As none of the commercially available antibodies against SDHC and SDHD we tested were reasonably specific, we cannot confirm the presence of fully assembled CII in the precipitate. In principle, it is possible that only the two hydrophilic subunits SDHA and SDHB are present in the SC with CV. Notwithstanding, this result is compatible with recent data showing the presence of CII as well as CV in the mitoK$_{ATP}$ channel complex, whose size was found to be approximately 940 kDa, similarly to CII$_{hmw}$ forms observed in tissues.

CII does not form SC with TCA cycle enzymes

CII can also potentially interact with components of the TCA cycle. We therefore used CNE to separate digitonin-solubilised (4 g/g) rat heart mitochondria and subsequently analysed the lysate by western blotting for the presence and distribution pattern of individual TCA cycle enzymes, which were then compared with the distribution of CII. We observed high molecular weight form complexes of fumarase and succinyl-CoA synthetase in the region above 670 kDa (Figure 8A). Although they dissociated into lower molecular forms after the addition of CBG, as was the case for CII (Figure 8B), the CNE migration pattern for both fumarase and succinyl-CoA synthetase was slightly different from that of CII, which does not support the existence of their direct interaction. Other digitonin-solubilised TCA cycle enzymes did not show any co-migration with CII on the CNE gels (not shown).

To check for the potential associations between CII and other TCA cycle enzymes, we immunoprecipitated CII from rat heart mitochondria using the monoclonal antibody against the

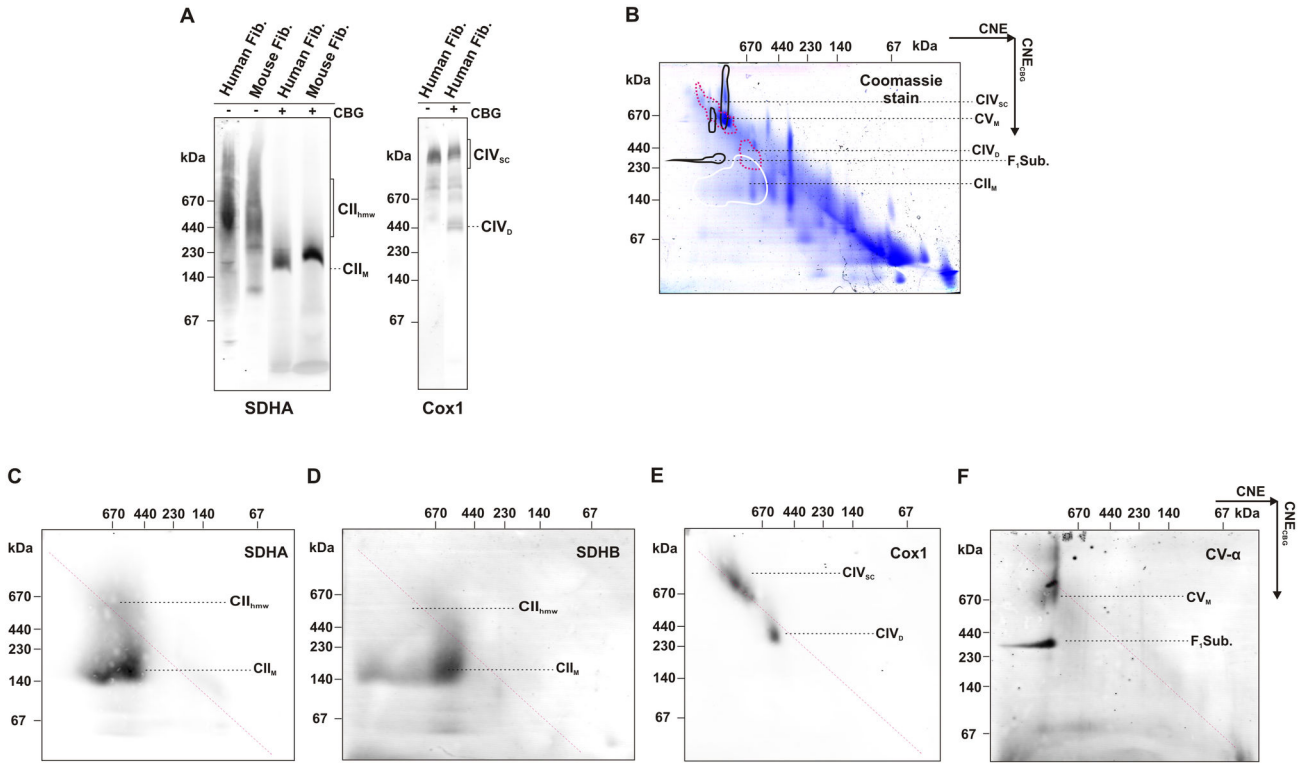

Figure 5. Low stability of CII$_{hmw}$ in fibroblasts. (A) Digitonin-solubilised (4 g/g protein; 20 µg protein load) mitochondrial proteins from control human fibroblasts or control mouse fibroblasts were resolved by CNE with (+) or without (-) CBG. (B–F) Two-dimensional CNE/CNE$_{CBG}$ analysis of mitochondrial proteins from control fibroblasts (50 µg protein load). After separation of mitochondrial proteins with CNE, the gel slices were incubated in CBG and subjected to CNE in the second dimension. One gel was stained in Coomassie blue stain and identical duplicate gel was used for western blot. The positions of individual OXPHOS complexes are highlighted on the stained gel (B) according to their immunodetection: full white line, CII monomer (CII$_M$); dashed red line, CIV dimer (CIV$_D$) and supercomplexes of CIV (CIV$_{SC}$); full black line, F$_1$ subcomplex of CV (F$_1$Sub.) and monomer of CV (CV$_M$) based on the signals of SDHA (C), SDHB (D), Cox1 (E) and CV-α (F) subunits.

doi: 10.1371/journal.pone.0071869.g005

SDHA subunit as above. The resulting immunoprecipitated CII contained no other TCA cycle enzymes, namely α-ketoglutarate dehydrogenase (subunit E1), aconitase, fumarase, citrate synthase, isocitrate dehydrogenase (subunit α), succinyl-CoA synthetase (subunit α) or malate dehydrogenase (Figure 8B).

Discussion

The key finding of this study is the discovery of CII propensity to form higher molecular structures (CII$_{hmw}$) in the IMM. We demonstrated that under sufficiently mild conditions, CII associates into CII$_{hmw}$ forms in both mammalian cultured cells and tissues. As the representative cell line/tissue we used human fibroblasts and rat heart, and we have clearly shown that CII$_{hmw}$ are present regardless of the species (rat, mouse, human), tissue type (heart, liver, brown adipose tissue) or the origin of the cell line (fibroblasts, kidney cells). As such, CII$_{hmw}$ can be found in mitochondria with a wide range of content of the respiratory chain complexes. The interactions responsible for CII$_{hmw}$ formation must be rather weak as the supramolecular structures are not retained under the conditions of the commonly used native electrophoretic techniques, such as BNE or hrCNE [26,28], where either negatively charged CBG or additional detergents are present and, presumably, disrupt the weak interactions responsible for CII$_{hmw}$ formation. Thus, these complexes can only be visualised using the CNE electrophoretic system, where proteins migrate according to their intrinsic charge routinely lost by the charged dyes or detergents used to introduce the net charge to the protein micelles formed during the solubilisation of the membrane. Despite the lower resolution of CNE in comparison with other native electrophoretic systems [31], we have shown that CII$_{hmw}$ forms differ in their apparent molecular mass between tissues (500 – over 1000 kDa) and cultured cells (400–670 kDa). The reasons for this difference are not immediately obvious. Possibly, this may be the effect of detergent (i.e. digitonin) and its concentrations used for solubilisation of proteins from the IMM. Apart from the critical micellar concentration [32], the ratio of the detergent and the protein can also dictate the outcome of

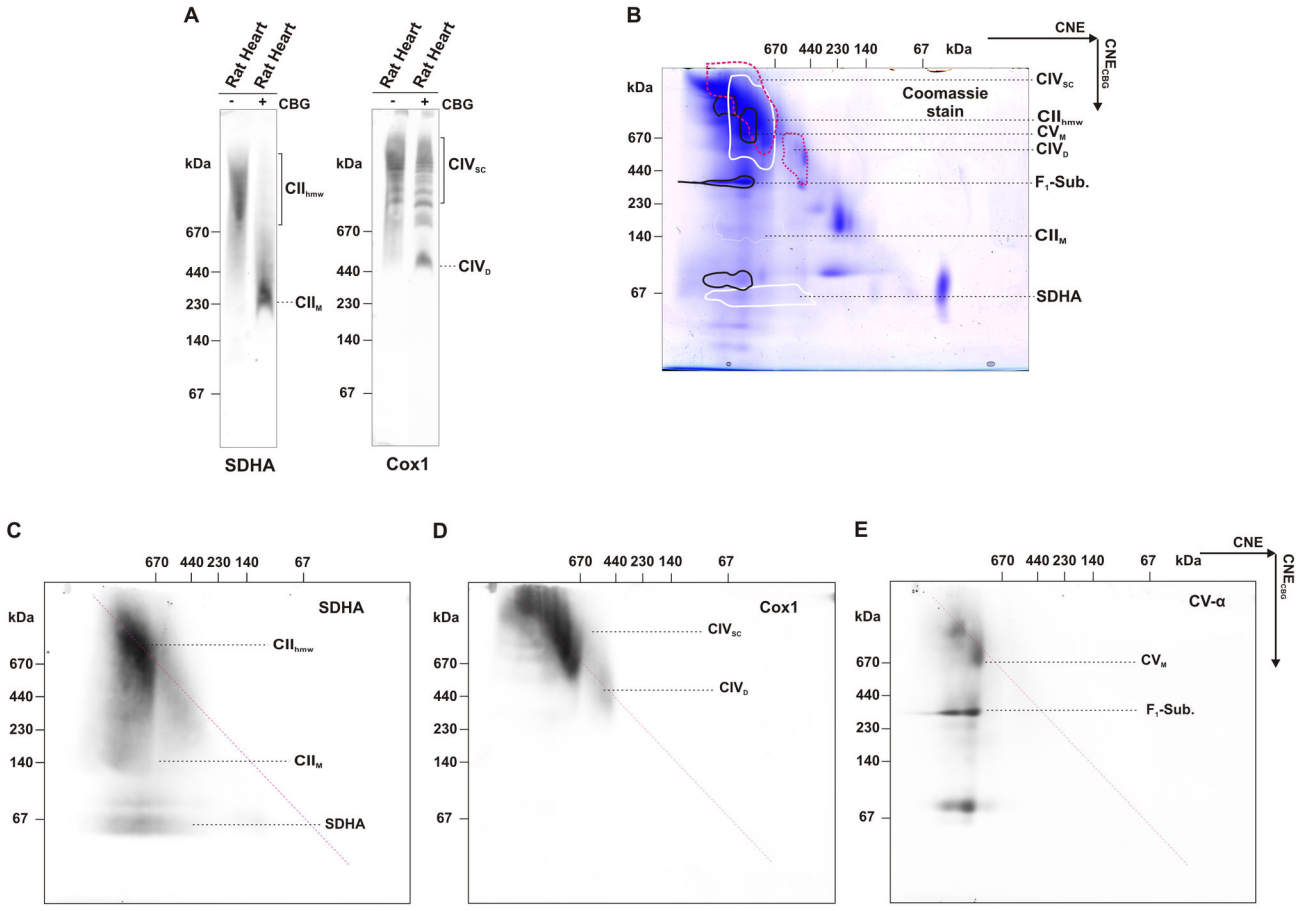

Figure 6. Low stability of CII_{hmw} in rat heart. (A) Digitonin-solubilised (4 g/g protein, 20 µg protein load) mitochondrial proteins from rat heart mitochondria were resolved by CNE with (+) or without (-) CBG. (B–F) Two-dimensional CNE/CNE_{CBG} analysis of mitochondrial proteins from rat heart (40 µg protein load). After separation of mitochondrial proteins with CNE, the gel slices were incubated in CBG and subjected to CNE in the second dimension. One gel was stained in Coomassie blue stain and identical duplicate gel was used for western blot. The positions of individual OXPHOS complexes are highlighted on the stained gel (B) according to their immunodetection: full white line, CII monomer (CII_M), high molecular weight forms of CII (CII_{hmw}), and the SDHA subunit of CII; dashed red line, CIV dimer (CIV_D) and supercomplexes of CIV (CIV_{SC}); full black line, F_1 subcomplex of CV (F_1Sub.) and monomer of CV (CV_M) based on the signals of SDHA (C), Cox1 (D), and CV-α (E) subunits.

doi: 10.1371/journal.pone.0071869.g006

the solubilisation process. As tissues display higher density of mitochondria than cultured cells, the use of the same detergent/protein ratio for both may yield different results when resolving the mitochondrial SCs. Another possible reason for the different mobility of CII_{hmw} from the two sources could be a different phospholipid composition of the IMM between cells and tissues, although the recent work indicates similarities in the relative abundance of mitochondrial phospholipids in tissues and cultured cells [33,34]. Ultimately, this difference may simply reflect a higher number of OXPHOS complexes in the IMM [33,35] and different energetic demands of tissues when compared with cells that lead to a higher probability of CII uptake into larger structures in the tissue mitochondria. Importantly, the observed differences between cells and tissues in CII_{hmw} size and stability as well as their dependence on mtDNA depletion, support the view that they reflect biological properties of complex II and do not represent an artefact of CNE electrophoresis.

When assessing the stability of CII_{hmw} complexes, we detected the CII_{hmw} as the dominant structural form of CII in digitonin solubilisates under the CNE separation conditions. The presence of either detergents (n-dodecyl-β-D-maltoside, deoxycholic acid) or CBG in the running buffer, i.e. conditions usually used to achieve better separation and resolution in the hrCNE and BNE electrophoretic systems, readily dissociated CII_{hmw} in both cells and tissues to CII monomers and individual subunits. Even the very low CBG concentration added to the sample (0.02%, 50-fold less than used in BNE samples) was sufficient for the complete CII_{hmw} dissociation. Similarly, incubation of the CNE gel slice with separated CII_{hmw} in a CBG solution also caused a partial dissociation of the CII_{hmw} structures, mainly in cultured cells. The addition of CBG to the

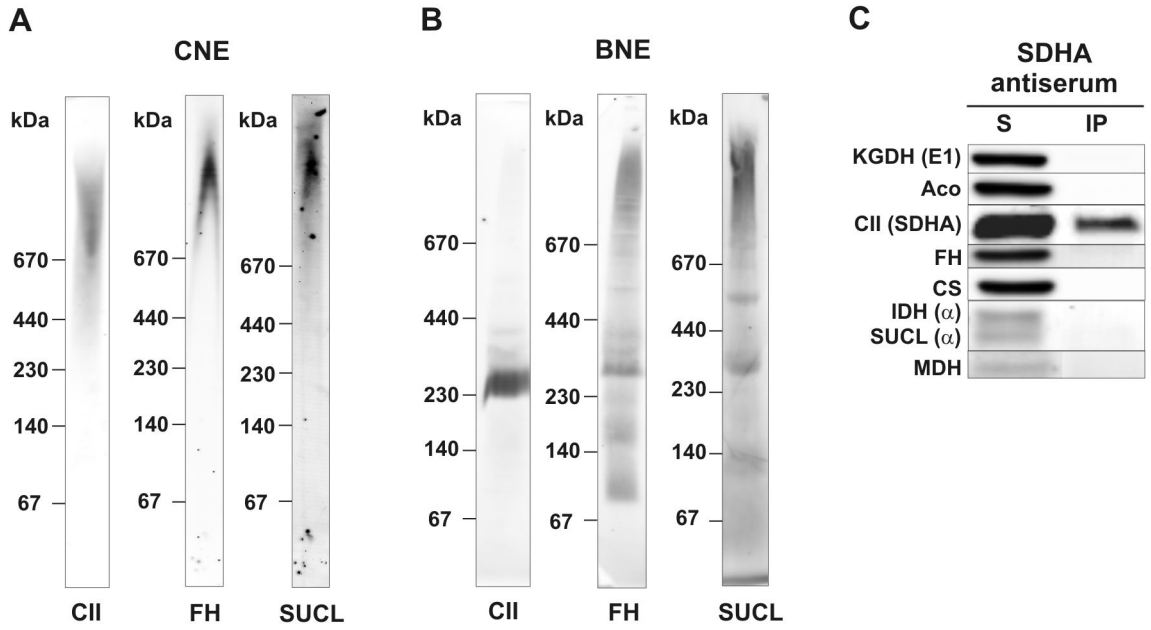

Figure 8. CII does not associate with other components of TCA cycle. (A) Mitochondrial membrane proteins from rat heart were solubilised with digitonin (4 g/g protein) and 20 µg protein aliquots separated using CNE. SDHA subunit of CII (CII), fumarase (FH) and subunit α of succinyl-CoA synthetase (SUCL) were detected with specific antibodies. (B) After digitonin solubilisation of mitochondria from rat heart, CII was immunoprecipitated with anti-SDHA antibody (SDHA antiserum). Proteins in the immunoprecipitate (IP) and solubilisate (S) were separated by SDS PAGE and analysed for the presence of individual components of the TCA cycle: α-ketoglutarate dehydrogenase subunit E1, KGDH (E1); aconitase, Aco; CII, SDHA; fumarase, FH; citrate synthase, CS; isocitrate dehydrogenase subunit α, IDH (α); succinyl-CoA synthetase (subunit α), SUCL (α); malate dehydrogenase, MDH.

doi: 10.1371/journal.pone.0071869.g008

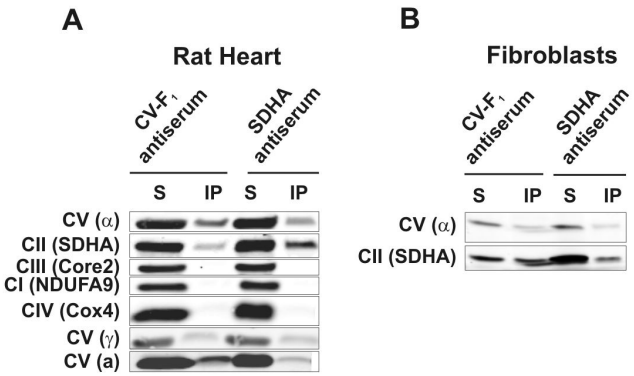

Figure 7. CII and CV co-immunoprecipitates. After digitonin solubilisation of mitochondria from the rat heart (A) and human fibroblasts (B), CV was immunoprecipitated with antibodies to its F_1 part and CII with anti-SDHA. Proteins in the immunoprecipitate (IP) and solubilisate (S) were separated by SDS PAGE and individual subunits of OXPHOS complexes detected as indicated with antibodies to CI, NDUFA9; CII, SDHA; CIII, Core2; CIV, Cox4; CV, α, γ, a.

doi: 10.1371/journal.pone.0071869.g007

sample/solution induces a dissociation effect by binding of the dye to proteins surface and introduction of a negative charge that can affect intermolecular interactions. Apparently, this process is more effective in solution than in the gel slice.

To understand the CII_{hmw} function, it is important to define CII interaction partners in CII_{hmw}. The most obvious candidates would be other OXPHOS complexes, but the putative presence of CII in the SCs with other OXPHOS complexes is still a matter of discussion. For example, single particle electron microscopy and X-ray imaging structural studies seem to contradict such idea [36,37]. These methods did not reveal the presence of CII in any type of SCs. It should be noted, though, that due to its relatively small size, CII may simply be below the detection limit of these techniques. Similarly, studies of the assembly kinetics of the CI+CIII+CIV SC did not reveal any participation of CII in this process [38]. On the other hand, at least some immunocapture and electrophoretic experiments demonstrated the existence of a large respirasome comprising respiratory chain complexes, including CII, as well as mobile electron carriers [17]. We therefore attempted to find any indication of the interaction between CII and other OXPHOS complexes. CNE analysis and in-gel activity staining in CNE gels pointed to a possible interaction with CIV or CV, but due to the low resolution of protein bands in the CNE gels it is hard to interpret this as genuine interactions. In the MW range 400–

670 kDa where CII_{hmw} are found in the cells, many other protein complexes and small SCs migrate. It is more likely that CII_{hmw} represents CII oligomers co-migrating with CV or CIV_D, as incorporation of CII into other complexes migrating in this range would require a shift in the electrophoretic mobility of the resulting SCs towards MW greater by at least 140 kDa, i.e. the molecular weight of the CII monomer. On the other hand, CII_{hmw} in the tissues with size over 1 MDa may represent CII as a part of OXPHOS SCs.

In another attempt to detect specific OXPHOS interacting partner(s) for CII, we studied cell lines with both isolated and combined deficiencies of OXPHOS complexes. With one of the interaction partners missing, the CII_{hmw} signal would be decreased or undetectable in the respective cell line. Such interdependency is well described for canonical OXPHOS SCs [12,17,38]. However, in our experiments, the levels and position of CII_{hmw} appear to be unchanged in cells with isolated defects of CI, CIV or CV, presenting additional evidence that no stable interaction is formed between CII and other OXPHOS complexes. On the other hand, when we analysed ρ^0 cells lacking mtDNA, unassembled subunits predominated over the CII monomer, and the CII_{hmw} structures were almost absent. The absence of the mtDNA-encoded subunits impedes the assembly and function of OXPHOS in ρ^0 cells [39]. Because CII is entirely encoded by the nuclear DNA, it was considered to be unchanged, but a recent study by Mueller et al. [40] reports a decreased level of CII with its activity reduced to 12%. Although the synthesis of the nuclear encoded subunits is unaffected in ρ^0 cells, mitochondrial protein import is disturbed as a consequence of decreased levels of ATP and the Tim44 protein, an essential effector of mitochondrial protein import [41]. Our experiments suggest that the CII and CII_{hmw} assembly depends on fully active mitochondria and the OXPHOS complexes of the IMM.

Immunoprecipitation was another independent approach we used to detect possible CII interaction partners. Here we identified CV as a plausible interaction partner of CII both in cultured cells and tissues. Generally, immunoprecipitation is more sensitive and selective than electrophoresis and can reveal rather weak interactions. Based on our experiments, we can conclude that CII, at least partially, co-immunoprecipitates with CV, constituting possibly a part of the mitoK$_{ATP}$ channel described in recent studies. Although the role for CII in mitoK$_{ATP}$ remains elusive, it was shown that SDH inhibitors modulate the channel activity and subsequently the process of ischemic preconditioning [18,42]. Only 0.4% of the CII present in mitochondria is necessary to activate the mitoK$_{ATP}$ and the inhibition of such a small portion of CII has no effect on the overall CII activity in OXPHOS [43]. The interaction of CII with CV is also not in conflict with our results with ρ^0 cells, as CV is assembled in ρ^0 cells, except for the two mtDNA-encoded subunits, ATP6 and ATP8 [44]. Such form of CV (lacking the two subunits) is sufficient for the survival of ρ^0 cells as it can hydrolyse ATP produced by glycolysis and allow for the maintenance of the transmembrane H^+ gradient by the electrogenic exchange of ATP for ADP by adenine nucleotide translocator [45,46].

An attractive proposal may be that CII may interact with other proteins from the TCA cycle, forming an organised multi-enzyme cluster. As the only membrane bound component of the TCA metabolism, CII would represent an anchor for the docking of TCA metabolism to the IMM into the spatial proximity of OXPHOS, in accordance with the known association of soluble TCA cycle enzymes with the mitochondrial membrane [47]. The existence of the metabolon composed of at least several TCA cycle proteins has been suggested [47,48]. However, most of the evidence points to the interactions of malate dehydrogenase, citrate synthase and, potentially, aconitase [19,20]. To date, no interaction involving CII has been demonstrated. Native electrophoretic systems represent a plausible model to study such interactions; although they involve solubilisation of membrane proteins by detergents, the solubilisates of whole mitochondria contain also matrix proteins. Naturally, any such interactions may be disrupted during the analysis. Here, crosslinking may help to capture such interactions in the future studies. Despite the fact that we did not identify any interacting partners for CII among the tested TCA cycle proteins, this deserves additional work as such interactions would appear functionally plausible.

It is possible that interactions of CII other than the one detected with CV do exist, and that such interactions may not even necessarily involve the whole of CII. For example, Gebert et al. [49] have published that the Sdh3 subunit of yeast CII (SDHC in mammals) has a dual function in mitochondria. It acts as a structural and functional subunit of CII and also plays a role in the biogenesis and assembly of the TIM22 complex via a direct interaction between Sdh3 and Tim18. Therefore, we cannot exclude that other CII subunits would have specific functions outside of the OXPHOS system. Notwithstanding these potential interactions of CII, our data lead to the conclusion that CII does form high molecular weight assemblies, but these structures are unlikely to represent traditional respiratory supercomplexes with CI, CIII and CIV as proposed previously by Acin-Perez et al. [17]. At least, some of these interactions are complexes with CV where CII plays a role as a regulatory component of mitoK$_{ATP}$ channel [42]. To summarise, our findings are consistent with the emerging notion that the individual OXPHOS complexes, or they subunits, have a role that may go beyond direct involvement in the mitochondrial bioenergetics.

Author Contributions

Conceived and designed the experiments: NK TM HN JN JH. Performed the experiments: NK TM HN EH. Analyzed the data: NK TM HN EH MV PP JH. Contributed reagents/materials/analysis tools: KH KK JR. Wrote the manuscript: NK TM PP JN JH.

References

1. Cecchini G (2003) Function and structure of complex II of the respiratory chain. Annu Rev Biochem 72: 77-109. doi:10.1146/annurev.biochem.72.121801.161700. PubMed: 14527321.
2. Sun F, Huo X, Zhai YJ, Wang AJ, Xu JX et al. (2005) Crystal structure of mitochondrial respiratory membrane protein complex II. Cell 121: 1043-1057. doi:10.1016/j.cell.2005.05.025. PubMed: 15989954.
3. Brière JJ, Favier J, El Ghouzzi V, Djouadi F, Bénit P et al. (2005) Succinate dehydrogenase deficiency in human. Cell Mol Life Sci 62: 2317-2324. doi:10.1007/s00018-005-5237-6. PubMed: 16143825.
4. Bardella C, Pollard PJ, Tomlinson I (2011) SDH mutations in cancer. Biochim Biophys Acta 1807: 1432-1443. doi:10.1016/j.bbabio.2011.07.003. PubMed: 21771581.
5. Burnichon N, Brière JJ, Libé R, Vescovo L, Rivière J et al. (2010) SDHA is a tumor suppressor gene causing paraganglioma. Hum Mol Genet 19: 3011-3020. doi:10.1093/hmg/ddq206. PubMed: 20484225.
6. Perry CG, Young WF Jr, McWhinney SR, Bei T, Stergiopoulos S et al. (2006) Functioning paraganglioma and gastrointestinal stromal tumor of the jejunum in three women: syndrome or coincidence. Am J Surg Pathol 30: 42-49. doi:10.1097/01.pas.0000178087.69394.9f. PubMed: 16330941.
7. Ricketts C, Woodward ER, Killick P, Morris MR, Astuti D et al. (2008) Germline SDHB mutations and familial renal cell carcinoma. J Natl Cancer Inst 100: 1260-1262. doi:10.1093/jnci/djn254. PubMed: 18728283.
8. Kluckova K, Bezawork-Geleta A, Rohlena J, Dong L, Neuzil J (2013) Mitochondrial complex II, a novel target for anti-cancer agents. Biochim Biophys Acta 1827: 552-564. doi:10.1016/j.bbabio.2012.10.015. PubMed: 23142170.
9. Ghezzi D, Goffrini P, Uziel G, Horvath R, Klopstock T et al. (2009) SDHAF1, encoding a LYR complex-II specific assembly factor, is mutated in SDH-defective infantile leukoencephalopathy. Nat Genet 41: 654-656. doi:10.1038/ng.378. PubMed: 19465911.
10. Shi YB, Ghosh MC, Tong WH, Rouault TA (2009) Human ISD11 is essential for both iron-sulfur cluster assembly and maintenance of normal cellular iron homeostasis. Hum Mol Genet 18: 3014-3025. doi: 10.1093/hmg/ddp239. PubMed: 19454487.
11. Hao HX, Khalimonchuk O, Schraders M, Dephoure N, Bayley JP et al. (2009) SDH5, a gene required for flavination of succinate dehydrogenase, is mutated in paraganglioma. Science 325: 1139-1142. doi:10.1126/science.1175689. PubMed: 19628817.
12. Bianchi C, Genova ML, Parenti Castelli G, Lenaz G (2004) The mitochondrial respiratory chain is partially organized in a supercomplex assembly: kinetic evidence using flux control analysis. J Biol Chem 279: 36562-36569. doi:10.1074/jbc.M405135200. PubMed: 15205457.
13. Shibata N, Kobayashi M (2008) The role for oxidative stress in neurodegenerative diseases. Brain Nerve 60: 157-170. PubMed: 18306664.
14. Strauss M, Hofhaus G, Schröder RR, Kühlbrandt W (2008) Dimer ribbons of ATP synthase shape the inner mitochondrial membrane. EMBO J 27: 1154-1160. doi:10.1038/emboj.2008.35. PubMed: 18323778.
15. Schägger H, Pfeiffer K (2000) Supercomplexes in the respiratory chains of yeast and mammalian mitochondria. EMBO J 19: 1777-1783. doi:10.1093/emboj/19.8.1777. PubMed: 10775262.
16. Wittig I, Schägger H (2009) Native electrophoretic techniques to identify protein-protein interactions. Proteomics 9: 5214-5223. doi:10.1002/pmic.200900151. PubMed: 19834896.
17. Acín-Pérez R, Fernández-Silva P, Peleato ML, Pérez-Martos A, Enriquez JA (2008) Respiratory active mitochondrial supercomplexes. Mol Cell 32: 529-539. doi:10.1016/j.molcel.2008.10.021. PubMed: 19026783.
18. Ardehali H, Chen Z, Ko Y, Mejía-Alvarez R, Marbán E (2004) Multiprotein complex containing succinate dehydrogenase confers mitochondrial ATP-sensitive K+ channel activity. Proc Natl Acad Sci U S A 101: 11880-11885. doi:10.1073/pnas.0401703101. PubMed: 15284438.
19. Meyer FM, Gerwig J, Hammer E, Herzberg C, Commichau FM et al. (2011) Physical interactions between tricarboxylic acid cycle enzymes in Bacillus subtilis: evidence for a metabolon. Metab Eng 13: 18-27. doi: 10.1016/j.ymben.2010.10.001. PubMed: 20933603.
20. Vélot C, Mixon MB, Teige M, Srere PA (1997) Model of a quinary structure between Krebs TCA cycle enzymes: a model for the metabolon. Biochemistry 36: 14271-14276. doi:10.1021/bi972011j. PubMed: 9400365.
21. Kovářová N, Cížková Vrbacká A, Pecina P, Stránecký V, Pronicka E et al. (2012) Adaptation of respiratory chain biogenesis to cytochrome c oxidase deficiency caused by SURF1 gene mutations. Biochim Biophys Acta 1822: 1114-1124. doi:10.1016/j.bbadis.2012.03.007. PubMed: 22465034.
22. Piekutowska-Abramczuk D, Magner M, Popowska E, Pronicki M, Karczmarewicz E et al. (2009) SURF1 missense mutations promote a mild Leigh phenotype. Clin Genet 76: 195-204. doi:10.1111/j.1399-0004.2009.01195.x. PubMed: 19780766.
23. Honzík T, Tesarová M, Mayr JA, Hansíková H, Jesina P et al. (2010) Mitochondrial encephalocardio-myopathy with early neonatal onset due to TMEM70 mutation. Arch Dis Child 95: 296-301. doi:10.1136/adc.2009.168096. PubMed: 20335238.
24. King MP, Attardi G (1996) Isolation of human cell lines lacking mitochondrial DNA. Methods Enzymol 264: 304-313. doi:10.1016/S0076-6879(96)64029-4. PubMed: 8965704.
25. Bentlage HA, Wendel U, Schägger H, ter Laak HJ, Janssen AJ et al. (1996) Lethal infantile mitochondrial disease with isolated complex I deficiency in fibroblasts but with combined complex I and IV deficiencies in muscle. Neurology 47: 243-248. doi:10.1212/WNL.47.1.243. PubMed: 8710086.
26. Wittig I, Braun HP, Schägger H (2006) Blue native PAGE. Nat Protoc 1: 418-428. doi:10.1038/nprot.2006.62. PubMed: 17406264.
27. Mrácek T, Pecinová A, Vrbacký M, Drahota Z, Houstek J (2009) High efficiency of ROS production by glycerophosphate dehydrogenase in mammalian mitochondria. Arch Biochem Biophys 481: 30-36. doi: 10.1016/j.abb.2008.10.011. PubMed: 18952046.
28. Wittig I, Karas M, Schägger H (2007) High resolution clear native electrophoresis for in-gel functional assays and fluorescence studies of membrane protein complexes. Mol Cell Proteomics 6: 1215-1225. doi: 10.1074/mcp.M700076-MCP200. PubMed: 17426019.
29. Schägger H, von Jagow G (1987) Tricine-sodium dodecyl sulfate-polyacrylamide gel electrophoresis for the separation of proteins in the range from 1 to 100 kDa. Anal Biochem 166: 368-379. doi: 10.1016/0003-2697(87)90587-2. PubMed: 2449095.
30. Moradi-Ameli M, Godinot C (1983) Characterization of monoclonal antibodies against mitochondrial F1-ATPase. Proc Natl Acad Sci U S A 80: 6167-6171. doi:10.1073/pnas.80.20.6167. PubMed: 6194526.
31. Wittig I, Schägger H (2005) Advantages and limitations of clear-native PAGE. Proteomics 5: 4338-4346. doi:10.1002/pmic.200500081. PubMed: 16220535.
32. Ko YH, Delannoy M, Hullihen J, Chiu W, Pedersen PL (2003) Mitochondrial ATP synthasome. Cristae-enriched membranes and a multiwell detergent screening assay yield dispersed single complexes containing the ATP synthase and carriers for Pi and ADP/ATP. J Biol Chem 278: 12305-12309. doi:10.1074/jbc.C200703200. PubMed: 12560333.
33. Lenaz G, Genova ML (2012) Supramolecular organisation of the mitochondrial respiratory chain: a new challenge for the mechanism and control of oxidative phosphorylation. Adv Exp Med Biol 748: 107-144. doi:10.1007/978-1-4614-3573-0_5. PubMed: 22729856.
34. Rosca M, Minkler P, Hoppel CL (2011) Cardiac mitochondria in heart failure: normal cardiolipin profile and increased threonine phosphorylation of complex IV. Biochim Biophys Acta 1807: 1373-1382. doi:10.1016/j.bbabio.2011.02.003. PubMed: 21320465.
35. Benard G, Faustin B, Passerieux E, Galinier A, Rocher C et al. (2006) Physiological diversity of mitochondrial oxidative phosphorylation. Am J Physiol Cell Physiol 291: C1172-C1182. doi:10.1152/ajpcell.00195.2006. PubMed: 16807301.
36. Dudkina NV, Eubel H, Keegstra W, Boekema EJ, Braun HP (2005) Structure of a mitochondrial supercomplex formed by respiratory-chain complexes I and III. Proc Natl Acad Sci U S A 102: 3225-3229. doi: 10.1073/pnas.0408870102. PubMed: 15713802.
37. Schäfer E, Seelert H, Reifschneider NH, Krause F, Dencher NA et al. (2006) Architecture of active mammalian respiratory chain supercomplexes. J Biol Chem 281: 15370-15375. doi:10.1074/jbc.M513525200. PubMed: 16551638.
38. Moreno-Lastres D, Fontanesi F, García-Consuegra I, Martín MA, Arenas J et al. (2012) Mitochondrial complex I plays an essential role in human respirasome assembly. Cell Metab 15: 324-335. doi:10.1016/j.cmet.2012.01.015. PubMed: 22342700.
39. Chevallet M, Lescuyer P, Diemer H, van Dorsselaer A, Leize-Wagner E et al. (2006) Alterations of the mitochondrial proteome caused by the absence of mitochondrial DNA: A proteomic view. Electrophoresis 27: 1574-1583. doi:10.1002/elps.200500704. PubMed: 16548050.
40. Mueller EE, Mayr JA, Zimmermann FA, Feichtinger RG, Stanger O et al. (2012) Reduction of nuclear encoded enzymes of mitochondrial energy metabolism in cells devoid of mitochondrial DNA. Biochem Biophys Res Commun 417: 1052-1057. doi:10.1016/j.bbrc.2011.12.093. PubMed: 22222373.

41. Mercy L, Pauw Ad, Payen L, Tejerina S, Houbion A et al. (2005) Mitochondrial biogenesis in mtDNA-depleted cells involves a Ca2+-dependent pathway and a reduced mitochondrial protein import. FEBS J 272: 5031-5055. doi:10.1111/j.1742-4658.2005.04913.x. PubMed: 16176275.
42. Wojtovich AP, Smith CO, Haynes CM, Nehrke KW, Brookes PS (2013) Physiological consequences of complex II inhibition for aging, disease, and the mKATP channel. Biochim Biophys Acta 1827: 598-611. doi: 10.1016/j.bbabio.2012.12.007. PubMed: 23291191.
43. Wojtovich AP, Nehrke KW, Brookes PS (2010) The mitochondrial complex II and ATP-sensitive potassium channel interaction: quantitation of the channel in heart mitochondria. Acta Biochim Pol 57: 431-434. PubMed: 21103454.
44. Carrozzo R, Wittig I, Santorelli FM, Bertini E, Hofmann S et al. (2006) Subcomplexes of human ATP synthase mark mitochondrial biosynthesis disorders. Ann Neurol 59: 265-275. doi:10.1002/ana.20729. PubMed: 16365880.
45. Buchet K, Godinot C (1998) Functional F1-ATPase essential in maintaining growth and membrane potential of human mitochondrial DNA-depleted rho degrees cells. J Biol Chem 273: 22983-22989. doi: 10.1074/jbc.273.36.22983. PubMed: 9722521.
46. García JJ, Ogilvie I, Robinson BH, Capaldi RA (2000) Structure, functioning, and assembly of the ATP synthase in cells from patients with the T8993G mitochondrial DNA mutation. Comparison with the enzyme in Rho(0) cells completely lacking mtdna. J Biol Chem 275: 11075-11081. doi:10.1074/jbc.275.15.11075. PubMed: 10753912.
47. Robinson JB Jr, Inman L, Sumegi B, Srere PA (1987) Further characterization of the Krebs tricarboxylic acid cycle metabolon. J Biol Chem 262: 1786-1790. PubMed: 2433288.
48. Haggie PM, Verkman AS (2002) Diffusion of tricarboxylic acid cycle enzymes in the mitochondrial matrix in vivo. Evidence for restricted mobility of a multienzyme complex. J Biol Chem 277: 40782-40788. doi:10.1074/jbc.M207456200. PubMed: 12198136.
49. Gebert N, Gebert M, Oeljeklaus S, von der Malsburg K, Stroud DA et al. (2011) Dual function of Sdh3 in the respiratory chain and TIM22 protein translocase of the mitochondrial inner membrane. Mol Cell 44: 811-818. doi:10.1016/j.molcel.2011.09.025. PubMed: 22152483.

Human Molecular Genetics, 2010, Vol. 19, No. 17 **3430–3439**
doi:10.1093/hmg/ddq254
Advance Access published on June 21, 2010

Mitochondrial ATP synthase deficiency due to a mutation in the *ATP5E* gene for the F_1 ε subunit

Johannes A. Mayr[1], Vendula Havlíčková[2], Franz Zimmermann[1], Iris Magler[1], Vilma Kaplanová[2], Pavel Ješina[2], Alena Pecinová[2], Hana Nůsková[2], Johannes Koch[1], Wolfgang Sperl[1] and Josef Houštěk[2,*]

[1]Department of Pediatrics, Paracelsus Medical University, Salzburg A5020, Austria and [2]Department of Bioenergetics, Institute of Physiology, Centre of Applied Genomics, Academy of Sciences of the Czech Republic, Prague 142 20, Czech Republic

Received May 7, 2010; Revised and Accepted June 15, 2010

F_1F_o-ATP synthase is a key enzyme of mitochondrial energy provision producing most of cellular ATP. So far, mitochondrial diseases caused by isolated disorders of the ATP synthase have been shown to result from mutations in mtDNA genes for the subunits ATP6 and ATP8 or in nuclear genes encoding the biogenesis factors TMEM70 and ATPAF2. Here, we describe a patient with a homozygous p.Tyr12Cys mutation in the ε subunit encoded by the nuclear gene *ATP5E*. The 22-year-old woman presented with neonatal onset, lactic acidosis, 3-methylglutaconic aciduria, mild mental retardation and developed peripheral neuropathy. Patient fibroblasts showed 60–70% decrease in both oligomycin-sensitive ATPase activity and mitochondrial ATP synthesis. The mitochondrial content of the ATP synthase complex was equally reduced, but its size was normal and it contained the mutated ε subunit. A similar reduction was found in all investigated F_1 and F_o subunits with the exception of F_o subunit c, which was found to accumulate in a detergent-insoluble form. This is the first case of a mitochondrial disease due to a mutation in a nuclear encoded structural subunit of the ATP synthase. Our results indicate an essential role of the ε subunit in the biosynthesis and assembly of the F_1 part of the ATP synthase. Furthermore, the ε subunit seems to be involved in the incorporation of subunit c to the rotor structure of the mammalian enzyme.

INTRODUCTION

Mitochondrial diseases caused by inborn defects in the mitochondrial ATP synthase (F_1F_o-ATP synthase, complex V) have been found less frequently than defects of the respiratory chain complexes; they are severe and affect predominantly the pediatric population (1).

The mitochondrial ATP synthase is a multisubunit complex composed of 16 different subunits (2) that form the globular, catalytic F_1 part connected by two stalks with the proton-translocating, membrane-spanning F_o part. Two subunits from the F_o part are encoded by the mitochondrial genome, subunits a and A6L (subunits 6 and 8) (3), whereas all the other ATP synthase subunits are encoded by nuclear genes. In addition, several other nuclear encoded proteins are specifically involved in the function and biogenesis of this enzyme. ATP synthase is regulated by the coupling factor B (4); two associated proteins MLQ (C14orf2) and AGP (5) are possibly involved in the formation of ATP synthase dimers and at least four other proteins, ATPAF1 (ATP11), ATPAF2 (ATP12), ATP23 and TMEM70, are supposed to take part in the biosynthesis and assembly of ATP synthase (6–9).

Mutations in both genomes were found to be responsible for different types of ATP synthase disorders. Maternally transmitted dysfunction of ATP synthase, known since 1990 (10), is mainly caused by mtDNA missense mutations in the *ATP6* gene (subunit a) (11). Several mutations of varying pathogenicity were described (see www.mitomap.org) to alter the function of the F_o proton channel and to result in the loss of ATP synthetic activity, whereas the hydrolytic activity and the amount of the enzyme are mostly retained.

*To whom correspondence should be addressed at: Department of Bioenergetics, Institute of Physiology, Academy of Sciences of the Czech Republic, Vídeňská 1083, 142 20 Prague 4, Czech Republic. Tel: +420 241062434; Fax: +420 241062149; Email: houstek@biomed.cas.cz

Patients present with neuropathy, ataxia, retinitis pigmentosa, maternally inherited Leigh syndrome, or bilateral striatal necrosis (11). More rarely, ATP synthase dysfunction can be caused by the lack of ATP6 protein due to altered processing of polycistronic *ATP8/ATP6/COX3* transcript (12,13) or by a mutation in the *ATP8* gene (14).

A distinct group of inborn defects of ATP synthase is represented by the enzyme deficiency due to nuclear genome mutations characterized by a selective inhibition of ATP synthase biogenesis (15). Biochemically, the patients show a generalized decrease in the content of ATP synthase complex which is <30% of the control. The insufficient ATP synthase phosphorylating capacity with respect to the respiratory chain results in an impaired energy provision and an increased ROS production due to an elevated mitochondrial membrane potential (1,16). The isolated ATP synthase deficiency appears to be a rather frequent mitochondrial disease, and more than 40 patients are known today. Most cases present with neonatal-onset hypotonia, lactic acidosis, hyperammonemia, hypertrophic cardiomyopathy, and 3-methylglutaconic aciduria. About a half of the patients die within few months or years (17–20). Since the demonstration of the nuclear gene involvement by cybrid complementation in 1999, pathogenic mutations were found in two genes, both coding for ancillary factors of ATP synthase biogenesis. In 2004, the first genetic defect was described in *ATPAF2* (*ATP12*), coding for a specific assembly factor of F_1 subunit α (21). The patient was homozygous for TGG-AGG missense mutation in exon 3 changing Trp94 to Arg, and presented with degenerative encephalopathy characterized by cortical and subcortical atrophy. Interestingly, this phenotype of marked brain atrophy differed significantly from other patients who lacked the *ATPAF2* mutation and presented with cardiomyopathy (18). In 2008, the expression profiling and homozygosity mapping identified a mutation in the second intron of *TMEM70* encoding a 30 kDa mitochondrial protein of unknown function, and ATP synthase-deficient patient fibroblasts were complemented by the wild-type TMEM70 protein (19). This protein turned out to be a novel ancillary factor of ATP synthase biosynthesis, interestingly, the first one specific for higher eukaryotes. The homozygous *TMEM70* c.317-2A>G mutation leading to aberrant splicing and to a loss of *TMEM70* transcript was found in 24 patients, and an additional patient was compound heterozygous for the c.317-2A>G and c.118_119insGT frameshift mutations (19). Since then, the *TMEM70* mutations were found in several other cases, constituting the most frequent cause of ATP synthase deficiency (20,22).

Nevertheless, one of the patients we analyzed had a distinct clinical phenotype of early-onset lactic acidosis, 3-methylglutaconic aciduria, no cardiac involvement, mild mental retardation, development of a severe peripheral neuropathy and survival to adulthood. In this case, neither *TMEM70* nor *ATPAF2* were affected, indicating the presence of a different genetic defect (P3 in reference 19).

RESULTS

Low ATP synthase activity in patient fibroblasts

As stated in our previous reports (18,23), the mitochondria of patient fibroblasts showed a normal activity of respiratory chain enzymes, but a decreased activity of mitochondrial ATP synthase (Table 1). A further analysis of patient fibroblasts showed a pronounced decrease of ATP synthase hydrolytic activity sensitive to oligomycin and aurovertin (67 and 77% decrease with respect to the control, respectively) (Fig. 1A). Likewise, the mitochondrial synthesis of ATP in the digitonin-permeabilized cells supplemented with ADP and respiratory substrates, using either pyruvate and malate or succinate, was decreased by 74 and 71% compared with the control, respectively (Fig. 1B). Therefore, a similar decrease in the synthetic and hydrolytic activity of ATP synthase was observed in the patient fibroblasts. Both types of measurements fully confirmed the presence of isolated defect of mitochondrial ATP synthase.

Table 1. Respiratory chain enzyme activities in frozen mitochondria isolated from the patient and control fibroblasts

Enzyme activities (mU/mg protein)	Patient	Controls
Citrate synthase	335	225–459
Complex I	16	15–52
Complex I + III	123	73–279
Complex II	98	64–124
Complex II + III	142	137–267
Complex III	861	208–648
Complex IV	370	202–403
Oligomycin-sensitive ATPase	<10	43–190

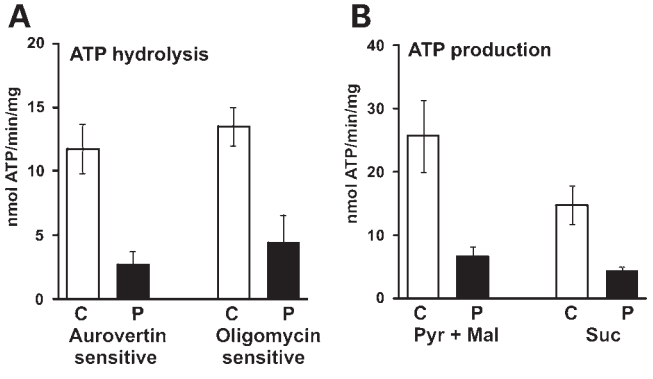

Figure 1. ATP synthase hydrolytic and synthetic activity. (**A**) Oligomycin- and aurovertin-sensitive hydrolysis was determined in the frozen/thawed fibroblasts. (**B**) ATP synthesis was measured in the digitonin-permeabilized fibroblasts supplied with respiratory substrates pyruvate (Pyr) + malate (Mal) or succinate (Suc). Values represent mean ± SD of four experiments, in control (C) and patient (P) cells.

Changes in cellular respiration and mitochondrial membrane potential

Respirometric measurements in the permeabilized patient fibroblasts supplemented with the combination of substrates glutamate, malate and succinate showed a pronounced decrease in the rate of ADP-stimulated respiration, although there was no apparent difference in FCCP-stimulated respiration compared with the control fibroblasts (Fig. 2A).

Cytofluorometric analysis of mitochondrial membrane potential ($\Delta\Psi_m$) in the permeabilized fibroblasts using tetramethylrhodamine methylester (TMRM) (Fig. 2B) revealed

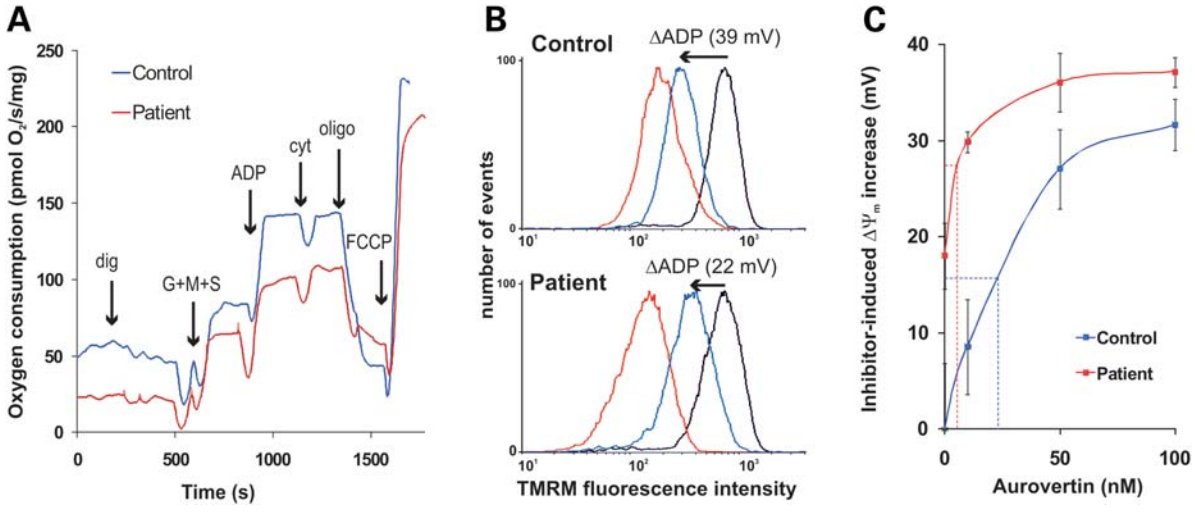

Figure 2. Respiration and mitochondrial membrane potential. (**A**) In the digitonin-permeabilized control (blue line) and patient (red line) fibroblasts, respiration with glutamate, malate and succinate (G + M + S) was measured in the presence of ADP, cytochrome *c* (cyt), oligomycin (oligo) and FCCP, as indicated. (**B**) Mitochondrial membrane potential ($\Delta\Psi_m$) was analyzed by TMRM cytofluorometry in the digitonin-permeabilized fibroblasts supplied with succinate (state 4, black line), after the addition of ADP (state 3-ADP, blue line) or FCCP (state 3-uncoupled, red line). (**C**) $\Delta\Psi_m$ at state 3-ADP was reversed back to state 4 by the inhibition of ATP synthase with aurovertin. Data show a titration with aurovertin in the control (blue line) and patient (red line) fibroblasts; the concentration of inhibitor for a 50% reversal is indicated.

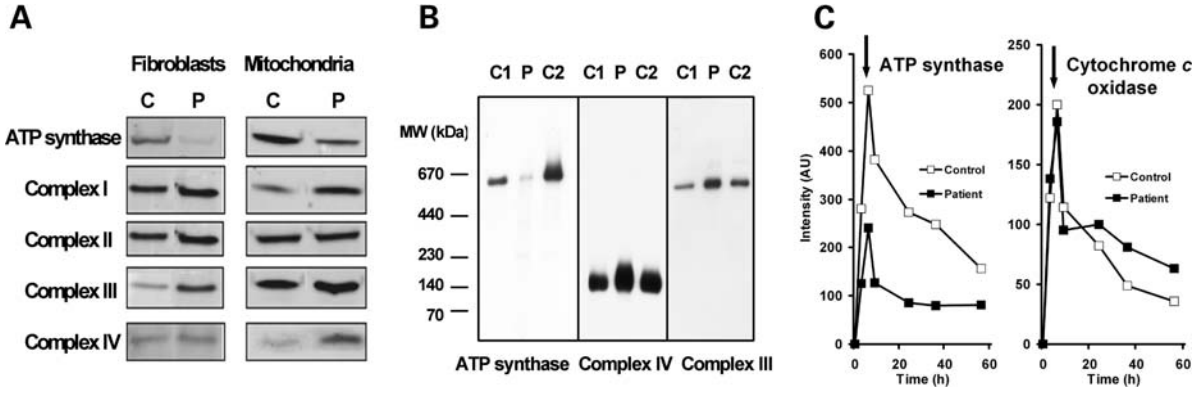

Figure 3. Specific content, size and biosynthesis of ATP synthase. (**A**) SDS–PAGE and WB analysis of ATP synthase and respiratory chain complexes in the control (C) and patient (P) fibroblasts (12 μg protein aliquots) and isolated mitochondria (3 μg protein aliquots), using antibodies to ATP synthase (F_1 α subunit), complex I (NDUFA9 subunit), complex II (SDH 70 kDa subunit), complex III (core 1 subunit) and complex IV (COX4 subunit). (**B**) BN-PAGE and WB analysis of DDM (1 g/g protein) solubilized proteins (10 μg protein aliquots) from the control (C1,C2) and patient (P) fibroblasts mitochondria, using antibodies to ATP synthase (F_1 α subunit), complex III (core1 subunit) and complex IV (COX1 subunit). The mobility of MW standards is shown on the left. (**C**) Metabolic labeling of ATP synthase and COX in cultivated fibroblasts. Fibroblasts were pulse-labeled with ^{35}S-methionine for 6 h and then chased with cold methionine (arrow). At the indicated times, the proteosynthesis was stopped by chloramphenicol and cycloheximide and mitoplasts isolated from the harvested cells were solubilized with DDM and subjected to 2D BN/SDS–PAGE. The radioactivity was quantified in assembled ATP synthase (subunits F_1 α + β) and COX (subunits COX2 + COX3 + COX4).

similar values of $\Delta\Psi_m$ at state 4 in the patient and control fibroblasts. In contrast (Fig. 2B), there was a much smaller decrease of $\Delta\Psi_m$ after an addition of ADP (i.e. at state 3-ADP) in the patient cells (20.29 ± 3.43 and 38.31 ± 6.85 mV in patient and controls, respectively), when mitochondria phosphorylate the added ADP at the expense of $\Delta\Psi_m$. In both patient and control cells, the inhibition of ATP synthase by aurovertin (or oligomycin) fully restored the $\Delta\Psi_m$ to the state 4 values. However, the titration of $\Delta\Psi_m$ at state 3-ADP with aurovertin showed a several-fold higher sensitivity of patient fibroblasts (Fig. 2C). Thus, all these functional measurements indicate that the patient cells possess an insufficient capacity of ATP synthase in relation to the capacity of respiratory chain.

Decreased content of ATP synthase complex

To determine the protein amount of ATP synthase and respiratory chain enzymes, SDS–polyacrylamide gel electrophoresis (PAGE) and western blot (WB) analysis was performed in both fibroblasts and isolated mitochondria. As shown in Fig. 3A, there was a pronounced decrease of ATP synthase

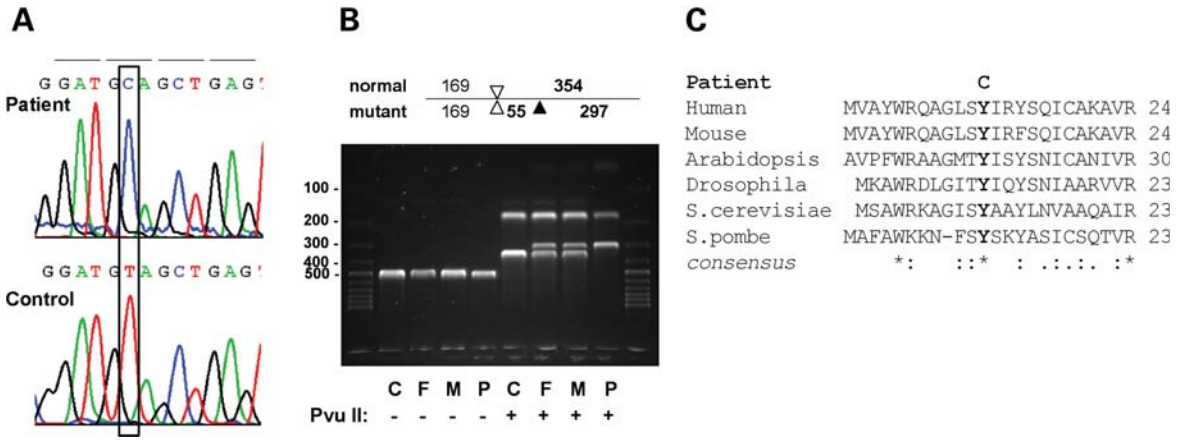

Figure 4. Presence of missense mutation c.35A>G in exon 2 of *ATP5E*, which leads to the amino acid exchange p.Tyr12Cys in the N-terminal conserved region of the subunit ε of ATP synthase. (**A**) Sequence analysis of the reverse complement cDNA of the patient (upper panel) and a control (lower panel). (**B**) RFLP analysis of genomic DNA isolated from the fibroblasts of control (C), father (F), mother (M) and patient (P). (**C**) Sequence alignment of the subunit ε from different organisms shows high conservation of the tyrosine 12 of the human protein.

F_1 α subunit content in the fibroblast homogenate corresponding to 70% reduction of the content of ATP synthase complex. The immunodetection of respiratory chain complexes with subunit-specific antibodies revealed a normal or increased content of the respiratory chain complexes I, II, III and IV corresponding to 100–150% of the control values. Analogous changes were observed in the isolated mitochondria (Fig. 3A) in accordance with the enzyme activity values (Table 1). Apparently, the observed biochemical changes are caused by an isolated decrease of the ATP synthase complex content, whereas the content of mitochondrial respiratory chain enzymes is unchanged or increased.

ATP synthase complex is fully assembled

The analysis of the ATP synthase complex in its native state was performed by blue native (BN)-PAGE and WB of dodecyl maltoside (DDM)-solubilized proteins of isolated fibroblast mitochondria. As shown in Fig. 3B, the migration of ATP synthase complex from the patient mitochondria was identical to that in the control, indicating that the complex has a normal size of about 620 kDa. The anti-F_1 α antibody showed that the ATP synthase defect in the patient cells is of quantitative character. There were two additional faint bands of lower molecular weight visible on the blot, which might be assembly or brake down intermediates; however, they did not accumulate at a high proportion. BN-PAGE analysis also confirmed an isolated decrease of the ATP synthase complex compared with the respiratory chain complexes III and IV.

Selective decrease of ATP synthase biosynthesis

The isolated decrease of ATP synthase can be caused by a decreased *de novo* synthesis of the enzyme and/or by its increased lability and thus enhanced degradation. To investigate the biosynthesis of mitochondrial oxidative phosphorylation complexes, we performed metabolic labeling with ^{35}S-methionine and followed its incorporation into the assembled oxidative phosphorylation complexes during a 6 h pulse labeling followed by a chase with unlabeled methionine. Mitoplasts were isolated from the labeled fibroblasts, and DDM-solubilized proteins were resolved by two-dimensional (2D) BN/SDS–PAGE.

The labeling of the full-sized, assembled ATP synthase holoenzyme (calculated from the labeling of two largest subunits, F_1 α and β) showed a near-linear increase during the 6 h pulse, in both control and patient cells (Fig. 3C), but the intensity of the labeling was 55% lower in patient cells. In contrast, there was no apparent difference in the intensity of the labeling of complex IV, cytochrome *c* oxidase (COX), quantified from the labeling of subunits COX2, COX3 and COX4. When the decay of the labeling of ATP synthase was quantified in the course of 50 h following the chase, an analogous time-dependent decrease was observed in the patient and control cells. Similarly, there was a comparable decay of COX labeling after the chase in the patient and control cells. These data indicate that the isolated defect of ATP synthase is caused by decreased *de novo* synthesis, whereas the half-life remains rather unchanged.

Patient cells harbor a homozygous missense mutation in the *ATP5E* gene

The genetic analysis excluded mutations in ATP synthase assembly factors and in the *TMEM70* gene (19), but sequencing of ATP synthase subunit genes at the cDNA level revealed the missense mutation c.35A>G in exon 2 of the *ATP5E* gene (Fig. 4A). This leads to the amino acid exchange p.Tyr12Cys, which corresponds to Tyr11 of the mature ε subunit which lacks the N-terminal methionine. The affected position is highly conserved among eukaryotes (Fig. 4C). This mutation introduces a restriction site for *Pvu*II into the sequence, which was used to verify the mutation by RFLP analysis at the level of genomic DNA. The mutation was homozygous and inherited from the parents who were both heterozygous carriers (Fig. 4B). The mutation was not found in 180 control chromosomes from the Austrian population.

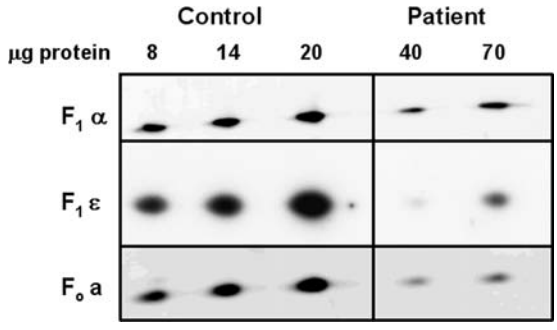

Figure 5. Mutated subunit ε is incorporated in the ATP synthase complex. DDM-solubilized mitochondrial proteins from the control and patient fibroblasts were separated by BN-PAGE in the first dimension; the gel pieces containing the full-size ATPase complex were dissected and subjected to SDS–PAGE in the second dimension. WB analysis was performed using antibodies to F_1 α, F_1 ε and F_o a subunits.

QT-PCR analysis revealed comparable levels of ε subunit mRNA (not shown), indicating that the transcription of the *ATP5E* gene is not altered in the patient cells.

ATP synthase complex contains mutated subunit ε

To examine whether the mutated ε subunit is incorporated into the ATP synthase holoenzyme in patient mitochondria, we performed 2D BN/SDS–PAGE and WB analysis using specific antibodies to F_1 subunits α and ε and F_o subunit a. As shown in Fig. 5, the anti-ε antibody reacted well with the mutated ε subunit, which could be identified in the assembled ATP synthase complex of patient mitochondria. The comparison of ε subunit signals to those of F_1 α and F_o a subunits showed similar proportions in the control and patient ATP synthase complex, indicating that although the amount of patient holoenzyme is profoundly reduced, it has a normal composition of its subunits. This means that most of the mutated ε subunit must be either degraded or present in an unassembled form or in intermediates.

Low content of ATP synthase subunit ε, but increased content of subunit c is present in patient mitochondria

We investigated whether there could be any accumulation of mutated subunit ε outside the ATP synthase holoenzyme in the patient mitochondria, and performed a detailed WB analysis of isolated fibroblasts mitochondria with the available antibodies to individual ATP synthase subunits. As shown in Fig. 6A, an analogous pronounced decrease compared with control mitochondria was found in F_1 subunits α, β and ε, as well as in F_o subunits a, d, OSCP and F6, supporting the assumption that only ATP synthase-assembled ε subunit is present in the patient cells.

However, in the patient mitochondria with the mutated ε subunit, we found an increased content of F_o subunit c that opposed the decrease of all other ATP synthase subunits. Interestingly, the content of subunit c was as low as that of all other ATP synthase subunits in the fibroblasts from the patients with the ATP synthase deficiency due to the *TMEM70* mutation (Fig. 6B). Apparently, the observed accumulation of subunit c was unique to the patients with the *ATP5E* mutation.

Accumulated subunit c is not associated with ATP synthase enzyme complex and is insoluble in DDM

When we performed 2D WB analysis of DDM-solubilized proteins from the patient mitochondria using antibodies to F_1 α and F_o c subunits, the subunit c was detected only in the full-size ATP synthase, and its content was very low, correlating with the low content of F_1 and F_o subunits. This indicated that the accumulated subunit c resisted DDM solubilization. Therefore, further experiments were performed to analyze both the DDM-soluble and DDM-insoluble material obtained after solubilization using up to 4 g DDM/g protein of mitochondria. As shown in Fig. 6C, there was a pronounced accumulation of c subunit in the DDM-insoluble fraction (pellet) of patient mitochondria, whereas almost no subunit c was found in the DDM-insoluble fraction from the control mitochondria. In the control, only 5% of the total c subunit was recovered in the pellet, whereas the pellet contained 56% of c subunit in the patient (Table 2). Thus, the subunit c content in the pellet was 17-fold higher in the patient mitochondria and the total content of subunit c was ~22% higher compared with the control. In contrast and as expected, the F_1 α subunit was mostly recovered in the soluble material (86–95%) both in the patient and control mitochondria (Fig. 6C). The respective F_o c/F_1 α ratio was similar in the patient and control DDM solubilisates, but it was 194-fold higher in DDM pellet from patient mitochondria compared with that of control (Table 2).

The pellet from the patient was analyzed also with antibodies to other F_o subunits, a and d. Their content was low and excluded any parallel accumulation with subunit c (Fig. 6C). These data clearly indicate that despite the isolated decrease of ATP synthase complex in the patient cells, the subunit c is produced and accumulates in mitochondria in the form of aggregates which cannot be solubilized with DDM, even at rather high detergent concentrations.

DISCUSSION

The present work demonstrates that in addition to nuclear encoded mutations in the assembly-biogenesis factors ATPAF2 and TMEM70, also a mutation of the subunit ε of the F_1 catalytic part can cause an isolated deficiency of ATP synthase leading to a mitochondrial disease. Mutations in all three genes lead to a very similar biochemical phenotype of selective inhibition of ATP synthase biogenesis, which apparently affects the early stage of enzyme assembly at the level of F_1. However, the mutation in the *ATP5E* gene presents with a distinct clinical phenotype as well as with a unique alteration of ATP synthase biogenesis at the level of subunit c, which contrasts with the manifestation of *TMEM70* (20) and *ATPAF2* (21) mutations.

The subunit ε of the F_1 catalytic part is one of the smallest subunits in the mitochondrial ATP synthase. Evolutionarily, it appeared probably during the formation of eukaryotic cell and is the only F_1 subunit that does not have a homolog in the

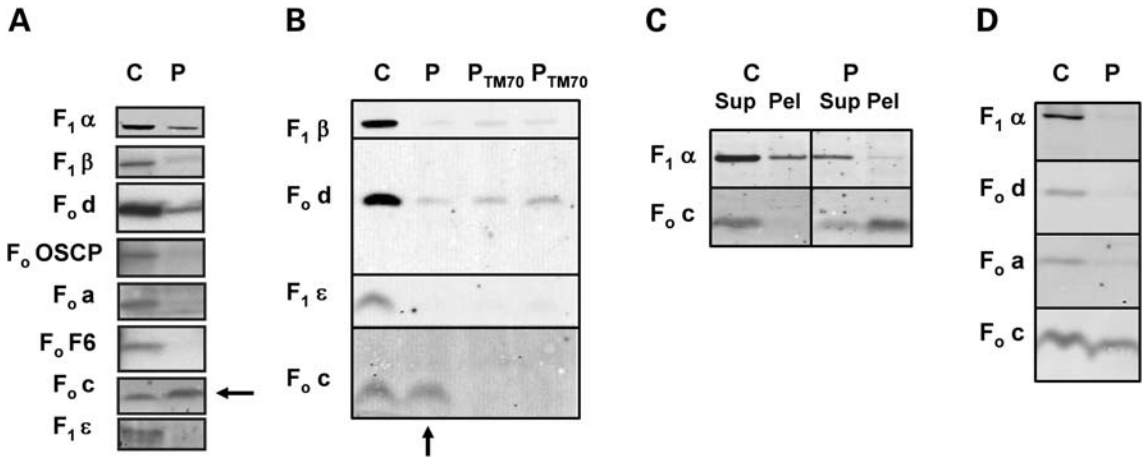

Figure 6. Patient mitochondria accumulate F_o subunit c of ATP synthase. SDS–PAGE and WB analysis of indicated ATP synthase subunits in the isolated fibroblast mitochondria (**A**) and fibroblasts (**B**) from control (C), patient with the *ATP5E* mutation (P) and two patients with a mutation in the *TMEM70* gene (P_{TM70}). (**C**) Accumulated F_o c subunits resist to DDM solubilization. Isolated mitochondria from patient and control fibroblasts were solubilized with DDM (4 g/g protein) and 29 000*g* supernatant (Sup) and pellet (Pel) were analyzed for the content of subunits F_1 α and F_o c. (**D**) Pellet from the patient accumulates F_o c but not the subunits F_o a or F_o d.

Table 2. Recovery of F_o c and F_1 α subunits in the supernatant and pellet of the patient and control fibroblast mitochondria solubilized with 4 g DDM/g protein

	Supernatant AU/mg prot	%Total	Pellet AU/mg prot	%Total	Total AU/mg prot
Patient F_1 α	1799	95.4	86	4.6	1885
Patient F_o c	1566	43.8	2009	56.2	3575
Patient F_o c/F_1 α	0.87		23.3		1.89
Control F_1 α	5872	86.4	922	13.6	6794
Control F_o c	2824	95.9	118	4.1	2942
Control F_o c/F_1 α	0.48		0.12		0.43

For quantification, 5 and 10 μg protein aliquots of 29 000 *g* supernatants and pellets were analyzed by SDS–PAGE and WB as in Fig. 6C.

bacterial and chloroplast enzyme. The mammalian ε (24) is a 51 amino acid protein that lacks the cleavable import sequence and exerts a high degree of homology with the slightly larger 62 amino acid yeast ε protein, encoded by the *ATP15* gene in *Saccharomyces cerevisiae*. The subunit ε is a part of the ATP synthase central stalk, and the function of this subunit is still unclear. The absence of ε subunit in *S. cerevisiae* (25) resulted in no detectable oligomycin-sensitive ATPase activity and in F_1 instability, but F_o subunits were still bound to F_1. The null mutation of the *ATP15* gene could be complemented by the bovine ε, indicating the structural and functional equivalence of corresponding subunits (26). Unlike in *S. cerevisiae*, the disruption of ε subunit gene in *Kluyveromyces lactis* completely eliminated the F_1-ATPase activity, indicating that the ε subunit may play an important role in the formation of the F_1 catalytic sector of eukaryotic ATP synthase (27). When the *ATP5E* gene in the mammalian HEK293 cells was knocked down, the biogenesis of ATP synthase was selectively inhibited, resulting in an isolated decrease of ATP synthase complex, insufficient ATP phosphorylating capacity, elevated levels of mitochondrial membrane potential ($\Delta\Psi_m$) and unexpected accumulation of subunit c (28).

The important finding of the present study is that the missense mutation c.35A>G (p.Tyr12Cys) in *ATP5E* results in a biochemical phenotype that is very similar to the downregulation of ε subunit biosynthesis. Interestingly, the function of ATP synthase assembled with the mutated ε subunit appears to be rather unaffected; it is able to utilize the mitochondrial membrane potential ($\Delta\Psi_m$) for ATP synthesis and also retains the sensitivity to oligomycin, which means that the F_1–F_o functional interactions are rather preserved, once the complex is formed.

The question arises at which stage of enzyme biogenesis the mutation of ε stalls the assembly process. The patient cells have similarly decreased oligomycin-sensitive and aurovertin-sensitive ATP synthase hydrolytic activities, which argues against the presence of free active F_1 catalytic part. They also do not show enhanced content of F_1 assemblies that are known to accumulate in rho^0 cells (29), upon mtDNA depletion (30), in *ATP6* mutations (31), and after the inhibition of mitochondrial protein synthesis by doxycycline (32). Also, there is no pronounced accumulation of free F_1 subunits α or β, nor their heterodimers. The initial formation of $\alpha_3\beta_3$ hetero-oligomer, which depends on the ATPAF1 and ATPAF2 factors, is expected to be followed by the addition of the γ, δ and ε subunits (6), but the eukaryotic F_1 assembly that involves the subunit ε is not much known. As the biochemical phenotype of patient cells indicates, a mutation in ε must be critical for the completion of F_1 or for its stability. Especially, the stability of the mutated F_1 might be a problem, and mutated F_1 could be degraded before it can establish further contacts with the F_o subunits.

As revealed by crystallographic studies (33), the ε subunit in the bovine enzyme is located in the protruding part of the central stalk and has a hairpin (helix–loop–helix) structure. It is in contact with (located between) the γ and δ subunits and is expected to play a role in the stability of the foot of the central stalk facing the c subunit oligomer. The C-terminus of ε subunit forms an extension of the β-sheet of the γ subunit, and the N-terminal region of ε subunit is in a shallow cleft of δ

subunit. Three of the five strictly conserved amino acids of the ε subunit are located at the N-terminus (Fig. 4C) and include Trp4, the only tryptophan within the mitochondrial F_1, Arg5 and Tyr11, which is replaced by Cys in our patient with the c.35A>G mutation in exon 2 of the *ATP5E* gene (amino acid numbering according to the mature ε that lacks the N-terminal methionine). Interestingly, this Tyr11 of the mature protein forms a part of the hydrophobic pocket for Trp4 and is involved in the hydrogen bonding to the δ subunit in a way that the ε subunit normally forms a stable heterodimer with the δ subunit (34,35). In the light of similarity between the Tyr11 to Cys replacement in the patient cells and the *ATP5E* knock-down in the HEK293 cells (28), it is possible to state that the disruption of these interactions at the level of stalk may be critical to the stability of the whole F_1 part of the ATP synthase. Interestingly, when the complete F_1F_o with mutated ε is formed, its stability appears to be normal.

Another important finding of our study is the accumulation of subunit c, the most hydrophobic ATP synthase subunit which forms an oligomeric ring in the F_o moiety. The accumulation of the subunit c, which appears to be present in an aggregated form, is comparable with that found in the *ATP5E* knock-down (28) and represents a substantial difference from the ATP synthase deficiency due to *TMEM70* or *ATPAF2* mutations. It also supports the view that the subunit ε plays an essential role in the incorporation and assembly of subunits c into the ATP synthase complex. Further studies are needed to test whether the p.Tyr12Cys replacement alters the F_1-c subunit oligomer formation via a changed conformation in the bottom part of the central stalk or whether the ε subunit interacts directly with the c subunits.

The accumulation of subunit c is known in neuronal ceroid lipofuscinosis (NCL), a neurodegenerative inherited lysosomal storage disease, where an altered degradation of hydrophobic proteins leads to a failure in the degradation of ATP synthase subunit c after its normal inclusion into mitochondria. Its consequent abnormal accumulation in lysosomes is apparent as autofluorescent storage bodies (lipopigment) (36). The impact of the NCL disease process differs substantially depending on the cell type. The brain neurons are most seriously affected and degenerate, whereas other cell types mostly survive without any detectable deterioration. NCL mitochondria were found to contain normal amounts of ATP synthase, and the oxidative phosphorylation was also normal (37,38). Up to now, about 160 NCL-causing mutations were found in eight NCL genes (39,40) but none of them appears to be associated with the ATP synthase biosynthesis and function.

In conclusion, the present work describes that a mutation in the third nuclear gene, *ATP5E*, leads to an isolated ATP synthase deficiency and mitochondrial disease. This is the first mutation in nuclear encoded subunit of mammalian ATP synthase that leads to an alteration of enzyme biosynthesis, and it provides with important information for the genetic diagnostics of mitochondrial diseases due to ATP synthase dysfunction. At the same time, this genetic disorder represents a unique model for further studies on the functional role of the ε subunit, one of the least understood subunits of the mitochondrial enzyme, in the biogenesis of the ATP synthase in eukaryotic cells.

MATERIALS AND METHODS

Case report

The girl was born after 37 weeks of gestation with the birth weight of 2440 g (small for gestational age). Pregnancy was uneventful; she is the first and only offspring of non-consanguineous, healthy Austrian parents. She was symptomatic from the first day of her life with poor sucking and respiratory distress. Laboratory investigations showed hyperlactacidemia (3.8 mmol/l) and 3-methylglutaconic aciduria. A metabolic disease was supposed; the girl recovered slowly and could be discharged home at the age of 2 months. The clinical course over the first years of life was marked by recurrent metabolic crises, mostly triggered by (upper airway) infections with elevated plasma lactate and partly hyperammonemia (up to 500 μmol/l). The girl started walking at the age of 18 months, the course of the disease stabilized at the age of 5–6 years. She entered and successfully completed a regular school and works now as an employee in an office. The diagnosis was finally established at the age of 17 years. The ATP synthase deficiency was diagnosed in cultured skin fibroblasts during a workup aimed at explaining her persistent 3-methylglutaconic aciduria and lactic acidosis. Electrophoretic analysis confirmed the isolated defect of the ATP synthase. The patient shows moderate ataxia, horizontal nystagmus, exercise intolerance and weakness, a strongly shortened walking distance and a severe peripheral neuropathy with the loss of tendon reflexes in the legs and mild hypertrophy of the left ventricle. The motor nerve conduction velocity of the peroneal nerve was severely reduced with a significantly diminished amplitude proofing mixed axonal and demyelizating neuropathy. Electromyography showed increased amplitudes and prolonged polyphasic potentials during the innervation as a symptom of reorganization. MRI showed slightly increased signal intensities in the caudate and lentiformis nuclei at the age of 14 years; MRI of the brain was normal 3 years later and the signal intensities disappeared.

Ethics

This study was carried out in accordance with the Declaration of Helsinki of the World Medical Association and was approved by the Committees of Medical Ethics at all collaborating institutions. Informed consent was obtained from the parents.

Cell cultures and isolation of mitochondria

Fibroblast cultures were established from skin biopsies and cells were cultivated in DMEM medium (Gibco BRL) with 10% fetal calf serum (Sigma, USA) at 37°C in 5% CO_2 in air. Cells were grown to ~90% confluence and harvested using 0.05% trypsin and 0.02% EDTA. Detached cells were diluted with ice-cold culture medium, sedimented by centrifugation and washed twice in cold phosphate-buffered saline (PBS; 8 g/l NaCl, 0.2 g/l KCl, 1.15 g/l Na_2HPO_4, 0.2 g/l KH_2PO_4). Mitochondria were isolated from the fibroblasts by the method of Bentlage *et al*. (41), utilizing the hypotonic shock cell disruption. To avoid proteolytic degradation, the isolation medium (250 mM sucrose, 40 mM KCl, 20 mM

Tris–HCl, 2 mM EGTA, pH 7.6) was supplemented with the protease inhibitor cocktail (Sigma P8340). The isolated mitochondria were stored at −70°C.

Enzyme activity measurements

The following respiratory chain enzyme activities were determined accordingly: citrate synthase (42), complex I and I + III (43), complex II and II + III (44), complex III (43), complex IV (45), with modifications described in Berger *et al*. (46). The ATPase hydrolytic activity was measured in ATP-regenerating system (47) using frozen–thawed fibroblasts or isolated mitochondria. The sensitivity to aurovertin and oligomycin was determined at 2 μM inhibitor concentration. All spectrophotometric measurements were performed at 37°C.

The rate of ATP synthesis was measured as described before (13) in fibroblasts permeabilized with digitonin (0.1 g/g protein; Fluka, USA) and supplemented with 1 mM ADP and respiratory substrates 10 mM pyruvate + 2.5 mM malate or 10 mM succinate. The reaction was started by the addition of fibroblasts; then, in time intervals of 5–15 min, samples were quenched with dimethylsulfoxide (1/1, v/v), and ATP content was measured by a luciferase assay (48). The ATP production was expressed in nmol ATP/min/mg protein.

The protein content was measured by the method of Bradford (49), using bovine serum albumin as a standard. Samples were sonicated for 20 s prior to the protein determination.

High-resolution oxygraphy

Oxygen consumption by cultured fibroblasts was determined at 30°C as described before (50) using Oxygraph-2k (Oroboros, Austria). Freshly harvested fibroblasts were suspended in a KCl medium (80 mM KCl, 10 mM Tris–HCl, 3 mM $MgCl_2$, 1 mM EDTA, 5 mM potassium phosphate, pH 7.4) and cells were permeabilized with digitonin (0.05 g/g protein). For measurements, 10 mM glutamate, 2.5 mM malate, 10 mM succinate, 1.5 mM ADP, 25 μM cytochrome *c*, 1 μM oligomycin and 0.5 μM FCCP were used. The oxygen consumption was expressed in pmol oxygen/s/mg protein.

Flow cytometry analysis of mitochondrial membrane potential ΔΨm

The cells were resuspended in the KCl medium used for oxygraphy at the protein concentration of 1 mg/ml. The aliquots of the cells (0.3 mg protein) were diluted in 1.5 ml KCl medium containing 10 mM succinate, permeabilized with 0.1 g digitonin/g protein and incubated with 20 nM TMRM (Molecular Probes, USA) for 15 min. For measurements, 1.5 mM ADP and 1 μM FCCP were used. Cytofluorometric analysis was performed on PAS-III flow cytometer (Partec, Germany) equipped with the 488 nm Ar–Kr laser, and TMRM fluorescence was analyzed in the FL2 channel (band pass filter 580 ± 30 nm). Data were acquired with FloMax software (Partec, Germany) and analyzed with Summit Offline V3.1 software (Cytomation, USA). The changes in ΔΨm were calculated in millivolts (51).

Electrophoresis and WB analysis

SDS–PAGE (52) was performed on 10% polyacrylamide slab minigels (MiniProtean II system; Bio-Rad). The samples were boiled for 3 min in a sample lysis buffer [2% (v/v) mercaptoethanol, 4% (w/v) SDS, 50 mM Tris–HCl, pH 7.0, 10% (v/v) glycerol], and the protein aliquots were loaded as indicated. Blue native-PAGE (BN-PAGE) (53) was performed on 6–15% gradient polyacrylamide slab minigels. Fibroblast mitochondria or mitoplasts were solubilized with 1–4 g/g protein of DDM for 20 min at 0°C and centrifuged for 20 min at 29 000*g*. The protein concentration in the supernatant was estimated and Serva Blue G was added at a ratio 0.25 g/g DDM. For 2D analysis, strips of gel from BN-PAGE were incubated for 1 h in 1% (v/v) mercaptoethanol, 1% (w/v) SDS and subjected to SDS–PAGE in the second dimension.

The gels were blotted onto a PVDF membrane (Immobilon P, Millipore) by the semidry electrotransfer for 1 h at 0.8 mA/cm^2, and the membrane was blocked in PBS, 0.1% Tween-20, 5% (w/v) fat-free dried milk. The membranes were incubated for 3 h with primary antibodies diluted in PBS with 0.3% (v/v) Tween-20 (PBST). The following antibodies were used: monoclonal antibodies from Mitosciences (USA) to SDH70 (MS204), Core 1 (MS303), COX4 (MS407), NDUFA9 (MS111), ATP synthase subunits α (MS502), β (MS503), d (MS504), OSCP (MS505), F6 (MS508) and porin (MSA03); Abnova (USA) antibody to ATP synthase subunit ε (H00000514-M01); polyclonal antibodies to ATP synthase subunits a (54) and c (55). Incubation with Alexa Fluor 680-labeled secondary antibodies (Molecular Probes) in PBST was performed for 1 h using either goat anti-mouse IgG (A21058) or goat anti-rabbit IgG (A21109). The fluorescence was detected using Odyssey Imager (LI-COR) and the signal was quantified using Aida 3.21 Image Analyzer software (Raytest).

DNA analysis

Genomic DNA was isolated from fibroblasts or blood with a standard technology (NucleoSpin, Machery-Nagel). Total RNA was extracted from fibroblasts (TRI reagent, MRC, Inc.), treated with DNase I (Ambion) for 15 min and reverse-transcribed (Superscript III, Invitrogen). The *ATP5E* gene was amplified from cDNA with the following forward ATP5E-F GACATTGCCGGCGTCTTG and reverse ATP5E-R TCCC ATGGAATGAGATCCTTT primers (5′ to 3′). Sequence analysis (CEQ-8000, Beckman Coulter) was performed according to the manufacturer. The presence of the c.35A>G mutation was assessed from the genomic DNA by PCR–RFLP analysis with the following forward ATP5E-intron1-F AGATCATCCATCCAAACACC and reverse ATP5E-intron2-R GCCAGGGGACTTCTATAACC primers employing a mutation-induced restriction site for *Pvu*II in the sequence.

Metabolic labeling

Fibroblasts were grown in 75 cm^2 flasks until 80% confluency. Cells were washed twice with PBS and then incubated for 3 h in methionine-free medium (Sigma D0422) with 10% dialyzed

FCS (Gibco BRL 26400-044) for the depletion of intracellular methionine. The met$^-$ medium was removed and labeling was started by the addition of 6 ml of met$^-$ medium with 10% FCS and 100 μCi ^{35}S-methionine (MP Radiochemicals No. 51004) into each flask. For chase, 10 mM methionine was added. Labeling was performed for the indicated time intervals and then stopped by 2.5 mM chloramphenicol and 2.5 mM cycloheximide. After 10 min, the cells were washed twice with PBS containing both inhibitors and harvested by trypsinization. Mitoplasts prepared by digitonin treatment [0.8 g/g protein (56)] were solubilized with DDM and analyzed by 2D BN/SDS–PAGE. Radioactivity of proteins was quantified in dried gels using BAS-5000 system (Fuji). The labeling of ATP synthase complex was calculated from the radioactivity of subunits α and β, and the labeling of COX was calculated from the radioactivity of subunits COX2, COX3 and COX4 identified in Coomassie Blue R-250-stained gels.

ACKNOWLEDGEMENTS

We thank Dr Peter Kurnik and Dr Silvia Stöckler-Ipsiroglu for sending in the patient fibroblasts and providing clinical data.

Conflict of Interest statement. None declared.

FUNDING

This work was supported by the Grant Agency of the Ministry of Health of the Czech Republic (NS9759), Ministry of Education, Youth and Sports of the Czech Republic (AV0Z 50110509, 1M0520), Charles University (UK97807), Oesterreichische Nationalbank (Jubiläumsfonds 12568) and the Vereinigung zur Pädiatrischen Forschung und Fortbildung Salzburg.

REFERENCES

1. Houštěk, J., Pickova, A., Vojtiskova, A., Mracek, T., Pecina, P. and Ješina, P. (2006) Mitochondrial diseases and genetic defects of ATP synthase. *Biochim. Biophys. Acta*, **1757**, 1400–1405.
2. Collinson, I.R., Skehel, J.M., Fearnley, I.M., Runswick, M.J. and Walker, J.E. (1996) The F_1F_0-ATPase complex from bovine heart mitochondria: the molar ratio of the subunits in the stalk region linking the F_1 and F_0 domains. *Biochemistry*, **35**, 12640–12646.
3. Anderson, S., Bankier, A.T., Barrell, B.G., de Bruijn, M.H.L., Coulson, A.R., Drouin, J., Eperon, I.C., Nierlich, D.P., Roe, B.A., Sanger, F. *et al.* (1981) Sequence and organization of the human mitochondrial genome. *Nature*, **290**, 457–465.
4. Belogrudov, G.I. and Hatefi, Y. (2002) Factor B and the mitochondrial ATP synthase complex. *J. Biol. Chem.*, **277**, 6097–6103.
5. Meyer, B., Wittig, I., Trifilieff, E., Karas, M. and Schagger, H. (2007) Identification of two proteins associated with mammalian ATP synthase. *Mol. Cell Proteomics*, **6**, 1690–1699.
6. Ackerman, S.H. and Tzagoloff, A. (2005) Function, structure, and biogenesis of mitochondrial ATP synthase. *Prog. Nucleic Acid Res. Mol. Biol.*, **80**, 95–133.
7. Zeng, X., Neupert, W. and Tzagoloff, A. (2007) The metalloprotease encoded by ATP23 has a dual function in processing and assembly of subunit 6 of mitochondrial ATPase. *Mol. Biol. Cell*, **18**, 617–626.
8. Osman, C., Wilmes, C., Tatsuta, T. and Langer, T. (2007) Prohibitins interact genetically with Atp23, a novel processing peptidase and chaperone for the F1FO-ATP synthase. *Mol. Biol. Cell*, **18**, 627–635.
9. Houštěk, J., Kmoch, S. and Zeman, J. (2009) TMEM70 protein—a novel ancillary factor of mammalian ATP synthase. *Biochim. Biophys. Acta*, **1787**, 529–532.
10. Holt, I.J., Harding, A.E., Petty, R.K.H. and Morgan-Hughes, J.A. (1990) A new mitochondrial disease associated with mitochondrial DNA heteroplasmy. *Am. J. Hum. Genet.*, **46**, 428–433.
11. Schon, E.A., Santra, S., Pallotti, F. and Girvin, M.E. (2001) Pathogenesis of primary defects in mitochondrial ATP synthesis. *Semin. Cell Dev. Biol.*, **12**, 441–448.
12. Seneca, S., Abramowicz, M., Lissens, W., Muller, M.F., Vamos, E. and de Meirleir, L. (1996) A mitochondrial DNA microdeletion in a newborn girl with transient lactic acidosis. *J. Inherit. Metab. Dis.*, **19**, 115–118.
13. Ješina, P., Tesarova, M., Fornuskova, D., Vojtiskova, A., Pecina, P., Kaplanová, V., Hansikova, H., Zeman, J. and Houštěk, J. (2004) Diminished synthesis of subunit a (ATP6) and altered function of ATP synthase and cytochrome *c* oxidase due to the mtDNA 2bp microdeletion of TA at positions 9205 and 9206. *Biochem. J.*, **383**, 561–571.
14. Jonckheere, A.I., Hogeveen, M., Nijtmans, L.G., van den Brand, M.A., Janssen, A.J., Diepstra, J.H., van den Brandt, F.C., van den Heuvel, L.P., Hol, F.A., Hofste, T.G. *et al.* (2008) A novel mitochondrial ATP8 gene mutation in a patient with apical hypertrophic cardiomyopathy and neuropathy. *J. Med. Genet.*, **45**, 129–133.
15. Houštěk, J., Klement, P., Floryk, D., Antonicka, H., Hermanska, J., Kalous, M., Hansikova, H., Hout'kova, H., Chowdhury, S.K., Rosipal, T. *et al.* (1999) A novel deficiency of mitochondrial ATPase of nuclear origin. *Hum. Mol. Genet.*, **8**, 1967–1974.
16. Mracek, T., Pecina, P., Vojtiskova, A., Kalous, M., Sebesta, O. and Houštěk, J. (2006) Two components in pathogenic mechanism of mitochondrial ATPase deficiency: energy deprivation and ROS production. *Exp. Gerontol.*, **41**, 683–687.
17. Houštěk, J., Mracek, T., Vojtiskova, A. and Zeman, J. (2004) Mitochondrial diseases and ATPase defects of nuclear origin. *Biochim. Biophys. Acta*, **1658**, 115–121.
18. Sperl, W., Ješina, P., Zeman, J., Mayr, J.A., Demeirleir, L., VanCoster, R., Pickova, A., Hansikova, H., Houst'kova, H., Krejcik, Z. *et al.* (2006) Deficiency of mitochondrial ATP synthase of nuclear genetic origin. *Neuromuscul. Disord.*, **16**, 821–829.
19. Cizkova, A., Stranecky, V., Mayr, J.A., Tesarova, M., Havlíčková, V., Paul, J., Ivanek, R., Kuss, A.W., Hansikova, H., Kaplanová, V. *et al.* (2008) TMEM70 mutations cause isolated ATP synthase deficiency and neonatal mitochondrial encephalocardiomyopathy. *Nat. Genet.*, **40**, 1288–1290.
20. Honzik, T., Tesarova, M., Mayr, J.A., Hansikova, H., Ješina, P., Bodamer, O., Koch, J., Magner, M., Freisinger, P., Huemer, M. *et al.* (2010) Mitochondrial encephalocardio-myopathy with early neonatal onset due to TMEM70 mutation. *Arch. Dis. Child.*, **95**, 296–301.
21. De Meirleir, L., Seneca, S., Lissens, W., De Clercq, I., Eyskens, F., Gerlo, E., Smet, J. and Van Coster, R. (2004) Respiratory chain complex V deficiency due to a mutation in the assembly gene ATP12. *J. Med. Genet.*, **41**, 120–124.
22. Wortmann, S.B., Rodenburg, R.J.T., Jonckheere, A., de Vries, M.C., Huizing, M., Heldt, K., van den Heuvel, L.P., Wendel, U., Kluijtmans, L.A., Engelke, U.F. *et al.* (2009) Biochemical and genetic analysis of 3-methylglutaconic aciduria type IV: a diagnostic strategy. *Brain*, **132**, 136–146.
23. Cizkova, A., Stranecky, V., Ivanek, R., Hartmannova, H., Noskova, L., Piherova, L., Tesarova, M., Hansikova, H., Honzik, T., Zeman, J. *et al.* (2008) Development of a human mitochondrial oligonucleotide microarray (h-MitoArray) and gene expression analysis of fibroblast cell lines from 13 patients with isolated F1Fo ATP synthase deficiency. *BMC Genomics*, **9**, 38.
24. Vinas, O., Powell, S.J., Runswick, M.J., Iacobazzi, V. and Walker, J.E. (1990) The epsilon-subunit of ATP synthase from bovine heart mitochondria. Complementary DNA sequence, expression in bovine tissues and evidence of homologous sequences in man and rat. *Biochem. J.*, **265**, 321–326.
25. Guelin, E., Chevallier, J., Rigoulet, M., Guerin, B. and Velours, J. (1993) ATP synthase of yeast mitochondria. Isolation and disruption of the ATP epsilon gene. *J. Biol. Chem.*, **268**, 161–167.
26. Lai-Zhang, J. and Mueller, D.M. (2000) Complementation of deletion mutants in the genes encoding the F1-ATPase by expression of the corresponding bovine subunits in yeast *S. cerevisiae*. *Eur. J. Biochem.*, **267**, 2409–2418.

27. Chen, X.J. (2000) Absence of F1-ATPase activity in *Kluyveromyces lactis* lacking the epsilon subunit. *Curr. Genet.*, **38**, 1–7.
28. Havlíčková, V., Kaplanová, V., Nůsková, H., Drahota, Z. and Houštěk, J. (2010) Knockdown of F(1) epsilon subunit decreases mitochondrial content of ATP synthase and leads to accumulation of subunit c. *Biochim. Biophys. Acta*, **1797**, 1124–1129.
29. Buchet, K. and Godinot, C. (1998) Functional F1-ATPase is essential in maintaining growth and membrane potential of human mitochondrial DNA-depleted rho degrees cells. *J. Biol. Chem.*, **273**, 22983–22989.
30. Carrozzo, R., Wittig, I., Santorelli, F.M., Bertini, E., Hofmann, S., Brandt, U. and Schagger, H. (2006) Subcomplexes of human ATP synthase mark mitochondrial biosynthesis disorders. *Ann. Neurol.*, **59**, 265–275.
31. Houštěk, J., Klement, P., Hermanska, J., Houstkova, H., Hansikova, H., van den Bogert, C. and Zeman, J. (1995) Altered properties of mitochondrial ATP-synthase in patients with a T —> G mutation in the ATPase 6 (subunit a) gene at position 8993 of mtDNA. *Biochim. Biophys. Acta*, **1271**, 349–357.
32. Nijtmans, L.G., Klement, P., Houštěk, J. and van den Bogert, C. (1995) Assembly of mitochondrial ATP synthase in cultured human cells: implications for mitochondrial diseases. *Biochim. Biophys. Acta*, **1272**, 190–198.
33. Gibbons, C., Montgomery, M.G., Leslie, A.G. and Walker, J.E. (2000) The structure of the central stalk in bovine F(1)-ATPase at 2.4 A resolution. *Nat. Struct. Biol.*, **7**, 1055–1061.
34. Penin, F., Deleage, G., Gagliardi, D., Roux, B. and Gautheron, D.C. (1990) Interaction between delta and epsilon subunits of F1-ATPase from pig heart mitochondria. Circular dichroism and intrinsic fluorescence of purified and reconstituted delta epsilon complex. *Biochemistry*, **29**, 9358–9364.
35. Orriss, G.L., Runswick, M.J., Collinson, I.R., Miroux, B., Fearnley, I.M., Skehel, J.M. and Walker, J.E. (1996) The delta- and epsilon-subunits of bovine F1-ATPase interact to form a heterodimeric subcomplex. *Biochem. J.*, **314**, 695–700.
36. Palmer, D.N., Fearnley, I.M., Medd, S.M., Walker, J.E., Martinus, R.D., Bayliss, S.L., Hall, N.A., Lake, B.D., Wolfe, L.S. and Jolly, R.D. (1989) Lysosomal storage of the DCCD reactive proteolipid subunit of mitochondrial ATP synthase in human and ovine ceroid lipofuscinoses. *Adv. Exp. Med. Biol.*, **266**, 211–222.
37. Palmer, D.N., Fearnley, I.M., Walker, J.E., Hall, N.A., Lake, B.D., Wolfe, L.S., Haltia, M., Martinus, R.D. and Jolly, R.D. (1992) Mitochondrial ATP synthase subunit c storage in the ceroid-lipofuscinoses (Batten disease). *Am. J. Med. Genet.*, **42**, 561–567.
38. Hughes, S.M., Moroni-Rawson, P., Jolly, R.D. and Jordan, T.W. (2001) Submitochondrial distribution and delayed proteolysis of subunit c of the H+-transporting ATP-synthase in ovine ceroid-lipofuscinosis. *Electrophoresis*, **22**, 1785–1794.
39. Jalanko, A. and Braulke, T. (2009) Neuronal ceroid lipofuscinoses. *Biochim. Biophys. Acta*, **1793**, 697–709.
40. Cooper, J.D., Russell, C. and Mitchison, H.M. (2006) Progress towards understanding disease mechanisms in small vertebrate models of neuronal ceroid lipofuscinosis. *Biochim. Biophys. Acta*, **1762**, 873–889.
41. Bentlage, H.A., Wendel, U., Schagger, H., ter Laak, H.J., Janssen, A.J. and Trijbels, J.M. (1996) Lethal infantile mitochondrial disease with isolated complex I deficiency in fibroblasts but with combined complex I and IV deficiencies in muscle. *Neurology*, **47**, 243–248.
42. Srere, P.A. (1969) Citrate synthase. *Methods Enzymol.*, **13**, 3–26.
43. Rustin, P., Chretien, D., Bourgeron, T., Gerard, B., Rotig, A., Saudubray, J.M. and Munnich, A. (1994) Biochemical and molecular investigations in respiratory chain deficiencies. *Clin. Chim. Acta*, **228**, 35–51.
44. Birch-Machin, M.A., Briggs, H.L., Saborido, A.A., Bindoff, L.A. and Turnbull, D.M. (1994) An evaluation of the measurement of the activities of complexes I–IV in the respiratory chain of human skeletal muscle mitochondria. *Biochem. Med. Metab. Biol.*, **51**, 35–42.
45. Trounce, I.A., Kim, Y.L., Jun, A.S. and Wallace, D.C. (1996) Assessment of mitochondrial oxidative phosphorylation in patient muscle biopsies, lymphoblasts, and transmitochondrial cell lines. *Methods Enzymol.*, **264**, 484–509.
46. Berger, A., Mayr, J., Meierhofer, D., Fötschl, U., Bittner, R., Budka, H., Grethen, C., Huemer, M., Kofler, B. and Sperl, W. (2003) Severe depletion of mitochondrial DNA in spinal muscular atrophy. *Acta Neuropathol.*, **105**, 245–251.
47. Baracca, A., Amler, E., Solaini, G., Parenti Castelli, G., Lenaz, G. and Houštěk, J. (1989) Temperature-induced states of isolated F1-ATPase affect catalysis, enzyme conformation and high-affinity nucleotide binding sites. *Biochim. Biophys. Acta*, **976**, 77–84.
48. Ouhabi, R., Boue-Grabot, M. and Mazat, J.P. (1998) Mitochondrial ATP synthesis in permeabilized cells: assessment of the ATP/O values *in situ*. *Anal. Biochem.*, **263**, 169–175.
49. Bradford, M.M. (1976) A rapid and sensitive method for the quantitation of microgram quantities of protein utilizing the principle of protein dye binding. *Anal. Biochem.*, **72**, 248–254.
50. Chowdhury, S.K., Drahota, Z., Floryk, D., Calda, P. and Houštěk, J. (2000) Activities of mitochondrial oxidative phosphorylation enzymes in cultured amniocytes. *Clin. Chim. Acta*, **298**, 157–173.
51. Plasek, J., Vojtiskova, A. and Houštěk, J. (2005) Flow-cytometric monitoring of mitochondrial depolarisation: from fluorescence intensities to millivolts. *J. Photochem. Photobiol. B*, **78**, 99–108.
52. Schagger, H. and von Jagow, G. (1987) Tricine-sodium dodecyl sulfate-polyacrylamide gel electrophoresis for the separation of proteins in the range from 1 to 100 kDa. *Anal. Biochem.*, **166**, 368–379.
53. Schagger, H. and von Jagow, G. (1991) Blue native electrophoresis for isolation of membrane protein complexes in enzymatically active form. *Anal. Biochem.*, **199**, 223–231.
54. Dubot, A., Godinot, C., Dumur, V., Sablonniere, B., Stojkovic, T., Cuisset, J.M., Vojtiskova, A., Pecina, P., Ješina, P. and Houštěk, J. (2004) GUG is an efficient initiation codon to translate the human mitochondrial ATP6 gene. *Biochem. Biophys. Res. Commun.*, **313**, 687–693.
55. Houštěk, J., Andersson, U., Tvrdik, P., Nedergaard, J. and Cannon, B. (1995) The expression of subunit c correlates with and thus may limit the biosynthesis of the mitochondrial F0F1-ATPase in brown adipose tissue. *J. Biol. Chem.*, **270**, 7689–7694.
56. Klement, P., Nijtmans, L.G., Van den Bogert, C. and Houštěk, J. (1995) Analysis of oxidative phosphorylation complexes in cultured human fibroblasts and amniocytes by blue-native-electrophoresis using mitoplasts isolated with the help of digitonin. *Anal. Biochem.*, **231**, 218–224.

Biochimica et Biophysica Acta 1797 (2010) 1124–1129

Contents lists available at ScienceDirect

Biochimica et Biophysica Acta

journal homepage: www.elsevier.com/locate/bbabio

Knockdown of F_1 epsilon subunit decreases mitochondrial content of ATP synthase and leads to accumulation of subunit c

Vendula Havlíčková, Vilma Kaplanová, Hana Nůsková, Zdeněk Drahota, Josef Houštěk *

Department of Bioenergetics, Institute of Physiology and Centre for Applied Genomics, Academy of Sciences of the Czech Republic, 142 20 Prague

ARTICLE INFO

Article history:
Received 3 November 2009
Received in revised form 11 December 2009
Accepted 13 December 2009
Available online 21 December 2009

Keywords:
Mitochondria
ATP synthase
Epsilon subunit
c subunit
Biogenesis

ABSTRACT

The subunit ε of mitochondrial ATP synthase is the only F_1 subunit without a homolog in bacteria and chloroplasts and represents the least characterized F_1 subunit of the mammalian enzyme. Silencing of the *ATP5E* gene in HEK293 cells resulted in downregulation of the activity and content of the mitochondrial ATP synthase complex and of ADP-stimulated respiration to approximately 40% of the control. The decreased content of the ε subunit was paralleled by a decrease in the F_1 subunits α and β and in the F_o subunits a and d while the content of the subunit c was not affected. The subunit c was present in the full-size ATP synthase complex and in subcomplexes of 200–400 kDa that neither contained the F_1 subunits, nor the F_o subunits. The results indicate that the ε subunit is essential for the assembly of F_1 and plays an important role in the incorporation of the hydrophobic subunit c into the F_1-c oligomer rotor of the mitochondrial ATP synthase complex.

1. Introduction

The mammalian ATP synthase (F_oF_1 ATPase) is a heterooligomeric complex of ~650 kDa localized in the inner mitochondrial membrane. It consists of at least 16 different types of subunits [1,2]. Six of them (α, β, γ, δ, ε and inhibitor protein IF_1) form the F_1-catalytic domain on the matrix side of the membrane. The remaining ten subunits (a, b, c, d, e, f, g, OSCP, A6L, F6), two of which (a and A6L) are encoded by mitochondrial DNA (mtDNA) [3], comprise the membrane-embedded F_o portion, functioning as a proton channel, and two stalks connecting the F_1 and F_o domains [4–7]. Two additional proteins MLQ and AGP are possibly involved in the dimerization of ATP synthase [8], and the enzyme function can be modulated by the coupling factor B [9].

The three largest subunits of the F_1 catalytic part of ATP synthase — α, β and γ — exert a varying degree of homology among ATP synthases from mitochondria, chloroplast and bacteria, while the mammalian subunit δ corresponds to the ε subunit in the bacterial enzyme [1]. The only F_1 subunit that does not have a homolog in bacteria and chloroplasts is the ε subunit [1], which is the smallest and functionally the least characterized mitochondrial F_1 subunit. The mammalian ε subunit [10] encoded by the *ATP5E* gene is a 51AA protein of 5.8 kDa that lacks a cleavable import sequence. It exerts a high degree of homology with the slightly larger yeast ε of 6.6 kDa, which is encoded by the *ATP15* gene, and consists of 62 AA in *S. cerevisiae* [11]. As revealed by complementation experiments, the yeast and mammalian ε are structurally and functionally equivalent [12].

The F_1 subunits γ, δ and ε together with the subunit c oligomer form the rotor of ATP synthase [13]. The subunit ε was shown to form heterodimers with the subunit δ [14,15] and presumably also makes contacts with F_o. As revealed by crystallographic studies [5,16], the mitochondrial ε subunit is located in the protruding part of the central stalk and it has a hairpin (helix–loop–helix) structure. It maintains contact with the γ and δ subunits and is expected to be involved in the stability of the foot of the central stalk facing the c subunit oligomer. The C-terminus of ε subunit forms an extension of the β-sheet of γ subunit and the N-terminal region of ε subunit is located in a shallow cleft of δ subunit [5].

The involvement of ε subunit in the ATP synthase biogenesis and function was repeatedly studied in yeast by means of disruption of the *ATP15* gene. The absence of ε subunit in *S. cerevisiae* resulted in no detectable oligomycin-sensitive ATPase activity, decreased content of γ, δ and F_o subunits in immunoprecipitated ATP synthase and F_1 instability. High proton leak, which was shown to be sensitive to oligomycin, indicated a conformationally changed F_o [17]. Also, disruption of the *ATP15* gene in *K. lactis* resulted in a complete elimination of F_1-ATPase activity, suggesting that the ε subunit may have an important role in the formation of the F_1 catalytic sector of eukaryotic ATP synthase [18]. In contrast, if the null mutations of F_1 subunits α, β, γ, δ and ε were made in *S. cerevisiae*, mutations in all but the ε subunit gene were unable to grow on a nonfermentable carbon source indicating that ε is not an essential component of the ATP synthase [11].

Abbreviations: DDM, dodecyl maltoside; F_1, catalytic part of ATP synthase; F_o, membrane-embedded part of ATP synthase

* Corresponding author. Institute of Physiology, Academy of Sciences of the Czech Republic, Vídeňská 1083, 142 20 Prague 4-Krč, Czech Republic. Tel.: +420 2 4106 2434; fax: +420 2 4106 2149.
E-mail address: houstek@biomed.cas.cz (J. Houštěk).

0005-2728/$ – see front matter © 2009 Elsevier B.V. All rights reserved.
doi:10.1016/j.bbabio.2009.12.009

With the aim to investigate the functional role of ε subunit in the biogenesis and formation of mammalian ATP synthase complex, we have downregulated the expression of *ATP5E* gene in HEK293 cells by means of RNA interference (RNAi). We have found that the inhibition of ε subunit biosynthesis has a pronounced effect on the mitochondrial content and activity of ATP synthase and leads to a relative accumulation of subunit c. Our results demonstrate the essential role of subunit ε in the assembly of F_1 and the incorporation of hydrophobic subunit c into the F_1-c oligomer rotor structure of mitochondrial ATP synthase in higher eukaryotes.

2. Materials and methods

2.1. Cell culture

Human embryonic kidney 293 cells (HEK293 from ATCC) were grown at 37 °C in a 5% (v/v) CO_2 atmosphere in high-glucose Dulbecco's modified Eagle's medium (PAA) supplemented with 10% (v/v) fetal calf serum (PAA). Cell transfections were carried out with a Nucleofector™ device (Amaxa) using the HEK293 cell-specific transfection kit.

2.2. RNAi

For the silencing of subunit ε of ATP synthase we used two miR-30-based shRNAs (shRNAmirs) shE1 (TGCTGTTGACAGTGAGCGAACAATGTCAATAAATTGAAATTAGTGAAGCCACAGATGTAATTTCAATTTATTGACATTGTCTGCCTACTGCCTCGGA) and shE2 (TGCTGTTGACAGTGAGCGAACATGTTATGGCAGATTGAAATAGTGAAGCCACAGATGTATTTCAATCTGCCATAACATGTGTGCCTACTGCCTCGGA) targeted to the coding sequence of human *ATP5E* gene, which were cloned to plasmid pGIPZ™ (V2LHS-77373 and V2LHS-773734, Open Biosystems). Plasmid DNA was isolated by an endotoxin-free kit (Qiagen) and HEK293 cells were transfected with the shE1 or shE2 shRNA constructs or with the non-silencing, empty vector (negative control, NS cells). At 48 h after the transfection the cells were split into culture medium containing 1.5 μg/ml puromycin (Sigma-Aldrich) and antibiotic-resistant colonies were selected over a period of three weeks.

ATP5E mRNA and *18S* RNA levels were determined in the transfected cells by QT RT-PCR. The total RNA was isolated with TRIzol reagent (Invitrogen) and cDNA was synthesized with SuperScript III reverse transcriptase using random primers (Invitrogen). PCR was performed on the LightCycler 480 instrument (Roche Diagnostics) with a SYBR Green Master kit (Qiagen) using *ATP5E* (F: 5′-GATGCACTGAAGACAGAATTCAAAG-3′, R: 5′-GCTGCCAGAAGTCTTCTCAGC-3′) and *18S* (F: 5′-ATCAGGGTTCGATTC CGGAG-3′, R: 5′-TTGGATGTGGTAGCCGTTTCT-3′) primers.

2.3. Isolation of mitochondria

Cells (~90% confluent) were harvested with 0.05% trypsin and 0.02% EDTA and washed twice in phosphate-buffered saline (PBS, 8 g/l NaCl, 0.2 g/l KCl, 1.15 g/l Na_2HPO_4, 0.20 g/l KH_2PO_4). Mitochondria were isolated by a method utilizing hypotonic shock cell disruption [19]. To avoid proteolytic degradation, isolation medium (250 mM sucrose, 40 mM KCl, 20 mM Tris–HCl, 2 mM EGTA, pH 7.6) was supplemented with protease inhibitor cocktail (Sigma P8340). The protein content was measured by the Bio-Rad Protein Essay (Bio-Rad Laboratories), using BSA as a standard. The isolated mitochondria were stored at −70 °C.

2.4. Electrophoresis

Blue-Native polyacrylamide gel electrophoresis (BN-PAGE) [20] was performed on a 6–15% polyacrylamide gradient minigels (Mini Protean, Bio-Rad). Mitochondria were solubilized with dodecyl maltoside (DDM, 2 g/g protein) for 20 min on ice in 1.75 M aminocaproic acid, 2 mM EDTA and 75 mM Bis–tris (pH 7.0). Samples were centrifuged for 20 min at 26000 × *g*, Serva Blue G (0.1 g/g detergent) was added to supernatants and the electrophoresis was run at 45 V for 30 min and then at 90 V.

SDS-Tricine polyacrylamide gel electrophoresis (SDS-PAGE) [21] was performed on 10% (w/v) polyacrylamide slab minigels. The samples were incubated for 20 min at 40 °C in 2% (v/v) mercaptoethanol, 4% (w/v) SDS, 10 mM Tris–HCl, 10% (v/v) glycerol. For two-dimensional (2D) analysis, the stripes of the first dimension BN-PAGE gel were incubated for 1 h in 1% (w/v) SDS and 1% (v/v) mercaptoethanol and then subjected to SDS-PAGE in the second dimension [21].

2.5. Western blot analysis

Gels were blotted on to PVDF membrane (Millipore) by semi-dry electrotransfer (1 h at 0.8 mA/cm^2). Blocked membranes (5% (w/v) non-fat dry milk in PBS) were incubated in PBS, 0.01% (v/v) Tween 20 with the following primary antibodies — polyclonal antibodies against F_o-a (1:500 [22]) and F_o-c (1:1000 [23]), monoclonal antibodies against F_1-α (1:1000, MS502, MitoSciences), F_1-β (1:2000, MS503, MitoSciences), F_1-ε (1:5000, Abnova), F_o-d (1:100; Molecular Probes), SDH70 (1:10000, MS204, Mitosciences), Core 2 (1:1000, MS304, Mitosciences) and porin (1:1000, MSA03, Mitosciences) and with fluorescent secondary antibodies (goat anti-mouse IgG, 1:3000, Alexa Fluor 680 A-21058 or goat anti-rabbit IgG, 1:3000, Alexa Fluor 680 A-21109, Molecular Probes). The fluorescence was detected on an ODYSSEY system (LI-COR) and the signal was quantified using Aida 3.21 Image Analyser software.

2.6. ATPase assay

The ATP synthase hydrolytic activity was measured in ATP-regenerating system as described by [24]. Digitonin (0.05 g/g protein) permeabilized cells were incubated in a medium containing 40 mM Tris–HCl (pH 7.4), 5 mM $MgCl_2$, 10 mM KCl, 2 mM phosphoenolpyruvate, 0.2 mM NADH, 1 μM rotenone, 3 μM FCCP, 0.1% (w/v) BSA, 5 U of pyruvate kinase, 5 U of lactate dehydrogenase for 2 min. The reaction was started by addition of 1 mM ATP. The sensitivity to aurovertin or oligomycin was determined by parallel measurements in the presence of 2 μM inhibitor.

2.7. Respiration measurements

Respiration was measured at 30 °C by an Oxygraph-2k (Oroboros). Freshly harvested cells were suspended in a KCl medium (80 mM KCl, 10 mM Tris–HCl, 3 mM $MgCl_2$, 1 mM EDTA, 5 mM potassium phosphate, pH 7.4) and permeabilized with digitonin (0.1 g/g of protein). Respiration was measured using 10 mM glutamate, 3 mM malate, 1.5 mM ADP, 1 μM oligomycin, 1 μM FCCP and 1 μM antimycin A. Oxygen consumption was expressed in pmol oxygen s^{-1} mg $protein^{-1}$.

2.8. Mitochondrial membrane potential $\Delta\Psi_m$ measurements

$\Delta\Psi_m$ was measured with TPP^+-selective electrode in 1 ml of KCl medium as described in [25]. Cells (2.5 mg protein/ml) were permeabilized with digitonin (0.05 g/g protein) and the following substrates and inhibitors were used: 10 mM succinate, 10 mM glutamate, 3 mM malate, 1.5 mM ADP, 1 μM oligomycin and 1 μM FCCP. The membrane potential was plotted as pTPP, *i.e.* natural logarithm of TPP^+ concentration (μM).

3. Results

3.1. Downregulation of ATP5E gene decreases the content and activity of ATP synthase

Transfections of HEK293 cells with miR-30-based shRNAs (shE1, shE2) targeted to the *ATP5E* gene encoding the ε subunit of ATP synthase were followed by puromycin selection and resulted in three shE2 stable lines that showed a variable decrease of *ATP5E* mRNA levels relative to 18S RNA. These shEa, shEb and shEc exhibited an *ATP5E* mRNA level of 16%, 47% and 29%, respectively, compared with the parental HEK293 cells transfected with empty vector (NS cells). The cell lines exerted normal viability under standard cultivation conditions. There was no significant difference in cell growth rate between the silenced and control cell lines.

The cell lines were analyzed for the content and activity of mitochondrial ATP synthase as well as the function of mitochondrial respiratory chain. Quantification of the cellular content of respiratory chain enzymes by SDS-PAGE and WB showed in all silenced cell lines normal content of complexes II and III, but decreased content of complex V — ATP synthase (Fig. 1A), indicating that the specific knockdown of *ATP5E* gene expression affected selectively the biogenesis of ATP synthase complex. Based on the immunodetection with the antibody to F_1 subunit β, the content of ATP synthase showed a decrease of 60–70%. The same result was obtained with the antibody to the α subunit (not shown). This was confirmed by analysis of ATP synthase at native conditions in dodecyl maltoside-solubilized proteins from isolated mitochondria using BN-PAGE and WB (Fig. 1B). In comparison with the controls (the original HEK293 and NS cells), the *ATP5E*-silenced cell lines contained reduced amounts of assembled ATP synthase complex, which, however, retained the same mobility as the ATP synthase complex from control cells corresponding to about 650 kDa. Control cells contained a small amount of F_1 subcomplex of ~370 kDa, which was not detected in silenced cell lines. The quantification of WB data from BN-PAGE revealed also a 60–70% reduction of ATP synthase complex in the *ATP5E*-silenced cell lines.

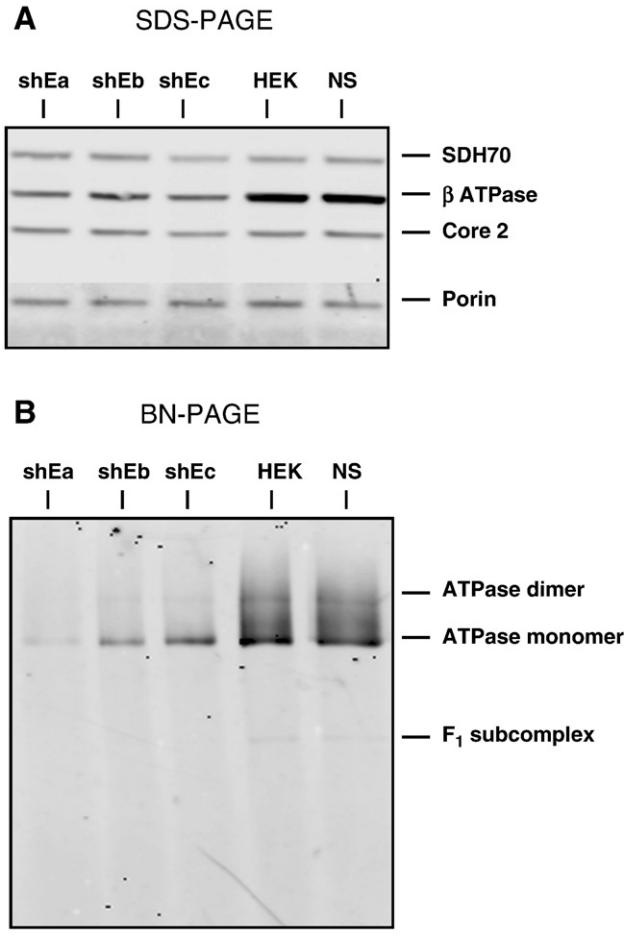

Fig. 1. Selective reduction of ATP synthase in *ATP5E*-silenced cell. (A) Isolated mitochondria (10 μg protein aliquots) from control (HEK293 and HEK293 transfected with empty vector (NS)) and *ATP5E*-silenced (shE2a, shE2b, shE2c) cells were analyzed by SDS-PAGE and WB with antibodies to ATP synthase (β) and to respiratory chain complexes II (SDH70) and III (Core 2). (B) DDM-solubilized (2 g/g protein) mitochondrial proteins (15 μg protein aliquots) from control (HEK293, NS) and *ATP5E*-silenced (shE2a, shE2b, shE2c) cells were analyzed by BN-PAGE and WB using antibody to ATP synthase β subunit.

Furthermore, the *ATP5E*-silenced cell lines had a low ATP synthase hydrolytic activity compared with the control HEK293 and NS cells. Oligomycin-sensitive ATP hydrolysis showed a 54–64% decrease of activity and aurovertin-sensitive ATP hydrolysis was 64–68% decreased in comparison with the control cells. The activity measurements data corresponded well with the electrophoretic analysis. The same results obtained with F_1-interacting aurovertin and F_o-interacting oligomycin indicated further that all remaining ATP hydrolytic activity was due to complete ATP synthase complexes with unaltered F_1–F_o interaction and not due to a presence of free and active F_1-ATPase molecules.

3.2. Downregulation of ATP5E gene decreases mitochondrial ATP production but does not uncouple oxidative phosphorylation

The functional effects of *ATP5E* silencing on mitochondrial energy conversion were analyzed by mitochondrial respiration in digitonin-permeabilized cells. As shown in Fig. 2A, mitochondria in the *ATP5E*-silenced cells were tightly coupled at state 4, but ADP-stimulated respiration was significantly lower although these cells had comparable respiratory capacity after uncoupling with FCCP (state 3 uncoupled) when compared with the control NS (Fig. 2A) or HEK293 (not shown) cells. The ADP-stimulated respiration in the *ATP5E*-silenced cells was fully sensitive to oligomycin. Direct measurements of mitochondrial membrane potential $\Delta\Psi_m$ with TPP^+-selective electrode (Fig. 2B) revealed comparable state 4 values of $\Delta\Psi_m$ in both control and *ATP5E*-silenced cells. In fact, an even higher state 4 value was found in the *ATP5E*-silenced cells (ΔpTPP, i.e. the difference of membrane potential with respect to the pTPP value with FCCP, was 0.47 and 0.64 in the control and silenced cells, respectively). Addition of ADP led to a much smaller decrease of $\Delta\Psi_m$ in the silenced cells (ΔpTPP decrease of 0.28 and 0.05 in the control and silenced cells, respectively), but the decrease was fully reversed by oligomycin, much the same as in control cells. Membrane potential measurements thus further supported the conclusion that the *ATP5E*-silenced cells are well coupled but the low content of ATP synthase complex limits the function of mitochondrial oxidative phosphorylation.

3.3. Silencing of the ATP5E gene leads to relative accumulation of F_o subunit c

An alteration of ATP synthase assembly due to low availability of ε subunit may lead to an accumulation of incomplete assemblies consisting of some enzyme subunits, e.g. F_1 ATPase subcomplexes, assuming that the ε subunit is added at the late stage of F_1 formation, i.e. after the γ and/or δ subunits. Having determined the cellular content of individual ATP synthase subunits, we found that *ATP5E* silencing reduced the content of the F_1 subunits α and ε as well as of the F_o subunits a and d (Fig. 3A) to a similar extent. The only subunit that was not reduced was the F_o subunit c. Normal content of subunit c was maintained in all cell lines with silenced *ATP5E*, demonstrating

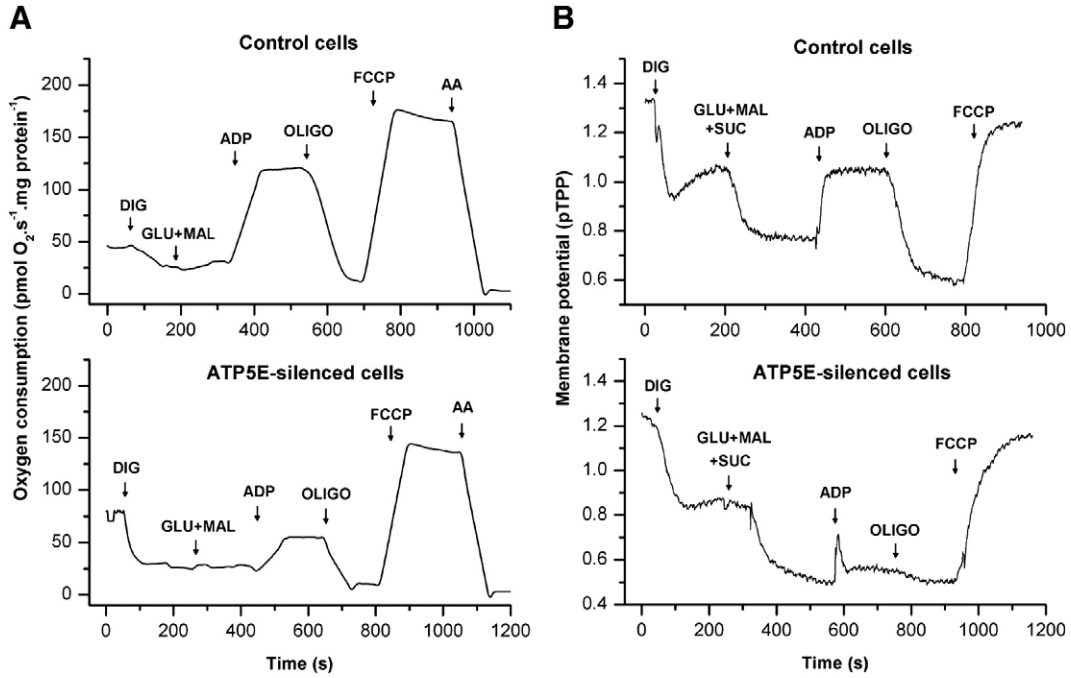

Fig. 2. ADP-stimulated respiration and ADP-induced decrease of mitochondrial membrane potential $\Delta\Psi_m$ in *ATP5E*-silenced cells. (A) Respiration and (B) $\Delta\Psi_m$ were measured in shE2a and NS cells permeabilized with digitonin (DIG) using 10 mM glutamate (GLU), 3 mM malate (MAL), 10 mM succinate (SUC), 1.5 mM ADP, 1 μM oligomycin (OLIGO), 1 μM FCCP and 1 μM antimycin A (AA). Respiration was expressed as oxygen consumption in pmol O2 s^{-1} mg $protein^{-1}$, mitochondrial membrane potential $\Delta\Psi_m$ measured with TPP^+-selective electrode was plotted as pTPP, *i.e.* natural logarithm of TPP^+ concentration (μM).

that if the ATP synthase assembly process was inhibited, the "excess" subunit c was not degraded and cleared out as other ATP synthase subunits.

To characterize further the accumulated subunit c, mitochondrial proteins were solubilized with DDM and analyzed for the content of ATP synthase subunits. As shown in Fig. 3B, the subunit c of *ATP5E*-silenced mitochondria was recovered in both soluble and insoluble fractions. In comparison with the control NS cells, both fractions from *ATP5E*-silenced cells showed a much higher content of subunit c relative to subunits α or d. Thus the solubilized proteins from *ATP5E*-silenced mitochondria were 2–2.5-fold enriched in subunit c and the DDM-insoluble pellet was enriched 4–10-fold.

When the solubilized mitochondrial proteins were subjected to 2D electrophoresis, BN/SDS-PAGE and WB analysis (Fig. 4), in control mitochondria all subunit c as well as subunit a were present in assembled F_oF_I ATP synthase complex and neither subunit c nor subunit a could be detected around 370 kDa where the F_1 subcomplex migrates. In mitochondria from the *ATP5E*-silenced cells, the subunit c signal was also present in the F_oF_1 complex, in a smaller amount, in a good correspondence with the reduced content of ATP synthase. In addition, significant signal of subunit c was found in the BN-PAGE region of about 200–400 kDa. In this region, however, no F_1 subunits α and β or F_o subunits a and d could be detected (Fig. 4).

4. Discussion

The present study demonstrates that the ε subunit is essential for the biosynthesis of F_1 catalytic part of mammalian ATP synthase complex and that a decreased amount of available subunit ε due to *ATP5E* silencing limits the cellular content of assembled and functional ATP synthase. As revealed by respiration and mitochondrial membrane potential $\Delta\Psi_m$ measurements, *ATP5E* silencing consequently decreases the activity of mitochondrial oxidative phosphorylation, not affecting the tight coupling of mitochondria. These data clearly indicate that the ε subunit plays an important role in the assembly and/or stability of F_1 moiety of mammalian ATP synthase.

The biogenesis of eukaryotic ATP synthase is a highly organized process depending on mutual action of different ancillary factors. At least 13 ATP synthase-specific factors exist in yeast. They are involved in transcription and translation of mtDNA-encoded subunits and in the assembly of the ATP synthase complex [26–29]. Much less is known about the mammalian enzyme where only 4 specific factors have been found so far. ATP11 and ATP12 are essential for the assembly of F_1 subunits α and β, similarly as their yeast homologues [30]. There is also a mammalian homologue of ATP23, yeast metalloprotease and chaperone of subunit 6 [27,31], but its function is not known. Recently, TMEM70 was identified as a novel factor of ATP synthase biogenesis in higher eukaryotes [32]. Its deficiency results in diminished amount of the full-size ATP synthase complex with detectable traces of the free F_1-part in some patients' tissues [33].

The biosynthesis and assembly of the F_1 catalytic part begins with the formation of $\alpha_3\beta_3$ oligomer catalyzed by ATP11 and ATP12 assembly factors [26] to which are then added subunits γ, δ and ε. It is not clear when and how exactly the subunit ε is inserted, but an ε null mutant of *S. cerevisiae* [17] indicated the presence of F_1 subcomplexes lacking also γ and δ subunits. Their expected size would be below that of $\alpha_3\beta_3\gamma\delta\varepsilon$ complex (ca. 370 kDa), and if they accumulate, they should be resolved by electrophoresis at native conditions. In our experiments with mammalian HEK293 cells, apparently neither ε-less F_1 molecules nor any smaller α/β-containing subassemblies could be detected after *ATP5E* silencing, indicating that either the lack of ε prevents their formation or such incomplete assemblies are very unstable and short-lived. This is in accordance with the observed low stability of F_1 in the ε null mutant in *S. cerevisiae* [17].

Another important finding of our study is that of unchanged content of subunit c in mitochondria upon *ATP5E* silencing. It demonstrates that in contrast to other ATP synthase subunits, the "excess" subunit c is not degraded. A major part of accumulated subunit c was resistant to solubilization with mild detergent DDM and likely represents insoluble and strongly hydrophobic subunit c aggregates. However, even the DDM-soluble fraction of *ATP5E*-silenced mitochondria was enriched in subunit c, this was resolved

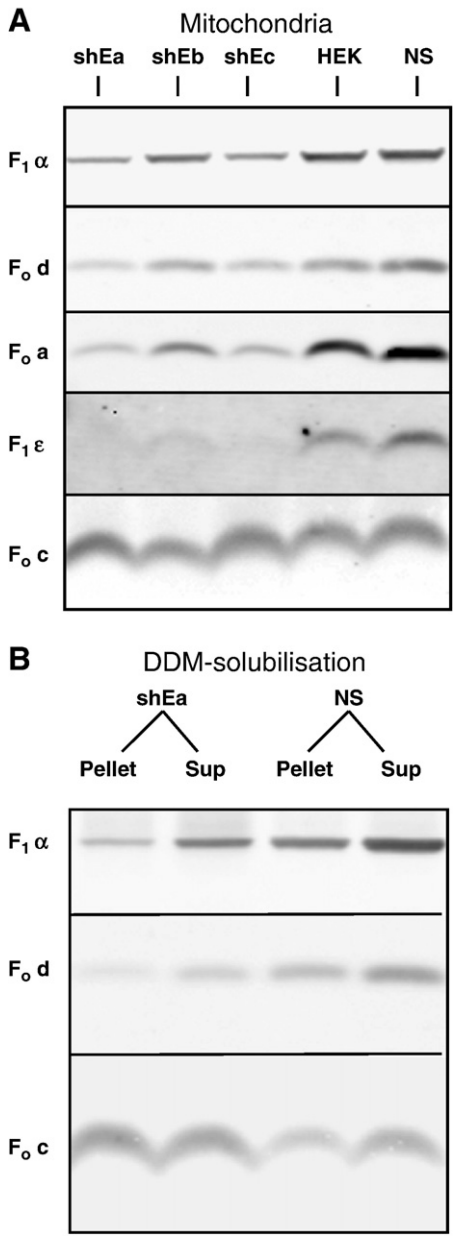

Fig. 3. Mitochondrial content of F_1 and F_o subunits in *ATP5E*-silenced cells. (A) Isolated mitochondria (10 μg protein aliquots) from silenced (shE2a, shE2b, shE2c) and control (HEK293, NS) cells and (B) 10 μg protein aliquots of 26000 ×*g* supernatant (Sup) and pellet (Pellet) from DDM-solubilized (2 g/g protein) mitochondria from silenced (shE2a) and control (NS) cells were analyzed by SDS-PAGE and WB. For detection antibodies to F_1 subunits α, and ε and F_o subunits a, d and c were used as indicated.

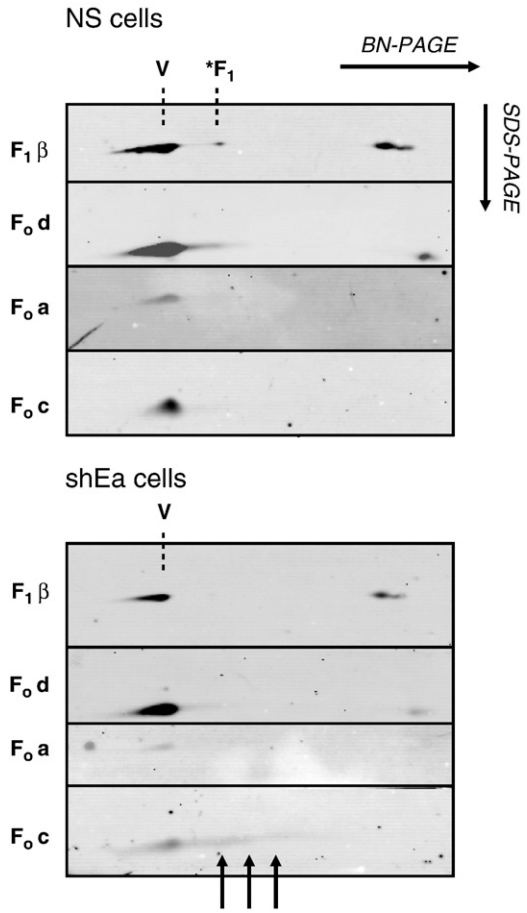

Fig. 4. Two-dimensional electrophoretic analysis of ATP synthase subunits in *ATP5E*-silenced cells. DDM-solubilized (2 g/g protein) proteins of mitochondria from shEa and NS cells were subjected to 2D electrophoresis and WB analysis was performed with indicated antibodies to ATP synthase subunits. V and $*F_1$ indicate position of ATP synthase monomer and F_1 subcomplex, arrows indicate accumulated subunit c.

by BN/SDS-PAGE in the second dimension corresponding to native complexes of about 200–400 kDa, which contained no F_1 subunits. Their origin is unclear at present, and they could represent breakdown products of subunit c oligomer attached to an unstable ε-lacking F_1 intermediate. However, their size is much larger than that of an oligomer of 10–12 copies of subunit c. Accumulated subunit c aggregates were also free of other F_o subunits, notably the subunit a, which is closely apposed to the c oligomer forming together the proton channel in the F_o structure. Apparently *ATP5E* silencing did not lead to enhanced proton conductivity of the inner mitochondrial membrane although a high proton leak was associated with ungated F_o structures in yeast ε null mutants [17]. Contrary to these findings, mitochondria of *ATP5E*-silenced cells showed an even tighter coupling than controls, in our work.

The accumulation of F_1 and larger assembly intermediates containing subunit c complexes of F_1 with subunit c oligomer were observed in various types of mammalian cultured cells or tissue samples with altered biogenesis of ATP synthase. They most likely represent dead-end products of a stalled assembly process resulting from a lack of mtDNA-encoded subunit a [34–36] or mutations in this subunit [36–38]. Upon *ATP5E* silencing in a human cell line, however, such intermediates are not present (Fig. 4). Interestingly, yeast F_1 mutants have been recently shown to inhibit translation of *ATP6* and *ATP8* mRNAs, but also in this case no F_1 or F_1-subunit c intermediates could be found in the *ΔATP15* strain [39].

Further studies are needed to resolve the properties and mechanism of subunit c accumulation, which is specifically induced by the absence of subunit ε and suggests a direct interaction and a regulatory role of ε in the assembly of ATP synthase rotor structure. Interestingly, no similar storage of subunit c could be found in mitochondria with ATP synthase deficiency of nuclear genetic origin due to mutations in *ATP12* [40] or *TMEM70* genes [32,41].

Acknowledgements

This work was supported by the Charles University (UK97807), the Grant Agency of the Ministry of Health of the Czech Republic (NS9759) and Ministry of Education, Youth and Sports of the Czech Republic (AV0Z 50110509, 1M0520).

References

[1] J.E. Walker, I.M. Fearnley, N.J. Gay, B.W. Gibson, F.D. Northrop, S.J. Powell, M.J. Runswick, M. Saraste, V.L. Tybulewicz, Primary structure and subunit stoichiometry of F1-ATPase from bovine mitochondria, J. Mol. Biol. 184 (1985) 677–701.

[2] I.R. Collinson, J.M. Skehel, I.M. Fearnley, M.J. Runswick, J.E. Walker, The F1F0-ATPase complex from bovine heart mitochondria: the molar ratio of the subunits in the stalk region linking the F1 and F0 domains, Biochemistry 35 (1996) 12640–12646.

[3] S. Anderson, A.T. Bankier, B.G. Barrell, M.H.L. de Bruijn, A.R. Coulson, J. Drouin, I.C. Eperon, D.P. Nierlich, B.A. Roe, F. Sanger, P.H. Schreier, A.J.H. Smith, R. Staden, I.G. Young, Sequence and organization of the human mitochondrial genome, Nature 290 (1981) 457–465.

[4] S. Karrasch, J.E. Walker, Novel features in the structure of bovine ATP synthase, J. Mol. Biol. 290 (1999) 379–384.

[5] C. Gibbons, M.G. Montgomery, A.G. Leslie, J.E. Walker, The structure of the central stalk in bovine F(1)-ATPase at 2.4 A resolution, Nat. Struct. Biol. 7 (2000) 1055–1061.

[6] J.L. Rubinstein, J.E. Walker, R. Henderson, Structure of the mitochondrial ATP synthase by electron cryomicroscopy, EMBO J. 22 (2003) 6182–6192.

[7] J.E. Walker, V.K. Dickson, The peripheral stalk of the mitochondrial ATP synthase, Biochim. Biophys. Acta 1757 (2006) 286–296.

[8] B. Meyer, I. Wittig, E. Trifilieff, M. Karas, H. Schagger, Identification of two proteins associated with mammalian ATP synthase, Mol. Cell. Proteomics 6 (2007) 1690–1699.

[9] G.I. Belogrudov, B. Factor, is essential for ATP synthesis by mitochondria, Arch. Biochem. Biophys. 406 (2002) 271–274.

[10] O. Vinas, S.J. Powell, M.J. Runswick, V. Iacobazzi, J.E. Walker, The epsilon-subunit of ATP synthase from bovine heart mitochondria. Complementary DNA sequence, expression in bovine tissues and evidence of homologous sequences in man and rat, Biochem. J. 265 (1990) 321–326.

[11] J. Lai-Zhang, Y. Xiao, D.M. Mueller, Epistatic interactions of deletion mutants in the genes encoding the F1-ATPase in yeast Saccharomyces cerevisiae, EMBO J. 18 (1999) 58–64.

[12] J. Lai-Zhang, D.M. Mueller, Complementation of deletion mutants in the genes encoding the F1-ATPase by expression of the corresponding bovine subunits in yeast S. cerevisiae, Eur. J. Biochem. 267 (2000) 2409–2418.

[13] D. Stock, A.G. Leslie, J.E. Walker, Molecular architecture of the rotary motor in ATP synthase, Science 286 (1999) 1700–1705.

[14] F. Penin, G. Deleage, D. Gagliardi, B. Roux, D.C. Gautheron, Interaction between delta and epsilon subunits of F1-ATPase from pig heart mitochondria. Circular dichroism and intrinsic fluorescence of purified and reconstituted delta epsilon complex, Biochemistry 29 (1990) 9358–9364.

[15] G.L. Orriss, M.J. Runswick, I.R. Collinson, B. Miroux, I.M. Fearnley, J.M. Skehel, J.E. Walker, The delta- and epsilon-subunits of bovine F1-ATPase interact to form a heterodimeric subcomplex, Biochem. J. 314 (1996) 695–700.

[16] V. Kabaleeswaran, N. Puri, J.E. Walker, A.G. Leslie, D.M. Mueller, Novel features of the rotary catalytic mechanism revealed in the structure of yeast F1 ATPase, EMBO J. 25 (2006) 5433–5442.

[17] E. Guelin, J. Chevallier, M. Rigoulet, B. Guerin, J. Velours, ATP synthase of yeast mitochondria. Isolation and disruption of the ATP epsilon gene, J. Biol. Chem. 268 (1993) 161–167.

[18] X.J. Chen, Absence of F1-ATPase activity in Kluyveromyces lactis lacking the epsilon subunit, Curr. Genet. 38 (2000) 1–7.

[19] H.A. Bentlage, U. Wendel, H. Schagger, H.J. ter Laak, A.J. Janssen, J.M. Trijbels, Lethal infantile mitochondrial disease with isolated complex I deficiency in fibroblasts but with combined complex I and IV deficiencies in muscle, Neurology 47 (1996) 243–248.

[20] H. Schägger, G. von Jagow, Blue native electrophoresis for isolation of membrane protein complexes in enzymatically active form, Anal. Biochem. 199 (1991) 223–231.

[21] H. Schagger, G. von Jagow, Tricine-sodium dodecyl sulfate-polyacrylamide gel electrophoresis for the separation of proteins in the range from 1 to 100 kDa, Anal. Biochem. 166 (1987) 368–379.

[22] A. Dubot, C. Godinot, V. Dumur, B. Sablonniere, T. Stojkovic, J.M. Cuisset, A. Vojtiskova, P. Pecina, P. Jesina, J. Houstek, GUG is an efficient initiation codon to translate the human mitochondrial ATP6 gene, Biochem. Biophys. Res. Commun. 313 (2004) 687–693.

[23] J. Houstek, U. Andersson, P. Tvrdik, J. Nedergaard, B. Cannon, The expression of subunit c correlates with and thus may limit the biosynthesis of the mitochondrial F0F1-ATPase in brown adipose tissue, J. Biol. Chem. 270 (1995) 7689–7694.

[24] A. Baracca, E. Amler, G. Solaini, G. Parenti Castelli, G. Lenaz, J. Houstek, Temperature-induced states of isolated F1-ATPase affect catalysis, enzyme conformation and high-affinity nucleotide binding sites, Biochim. Biophys. Acta 976 (1989) 77–84.

[25] A. Labajova, A. Vojtiskova, P. Krivakova, J. Kofranek, Z. Drahota, J. Houstek, Evaluation of mitochondrial membrane potential using a computerized device with a tetraphenylphosphonium-selective electrode, Anal. Biochem. 353 (2006) 37–42.

[26] S.H. Ackerman, A. Tzagoloff, Function, structure, and biogenesis of mitochondrial ATP synthase, Prog. Nucleic Acid Res. Mol. Biol. 80 (2005) 95–133.

[27] X. Zeng, W. Neupert, A. Tzagoloff, The metalloprotease encoded by ATP23 has a dual function in processing and assembly of subunit 6 of mitochondrial ATPase, Mol. Biol. Cell 18 (2007) 617–626.

[28] X. Zeng, A. Hourset, A. Tzagoloff, The Saccharomyces cerevisiae ATP22 gene codes for the mitochondrial ATPase subunit 6-specific translation factor, Genetics 175 (2007) 55–63.

[29] X. Zeng, M.H. Barros, T. Shulman, A. Tzagoloff, ATP25, a new nuclear gene of Saccharomyces cerevisiae required for expression and assembly of the Atp9p subunit of mitochondrial ATPase, Mol. Biol. Cell 19 (2008) 1366–1377.

[30] S.H. Ackerman, Atp11p and Atp12p are chaperones for F(1)-ATPase biogenesis in mitochondria, Biochim. Biophys. Acta 1555 (2002) 101–105.

[31] C. Osman, C. Wilmes, T. Tatsuta, T. Langer, Prohibitins interact genetically with Atp23, a novel processing peptidase and chaperone for the F1FO-ATP synthase, Mol. Biol. Cell 18 (2007) 627–635.

[32] A. Cizkova, V. Stranecky, J.A. Mayr, M. Tesarova, V. Havlickova, J. Paul, R. Ivanek, A.W. Kuss, H. Hansikova, V. Kaplanova, M. Vrbacky, H. Hartmannova, L. Noskova, T. Honzik, Z. Drahota, M. Magner, K. Hejzlarova, W. Sperl, J. Zeman, J. Houstek, S. Kmoch, TMEM70 mutations cause isolated ATP synthase deficiency and neonatal mitochondrial encephalocardiomyopathy, Nat. Genet. 40 (2008) 1288–1290.

[33] J. Houstek, S. Kmoch, J. Zeman, TMEM70 protein — a novel ancillary factor of mammalian ATP synthase, Biochim. Biophys. Acta 1787 (2009) 529–532.

[34] L.G. Nijtmans, P. Klement, J. Houstek, C. van den Bogert, Assembly of mitochondrial ATP synthase in cultured human cells: implications for mitochondrial diseases, Biochim. Biophys. Acta 1272 (1995) 190–198.

[35] P. Jesina, M. Tesarova, D. Fornuskova, A. Vojtiskova, P. Pecina, V. Kaplanova, H. Hansikova, J. Zeman, J. Houstek, Diminished synthesis of subunit a (ATP6) and altered function of ATP synthase and cytochrome c oxidase due to the mtDNA 2 bp microdeletion of TA at positions 9205 and 9206, Biochem. J. 383 (2004) 561–571.

[36] R. Carrozzo, I. Wittig, F.M. Santorelli, E. Bertini, S. Hofmann, U. Brandt, H. Schagger, Subcomplexes of human ATP synthase mark mitochondrial biosynthesis disorders, Ann. Neurol. 59 (2006) 265–275.

[37] J. Houstek, P. Klement, J. Hermanska, H. Houstkova, H. Hansikova, C. van den Bogert, J. Zeman, Altered properties of mitochondrial ATP-synthase in patients with a T —> G mutation in the ATPase 6 (subunit a) gene at position 8993 of mtDNA, Biochim. Biophys. Acta 1271 (1995) 349–357.

[38] L.G. Nijtmans, N.S. Henderson, G. Attardi, I.J. Holt, Impaired ATP synthase assembly associated with a mutation in the human ATP synthase subunit 6 gene, J. Biol. Chem. 276 (2001) 6755–6762.

[39] M. Rak, A. Tzagoloff, F1-dependent translation of mitochondrially encoded Atp6p and Atp8p subunits of yeast ATP synthase, Proc. Natl. Acad. Sci. USA 106 (2009) 18509–18514.

[40] L. De Meirleir, S. Seneca, W. Lissens, I. De Clercq, F. Eyskens, E. Gerlo, J. Smet, R. Van Coster, Respiratory chain complex V deficiency due to a mutation in the assembly gene ATP12, J. Med. Genet. 41 (2004) 120–124.

[41] J.A. Mayr, J. Paul, P. Pecina, P. Kurnik, H. Förster, U. Fötschl, W. Sperl, J. Houstek, Reduced respiratory control with ADP and changed pattern of respiratory chain enzymes due to selective deficiency of the mitochondrial ATP synthase, Pediatr. Res. 55 (2004) 1–7.

Biochem. J. (2015) **466**, 601–611 (Printed in Great Britain) doi:10.1042/BJ20141462

Alteration of structure and function of ATP synthase and cytochrome *c* oxidase by lack of F_o-a and Cox3 subunits caused by mitochondrial DNA 9205delTA mutation

Kateřina Hejzlarová*, Vilma Kaplanová*, Hana Nůsková*, Nikola Kovářová*, Pavel Ješina*, Zdeněk Drahota*, Tomáš Mráček*, Sara Seneca† and Josef Houštěk*[1]

*Institute of Physiology Academy of Sciences of the Czech Republic v.v.i., Vídeňská 1083, 14220 Prague 4, Czech Republic
†Center for Medical Genetics, UZ Brussel, Vrije Universiteit Brussel, Laarbeeklaan 101, 1090 Brussels, Belgium

Mutations in the *MT-ATP6* gene are frequent causes of severe mitochondrial disorders. Typically, these are missense mutations, but another type is represented by the 9205delTA microdeletion, which removes the stop codon of the *MT-ATP6* gene and affects the cleavage site in the *MT-ATP8/MT-ATP6/MT-CO3* polycistronic transcript. This interferes with the processing of mRNAs for the Atp6 (F_o-a) subunit of ATP synthase and the Cox3 subunit of cytochrome *c* oxidase (COX). Two cases described so far presented with strikingly different clinical phenotypes – mild transient lactic acidosis or fatal encephalopathy. To gain more insight into the pathogenic mechanism, we prepared 9205delTA cybrids with mutation load ranging between 52 and 99 % and investigated changes in the structure and function of ATP synthase and the COX. We found that 9205delTA mutation strongly reduces the levels of both F_o-a and Cox3 proteins. Lack of F_o-a alters the structure but not the content of ATP synthase, which assembles into a labile, ∼60 kDa smaller, complex retaining ATP hydrolytic activity but which is unable to synthesize ATP. In contrast, lack of Cox3 limits the biosynthesis of COX but does not alter the structure of the enzyme. Consequently, the diminished mitochondrial content of COX and non-functional ATP synthase prevent most mitochondrial ATP production. The biochemical effects caused by the 9205delTA microdeletion displayed a pronounced threshold effect above ∼90 % mutation heteroplasmy. We observed a linear relationship between the decrease in subunit F_o-a or Cox3 content and the functional presentation of the defect. Therefore we conclude that the threshold effect originated from a gene–protein level.

Key words: ATP synthase, cytochrome *c* oxidase, mitochondrial diseases, mtDNA *MT-ATP6* mutation, oxidative phosphorylation, threshold effect.

INTRODUCTION

Mitochondrial diseases due to disorders of the oxidative phosphorylation system (OXPHOS) are frequently caused by mitochondrial DNA (mtDNA) point mutations in protein-coding genes [1]. They alter the amino acid composition or (less frequently) lead to the formation of truncated protein if a premature stop codon has been formed. Up to now, over 200 point mutations of mtDNA have been reported. By their nature, they can be either homoplasmic and/or heteroplasmic and affect different mitochondrially synthesized subunits (www.mitomap.org [2]). In 1996, Seneca et al. [3] found a new type of mtDNA mutation that affects the *MT-ATP6* and *MT-CO3* genes by microdeletion of two bases, TA, in mtDNA at positions 9205–9206 (9205delTA). This mutation removes the stop codon of the *MT-ATP6* gene and alters the splicing site for processing of the polycistronic *MT-ATP8/MT-ATP6/MT-CO3* transcript. The 9205delTA mutation can be expected to alter the levels of *MT-ATP6* and *MT-CO3* transcripts and thus the synthesis of the F_o-a (Atp6) subunit of ATP synthase and the Cox3 subunit of cytochrome *c* oxidase (COX), which could limit the biogenesis of these two respiratory chain complexes.

The first case with the 9205delTA mutation presented with a relatively mild phenotype – seizures with several episodes of transient lactic acidosis [3]. Analysis of patient fibroblasts with the reported homoplasmic mutation revealed no changes in *MT-ATP6* and *MT-CO3* mRNA processing, a significant increase in deadenylation of *MT-ATP8/MT-ATP6* bicistron [4], and relatively insignificant biochemical changes [5]. The second case of the 9205delTA mutation was a child with severe encephalopathy and hyperlactacidaemia [6]. In correspondence with the fatal clinical course, the patient fibroblasts showed a pronounced alteration of ATP synthase structure and a low activity and protein content of COX resulting in a ∼70 % decrease in mitochondrial ATP synthesis [7]. There was a marked and specific decrease in *MT-ATP8/MT-ATP6/MT-CO3* primary transcript processing. F_o-a subunit content and its *de novo* synthesis were reduced 10-fold when compared with the other ATP synthase subunits. Both cases were reported to be homoplasmic and therefore we speculated that an additional nuclear-encoded mitochondrial factor might be involved in processing of the *MT-ATP8/MT-ATP6/MT-CO3* transcript and modulate the deleterious effects of the 9205delTA mutation [7]. It was of interest to compare the cells from both cases. While both cases were supposedly homoplasmic,

Abbreviations: BNE, blue native electrophoresis; COX, cytochrome *c* oxidase; DDM, *n*-dodecyl-β-D-maltoside; DMEM, Dulbecco's modified Eagle's medium; FCCP, carbonyl cyanide *p*-trifluoromethoxyphenylhydrazone; hrCNE1, high-resolution clear native electrophoresis; LLS, Leigh-like syndrome; LS, Leigh syndrome; MILS, maternally inherited LS; NARP, neurogenic muscle weakness, ataxia and retinitis pigmentosa; OSCP, oligomycin-sensitivity conferral protein; OXPHOS, oxidative phosphorylation system; TMPD, *N,N,N′,N′*-tetramethyl-*p*-phenylenediamine; TPP^+, tetraphenylphosphonium; WB, Western blot.

[1] To whom correspondence should be addressed (email houstek@biomed.cas.cz).

methodological limitations mean that they can only be claimed to have a mutation load >98 %. Later we identified heteroplasmy of the 9205delTA mutation in the fibroblasts of high passage from the first patient, indicating that negative segregation of the mutation occurred during the prolonged cultivation and unmasked the mutation heteroplasmy. The phenotypic differences between the two patients may therefore be caused by a threshold effect with a very steep dependence close to homoplasmy [8] and tissue-specific differences in heteroplasmy.

To gain more insight into the pathogenic mechanism of the 9205delTA mutation, we prepared cybrid cell lines with a varying load of the mtDNA 9205delTA mutation and investigated changes in the structure and function of ATP synthase and COX. We found that the 9205delTA mutation strongly reduces the levels of both F_o-a and Cox3 proteins, alters the structure of ATP synthase, decreases the content of COX, and prevents most of the mitochondrial ATP synthesis. All of the biochemical effects exerted a pronounced threshold effect above 90 % heteroplasmy. In addition, we found that a slightly smaller ATP synthase complex devoid of the F_o-a subunit is formed but it is rather labile and unable to synthesize ATP.

MATERIALS AND METHODS

Chemicals

Unless otherwise indicated, chemicals of the highest purity were obtained from Sigma–Aldrich.

Preparation of cybrids and isolation of mitochondria

Transmitochondrial cybrids were prepared according to [9]. Fibroblasts from the two patients P1 [3] and P2 [7] harbouring the 9205delTA mutation and from controls were enucleated by centrifugation in Dulbecco's modified Eagle's medium (DMEM, BioTech) containing 10 μg/ml cytochalasin B and then fused with mtDNA-less (ρ^0) 143B TK$^-$ osteosarcoma cells by adding a 50 % (w/v) solution of PEG with 10 % (v/v) DMSO. Cells were selected for 3 weeks in DMEM containing 5 % (v/v) fetal bovine serum, 0.1 mg/ml 5-bromodeoxyuridine and lacking uridine. The ring-cloned and subcloned cybrid cells were grown to ~90 % confluence, harvested using 0.05 % (w/v) trypsin and 0.02 % (w/v) EDTA, and washed twice in PBS before use.

Mitochondria from cybrid or fibroblast cells were isolated at 4 °C by a hypo-osmotic shock method [10]. The freshly harvested cells were disrupted in 10 mM Tris/HCl, pH 7.4, homogenized in a Teflon/glass homogenizer (10 % homogenate, w/v) and then sucrose was added to a final concentration of 0.25 M. Mitochondria were sedimented from the 600 ***g*** postnuclear supernatant by 10 min centrifugation at 10000 ***g***, washed, and resuspended in 0.25 M sucrose, 2 mM EGTA, 40 mM KCl and 20 mM Tris/HCl, pH 7.4.

In some experiments we also used the membrane fraction obtained by 10 min centrifugation of cell homogenate (10 % (w/v) in 83 mM sucrose and 6.6 mM imidazole, pH 7.0) at 15000 ***g*** [11]. Samples were stored at − 80 °C.

PCR and restriction analysis

To determine the amount of 9205delTA mtDNA, the isolated DNA was amplified by PCR using mismatch primers (bold) 5′-CCT CTA CCT GCA CGA CAA T**GC** A-3′ (forward) and 5′-CGT TAT G**C**A **T**TG GAA GTG AAA TCA C-3′ (reverse), corresponding to nt 9183–9329 (147 bp) [5]. Mismatch primers generated two *Nsi*I restriction sites in the case of wild-type mtDNA (fragments 116 + 22 + 9 bp) and one *Nsi*I restriction site in the case of mutated mtDNA (138 + 9 bp). PCR products were digested with *Nsi*I (Roche) for 3 h at 37 °C, the enzyme was inactivated for 15 min at 65 °C, and DNA fragments were separated on 1.5 % (w/v) agarose in TBE buffer (0.09 M Tris/HCl, 0.09 M H_3BO_3 and 2 mM sodium EDTA, pH 8.0). Ethidium bromide-stained gels were visualized on the transiluminator BioDocAnalyze (Biometra) and the signal was quantified using Aida 3.21 Image Analyzer. Heteroplasmy was expressed as a percentage of mutated mtDNA relative to the total signal of amplified mtDNA.

Electrophoresis, Western blot analysis, in-gel ATPase activity

SDS-PAGE [12] was performed on 10 % (w/v) polyacrylamide slab minigels (MiniProtean System, Bio-Rad Laboratories) at room temperature. Samples of whole cells or isolated mitochondria were heated for 20 min at 40 °C in a sample lysis buffer (2 % (v/v) 2-mercaptoethanol (Fluka), 4 % (w/v) SDS (Serva), 50 mM Tris/HCl (pH 7.0) and 10 % (v/v) glycerol).

Separation of native OXPHOS complexes by blue native (BNE) [11,13] or high-resolution clear native electrophoresis (hrCNE1 system) [14] was performed on polyacrylamide gradient (6–15 % for COX analysis, 4–13 % for ATP synthase analysis) minigels at 7 °C. Mitochondrial or membrane fraction proteins were solubilized with *n*-dodecyl-β-D-maltoside (DDM) or digitonin at the indicated detergent/protein ratio for 15 min on ice. The samples were centrifuged for 20 min at 4 °C and 30000 ***g***, and either Coomassie Brilliant Blue G dye (Serva Blue G-250, 0.125 g/g detergent) or Ponceau Red dye (0.005 %) and 5 % glycerol were added to the supernatants before electrophoresis. For two-dimensional (2D) analysis, strips of the first dimension native gels were incubated for 1 h in 1 % (w/v) SDS and 1 % (v/v) 2-mercaptoethanol at room temperature, washed in water and subjected to SDS-PAGE for separation in the second dimension.

Gels were blotted onto PVDF membrane (Millipore) by semi-dry electrotransfer (1 h at 0.8 mA/cm^2) and the membrane was blocked in 5 % defatted milk (Promil) in TBS (150 mM NaCl and 10 mM Tris/HCl, pH 7.5). The membranes were washed twice in TBST (TBS with 0.1 % (v/v) Tween-20) and immunodecorated with the following primary antibodies diluted in TBST: rabbit polyclonal antibodies to subunits F_o-c (1:1000) and F_o-a (1:500) [7], mouse monoclonal antibodies from Abcam to subunits F_1-α (1:1000, ab110273), F_1-β (1:2000, ab14730), F_o-d (1:700, ab110275), OSCP (oligomycin-sensitivity conferral protein) (1:250, ab110276), Cox1 (1:1000, ab14705), Cox2 (1:1000, ab110258), Cox4 (1:1000, ab110261), Cox5a (1:500, ab110262), Cox6c (1:500, ab110267), Core2 subunit (1:1000, ab14745) and pyruvate dehydrogenase (PDH, 1:1000, ab110334). Goat polyclonal antibody to Cox3 (1:200 in TBST with 3 % (w/v) BSA) was from Santa Cruz Biotechnology (sc-23986), rabbit polyclonal antibody to porin (1:1000) was a gift from Professor Vito de Pinto (Dipartimento di Scienze Chimiche - Università di Catania, Catania, Italy). For a quantitative detection, the following infra-red fluorescent secondary antibodies (Alexa Fluor 680, Life Technologies; IRDye 800, Rockland Immunochemicals) diluted in TBST were used: goat anti-mouse IgG (1:3000, A21058), goat anti-rabbit IgG (1:3000, A21109), donkey anti-rabbit IgG (1:3000, 611-732-127), and donkey anti-goat IgG (1:3000, A21084). The fluorescence was detected using ODYSSEY infra-red imaging system (LI-COR Biosciences) and the signal was quantified using Aida 3.21 Image Analyzer software.

ATPase hydrolytic activity was detected on native gels immediately after electrophoresis according to [15]. Briefly, gels were incubated for 1 h in 35 mM Tris/HCl, 270 mM glycine, 14 mM $MgSO_4$, 0.2 % (w/v) $Pb(NO_3)_2$ and 8 mM ATP, pH 8.3,

and white lead phosphate precipitates were documented by scanning.

High-resolution oxygraphy

Oxygen consumption by cybrid cells (0.75 mg protein/ml) was determined at 30 °C in a KCl medium (80 mM KCl, 10 mM Tris/HCl, 3 mM $MgCl_2$, 1 mM EDTA and 5 mM potassium phosphate, pH 7.4) as described previously [16], using Oxygraph-2k (Oroboros). Cells were permeabilized by 0.05 g of digitonin/g of protein. Respiration was measured with 10 mM succinate in the presence of 2.5 μM rotenone and 25 μM Ap5A (P^1,P^5-di(adenosine-5′)pentaphosphate), then 1.25 mM ADP was added. ADP-stimulated respiration was inhibited after 6 min with 1 μM oligomycin and after 2 min, 0.1 μM FCCP (carbonyl cyanide *p*-trifluoromethoxyphenylhydrazone) was added. Activity of COX was measured with 5 mM ascorbate and 1 mM TMPD (*N,N,N′,N′*-tetramethyl-*p*-phenylenediamine) in the presence of 1 mg/ml antimycin A and was corrected for substrate autoxidation insensitive to 0.33 mM KCN. Oxygen consumption was expressed in pmol of oxygen/s/mg of protein.

Mitochondrial membrane potential $\Delta\psi_m$ measurements

$\Delta\psi_m$ was measured with TPP^+ (tetraphenylphosphonium)-selective electrode in 1 ml of KCl medium as described in [16]. Cells (2 mg of protein/ml) were permeabilized with digitonin (0.04 g/g of protein) and the following substrates and inhibitors were used: 10 mM succinate, 10 mM glutamate, 3 mM malate, 1.5 mM ADP, 1 μM oligomycin and 1 μM FCCP. The membrane potential was plotted as pTPP, i.e. negative decimal logarithm of TPP^+ concentration.

ATP synthesis

During respiration measurements, 10 μl samples were collected from the oxygraphic chamber (before and 6 min after ADP addition) and immediately mixed with the same volume of 100 % DMSO. ATP content was then determined in DMSO-quenched samples by a luciferin–luciferase reaction [17]. Bioluminescence was measured in the medium containing 25 mM tricine, 5 mM $MgSO_4$, 0.1 mM EDTA, 1 mM dithiothreitol, 0.6 mM luciferin (Promega) and 6×10^7 luciferase units/ml luciferase (Promega), pH 7.8, using 1250 Luminometer (BioOrbit). Calibration curve was measured in the range 0–10 pmol of ATP. ATP production was expressed in nmol of ATP/min/mg of protein.

Ethics

The present study was carried out in accordance with the Declaration of Helsinki of the World Medical Association and was approved by the Committee of Medical Ethics of Institute of Physiology Academy of Sciences of the Czech Republic. Informed consent from the parents of the patients was obtained.

RESULTS

Cybrids with mtDNA 9205delTA mutation

The cybrid cell lines used in the present study were derived from the fibroblasts of two patients (P1 and P2) with the 9205delTA mutation (Figure 1A) and included cybrid clones of varying mutation heteroplasmy. To estimate the relationship between biochemical consequences and the 9205delTA mutation load we used wild-type mtDNA homoplasmic control cybrids, several clones of 9205delTA heteroplasmic cybrids with the content of

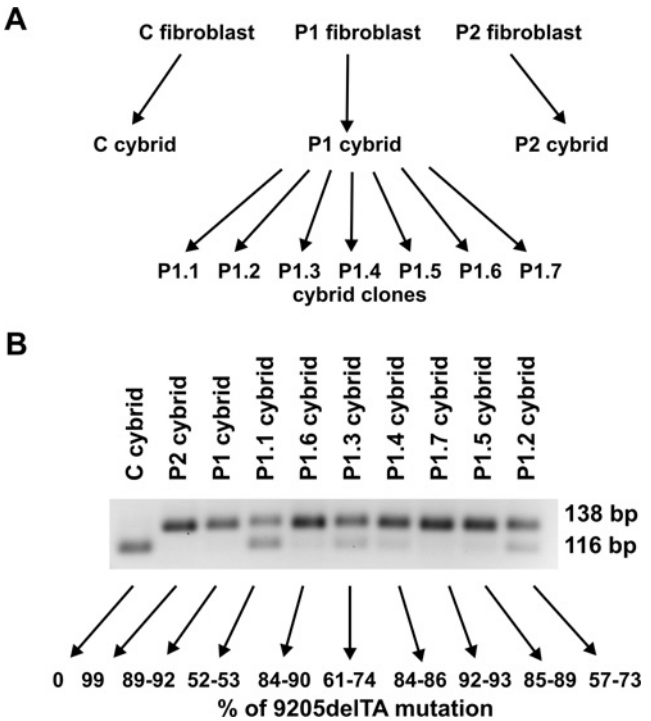

Figure 1 Cybrid cell lines used in the study

(**A**) Fibroblasts from two patients with the mtDNA 9205delTA microdeletion and from a control were enucleated and then fused with mtDNA-less (ρ^0) 143B TK^- osteosarcoma cells to produce transmitochondrial cybrid cell lines. (**B**) Mutation load in cybrid clones and subclones was analysed by restriction analysis with *Nsi*I of nt 9183–9329 mtDNA PCR products and was calculated from the amounts of 138 bp and 116 bp fragments corresponding to the mutated and wild-type mtDNA, respectively.

9205delTA mtDNA ranging between 52 and 92 % (derived from P1 fibroblasts) and 9205delTA cybrids with >99 % of mutated mtDNA (derived from P2 fibroblasts).

Throughout the course of the studies, individual cybrid cell lines maintained a stable heteroplasmy level, which was routinely checked by restriction analysis of PCR products and was expressed as a percentage of the mutated mtDNA relative to the total mtDNA (Figure 1B).

Changes in mitochondrial content and composition of ATP synthase and cytochrome *c* oxidase subunits in 9205delTA homoplasmic cells

Previous analysis of fibroblasts from the P2 patient demonstrated a very strong reduction in subunit F_o-a content [7]. The reduced content of COX subunits Cox1, Cox4 and Cox6c as well as altered maturation of Cox3 mRNA further indicated that the 9205delTA mutation may also disrupt the synthesis of subunit Cox3. To verify this assumption, we analysed cell homogenates and isolated mitochondria from control and 9205delTA homoplasmic cybrids by SDS-PAGE and Western blot (WB) (Figure 2A) using antibodies against several subunits of ATP synthase and COX. To quantify their specific content, the signals of individual subunits were normalized to those of porin and expressed as a percentage of control (Figure 2B).

The subunit F_o-a content was strongly reduced in 9205delTA homoplasmic cybrid cells; only a very low amount of F_o-a could be detected in isolated mitochondria. In contrast, F_1-α and F_1-β subunits of the catalytic part were present in near-normal levels

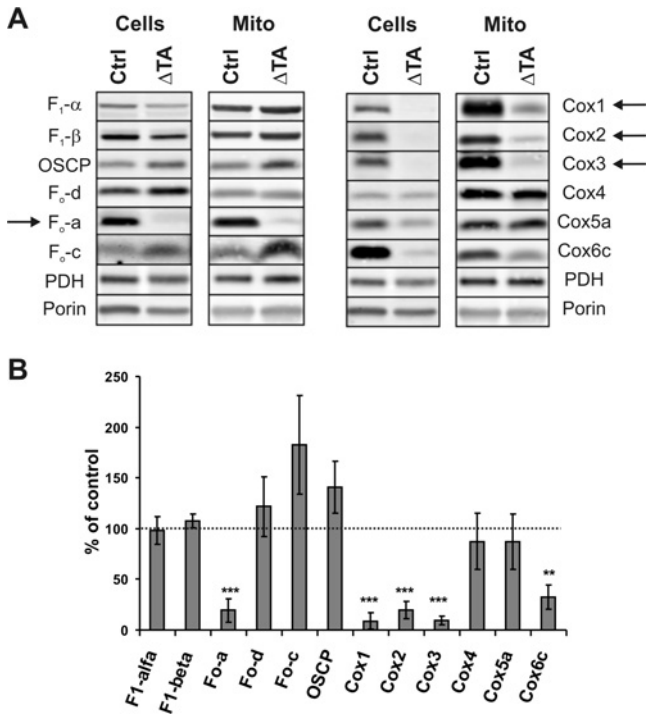

Figure 2 Specific content of ATP synthase and cytochrome *c* oxidase subunits in control and 9205delTA cybrid cells and isolated mitochondria

(**A**) Protein aliquots of cell homogenate (Cells, 15 μg) and isolated mitochondria (Mito, 10 μg) from control (Ctrl) and 9205delTA homoplasmic (ΔTA) cybrids were analysed by SDS-PAGE and WB with antibodies against indicated subunits. (**B**) Specific content of each subunit in 9205delTA samples was normalized for the signal of porin and expressed as a percentage of the content in the control. Data are the means $\pm$ S.E.M. for five experiments. $^{***}P < 0.001$, $^{**}P < 0.01$ (Student's *t* test).

in both cell homogenates and isolated mitochondria. Similarly, a normal or even increased content was found in the case of several subunits of F_o membrane part (F_o-d, OSCP and F_o-c; Figure 2B). Thus, with the exception of subunit F_o-a which was reduced to less than 20 %, all other ATP synthase subunits were present in normal or increased levels in homoplasmic 9205delTA cybrids when compared with the control cybrids.

The analysis of Cox3 clearly showed that the content of this subunit was strongly reduced due to the 9205delTA mutation. Interestingly, all mitochondrially encoded COX subunits (Cox1, Cox2 and Cox3) were similarly decreased in whole cells and isolated mitochondria (Figure 2A) and their respective content in 9205delTA homoplasmic cybrids was 8–20 % of the control (Figure 2B). Nuclear-encoded subunits were less affected and their content varied – Cox4 was almost normal in whole cells and isolated mitochondria, Cox6c was decreased to ~40 % of control in both samples, and Cox5a was decreased in the whole cells but not in isolated mitochondria (Figure 2A).

Changes in the assembled complexes of ATP synthase and cytochrome *c* oxidase in 9205delTA homoplasmic cells

Further, we were interested how the primary lack of F_o-a and Cox3 alters the properties of the assembled ATP synthase and COX. Mitochondria from the control and homoplasmic 9205delTA cybrids were solubilized by DDM or digitonin, resolved by BNE and visualized by WB using subunit-specific antibodies.

As shown in Figures 3A and 3B, in DDM-solubilized mitochondrial proteins of control cells, practically all F_1-β was recovered in ATP synthase monomer (complex V, cV) of approximately 600 kDa and a small amount, less than 10 %, was present in subcomplexes of 460 and 350 kDa. In 9205delTA cybrids, the pattern detected by anti-F_1-β antibody was completely different and revealed a strongly reduced amount of ATP synthase monomer (cV) but a high content of smaller sub-assemblies. The largest one, cV*, was approximately 60 kDa smaller than the cV monomer. Judging from the presence of subunits F_o-c and F_o-a, this could represent an almost complete cV without subunit F_o-a and possibly some other small subunit(s) (Figure 3A). This cV* was present in a similar amount as cV in 9205delTA cybrids but was completely absent from control cells. The majority of F_1-β was present in the three other, smaller, subcomplexes with the largest one being also the most abundant. None of those subcomplexes contained the F_o-a subunit. As similar subcomplexes were repeatedly described in *MT-ATP6* patients and ρ° cells [18–21], one may predict their composition. The 460 kDa subcomplex is thus expected to contain F_1 with the ring of F_o-c subunits (c-ring) and the inhibitory factor IF_1 (F_1IF_1c); the 380 kDa subcomplex corresponds to F_1IF_1, and the 350 kDa subcomplex represents F_1 alone. Judging from the F_1-β signal the relative content of these forms was 16:23:46:8:7 % for F_1:F_1IF_1:F_1IF_1c:cV*:cV, respectively. Importantly, the total amount of DDM-solubilized F_1-β signal, and thus of various cV assembly intermediates, in 9205delTA cybrids was the same or even higher than in control cells. The increase in DDM concentration from 2 g/g of protein to 4 g/g of protein did not affect the observed pattern of ATP synthase assembly forms (Figure 3A).

While it was previously proposed that ATP synthase subcomplexes observed in cells with *MT-ATP6* mutations do represent the breakdown products of assembled ATP synthase with mutated F_o-a [19], their formation may also be an artefact of the stringent conditions during BNE separation as was observed in ρ° cells [22]. Therefore, we used hrCNE1 to analyse ATP synthase assembly in 9205delTA cells. As shown in Figure 3C, when the DDM-solubilized proteins were resolved by hrCNE1, predominantly a single form of 9205delTA ATP synthase was present with a molecular mass of about 540 kDa that corresponded to the cV* detected on BNE. In-gel ATPase activity and WB analysis showed that this complex contains F_o subunits F_o-c and F_o-d but not F_o-a. A similar incomplete ATP synthase complex was described in ρ° cells, lacking both subunits F_o-a and A6L, with the mass around 550 kDa [22]. When the dye Coomassie Blue G was added to the 9205delTA sample before hrCNE1 (Figure 3C), the complex cV* broke down to the same 460 kDa and 350 kDa subcomplexes demonstrated in Figure 3A. Their composition detected by 2D analysis is shown in detail in Figure 3D. These experiments thus provide clear evidence supporting the view that mammalian ATP synthase can assemble even without the F_o-a subunit, but that the complex is unstable and dissociates easily.

When COX was analysed by BNE (Figures 4A and 4B) in control mitochondria solubilized by DDM (1 g/g protein), Cox1- and Cox4-specific antibodies detected most of the signal in the form of COX monomer (respiratory chain complex IV, cIV). A small amount was also present in higher structures – as COX dimer (cIV_2) and a supercomplex of two copies of complexes III and one copy of COX ($cIII_2cIV$), which was also detected by the antibody against cIII subunit Core2 (not shown). A small amount of both a 180 kDa subcomplex, which appears to represent the COX assembly intermediate S3, and free Cox1 subunit was also present. At a higher DDM concentration (4 g/g of protein), less supercomplex and cIV_2 but more S3 could be seen. In 9205delTA cybrid mitochondria (Figures 4A and 4B), we found no cIV_2 and strong reduction in other forms of COX compared with the control – $cIII_2cIV$, cIV and S3 were similarly decreased to 14 %,

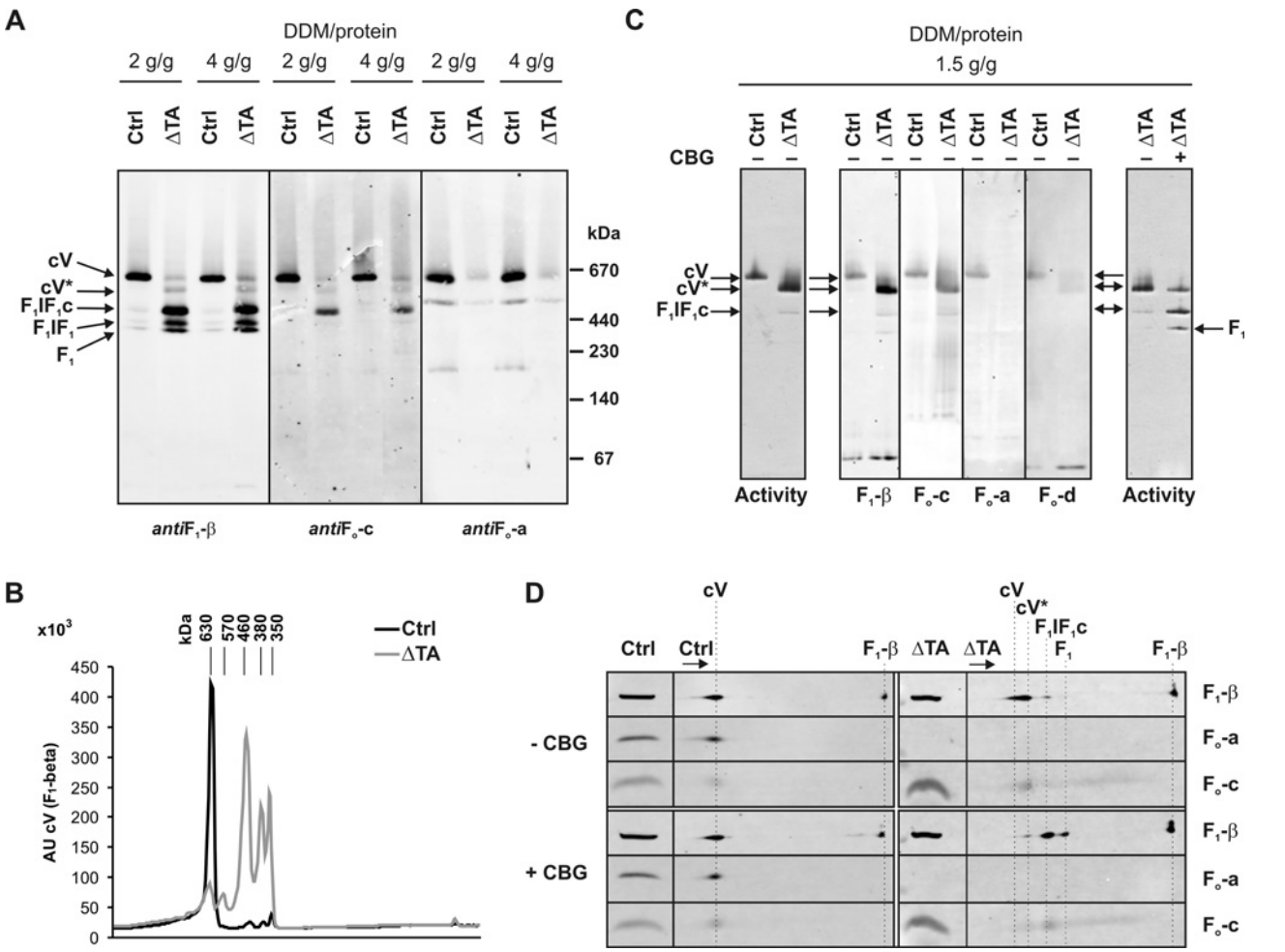

Figure 3 BNE analysis of ATP synthase complex in control and 9205delTA cybrid mitochondria

(**A**) Isolated mitochondria from control (Ctrl) and 9205delTA homoplasmic (ΔTA) cybrids were solubilized with indicated concentrations of *n*-dodecyl-β-D-maltoside (DDM) and analysed by BNE and WB using antibodies against indicated ATP synthase subunits. cV – ATP synthase complex; cV* – ATP synthase complex lacking subunit F_o-a; F_1IF_{1c} – subcomplex of F_1 with c-ring and IF_1 inhibitory factor; F_1IF_1 – subcomplex F_1 with IF_1; F_1 – F_1 alone. In (**B**) quantitative distribution of F_1-β subunit in samples solubilized at 4 g of DDM/g of protein is shown. (**C** and **D**) Mitochondrial membranes were solubilised with 1.5 g of DDM and samples with or without Coomassie Blue G dye (CBG) were analysed by hrCNE1 and 2D hrCNE1/SDS-PAGE. (**C**) ATPase activity staining and WB analysis of the hrCNE1 first dimension. (**D**) WB analysis of the hrCNE1/SDS PAGE second dimension. Aliquots of 15 μg of DDM-solubilized proteins were used.

20 % and 37 %, respectively. In contrast, the amount of free Cox1 subunit was comparable between 9205delTA and control cybrids suggesting that the early biogenesis of COX is not affected. Given the decrease in assembled enzyme, free Cox1 represented 55 % of the total Cox1 signal in 9205delTA cybrids and only 17 % in controls. Digitonin solubilization and subsequent BNE analysis achieves better resolution of supramolecular COX forms such as S2 intermediate of ∼100–140 kDa. While S2 is specifically increased in cells with COX deficiency due to *SURF1* mutations [23], Figure 4B clearly shows that this is not the case with 9205delTA cybrids.

9205delTA heteroplasmy-dependent variation in the subunit F_o-a and Cox3 content

It can be expected that the primary effect of the 9205delTA mutation is impaired synthesis of subunits F_o-a and Cox3, which leads to the formation of defective and unstable ATP synthase complex and decreased content of the fully assembled COX. To estimate how the subunit F_o-a content varies with the mutation load, we analysed several cybrid cell lines for the content of F_o-a (Figure 5A). The protein level of subunit F_o-a in 9205delTA cybrid cells did not change, until the heteroplasmy reached ∼90 %. When the mutation load exceeded this threshold, the F_o-a content progressively declined towards homoplasmy.

When we performed analogous analyses of the effect of 9205delTA mutation on the amount of Cox3 subunit (Figure 5B), again a pronounced threshold dependence could be observed. The normal amount of Cox3 subunit was present up to ∼90 % heteroplasmy, followed by a steep decrease in Cox3 content afterwards. Altogether, the contents of F_o-a and Cox3 were decreased 5 times and 10 times, respectively, in the homoplasmic cybrid cell line.

9205delTA heteroplasmy-dependent changes in the mitochondrial energetic function

9205delTA mutation affects both ATP synthase and COX, yet the functional outcome seems to be different. As shown in Figure 6, the mutation strongly affects both the generation of mitochondrial membrane potential by substrate oxidation and its utilization for ATP synthesis. In homoplasmic 9205delTA cybrids,

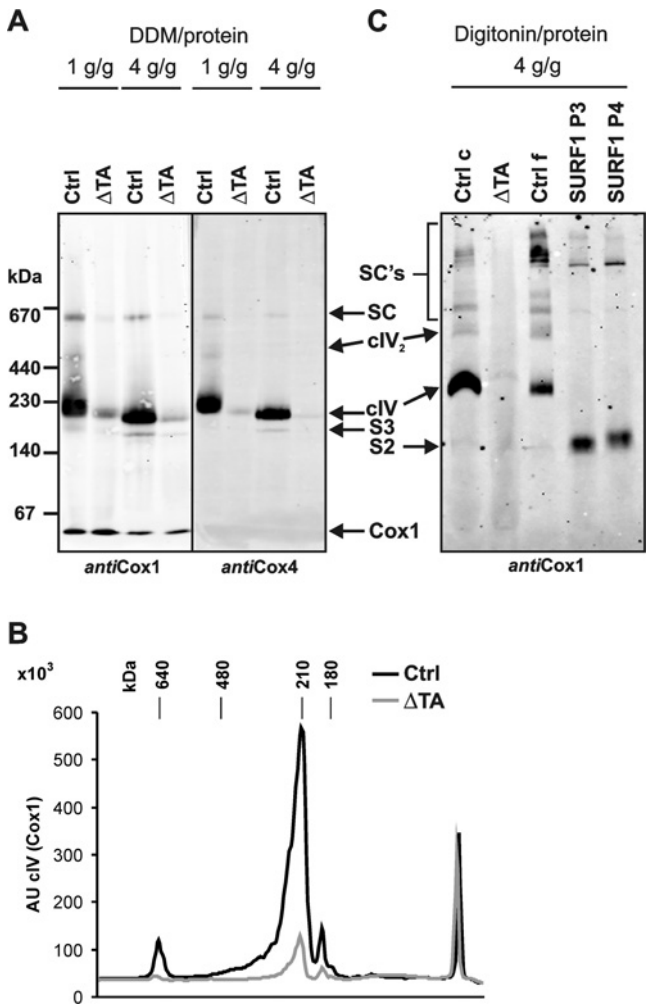

Figure 4 BNE analysis of cytochrome *c* oxidase complex in control and 9205delTA cybrid mitochondria

Isolated mitochondria of control (Ctrl) and 9205delTA homoplasmic (ΔTA) cybrids and of control (Ctrl f) and SURF1 patient (P3 and P4) fibroblasts were solubilized with given concentrations of (**A**) *n*-dodecyl-β-D-maltoside (DDM) or (**C**) digitonin, and analysed by BNE and WB using antibodies to indicated subunits of cytochrome *c* oxidase. SC's – COX supercomplexes, SC – $cIII_2cIV$ supercomplex of COX with two complexes III, cIV_2 – COX dimer, cIV – COX monomer, S3 and S2 – COX assembly intermediates. In (**B**) quantitative distribution of Cox1 subunit in samples solubilized at 4 g of DDM/g of protein is shown. Aliquots of 20 μg of DDM-solubilized proteins were used in (**A**). In (**C**) digitonin-solubilized proteins were loaded as follows: 20 μg of control cybrids and 30 μg of ΔTA cybrids, 10 μg of control fibroblasts and 30 μg of the SURF1 patient fibroblasts (P3 and P4).

the mitochondrial membrane potential $\Delta\psi_m$, expressed relatively to state 3-FCCP, was very low at state 2 and state 4 (3.1-times and 3.6-times lower in 9205delTA compared with the control cybrids, respectively). This clearly shows that the low content of COX drastically decreases the overall H^+-pumping activity of the respiratory chain. Only a minor decrease in state 2 $\Delta\psi_m$ was observed after the addition of ADP (state 3-ADP), the effect of which was oligomycin-sensitive. In accordance, the respiration in 9205delTA cybrids was only negligibly stimulated by ADP and the rate of respiration at state 3-ADP as well as at state 3-FCCP was very low. The both types of measurements excluded the possibility that alterations in ATP synthase structure would induce an enhanced proton leak.

In further experiments, we used cybrid cell lines with a varying 9205delTA mutation load and investigated how the mutation load affects the function of mitochondrial OXPHOS. We performed combined analysis of respiration by oxygraphic measurements of digitonin-permeabilized cells and of ATP production by estimating the ATP content in the course of coupled respiration with succinate as substrate. The rate of ADP-stimulated oxygen consumption was determined as the oligomycin-sensitive respiration in the presence of an excess of ADP (1.25 mM). Samples were collected during respiration measurements and content of the generated ATP was analysed by a coupled luciferase assay. In the same experiment, we also determined the activity of COX as the KCN-sensitive respiration induced by ascorbate + TMPD in the presence of antimycin A. In 9205delTA cybrid cell lines, both the oligomycin-sensitive ADP-stimulated respiration (Figure 7A) and ATP production (Figure 7B) were maintained at the control levels up to circa 90 % heteroplasmy. Both parameters decreased rapidly beyond this threshold. As shown in Figure 7C, COX activity displayed an analogous dependence on the mutation load. In 9205delTA homoplasmic cell line, the ADP-stimulated oligomycin-sensitive respiration, ATP production and COX activity were reduced to 10 %, 27 % and 16 % of the control values, respectively.

Altogether, these attempts to correlate the OXPHOS function, COX and ATP synthase activities as well as the primary changes in the F_o-a and Cox3 subunits with the 9205delTA mutation load revealed a highly similar threshold dependence. This implies that the energetic function of the mitochondrial OXPHOS could be proportionally related to the available quantity of these subunits. Figure 8 demonstrates that this was indeed the case as a near-linear relationship was observed between the content of the F_o-a and Cox3 subunits and the measured functional parameters: ADP-stimulated respiration, ATP synthesis and COX activity.

DISCUSSION

In the present study, we investigated a unique model of mitochondrial dysfunction based on selective down-regulation of biosynthesis of two OXPHOS subunits encoded by the mtDNA *MT-ATP6* and *MT-CO3* genes due to the altered processing and maturation of their mRNAs, caused by the mtDNA 9205delTA microdeletion.

The 9205delTA mutation has so far been found in only two cases that differed markedly in biochemical and clinical phenotypes, although both showed a nearly homoplasmic mutation load [3,7]. This could suggest the involvement of a nuclear-encoded factor that would take part in posttranscriptional regulation of F_o-a/Atp6 biosynthesis and thus modulate the presentation of homoplasmic mutation [7]. However, it is relatively difficult to rule out that in the "homoplasmic" cases, there are not trace amounts of wild-type mtDNA present. Indeed, after extended cultivation and numerous passages of fibroblasts from P1 (with a milder presentation) the presence of increased and detectable level of wild-type mtDNA became apparent. This suggests that at least P1 was not 100 % homoplasmic for the 9205delTA mutation. The distinct phenotypic presentation of the two cases thus could results from differences in the mutation load with a critical threshold for disease manifestation present at a very high heteroplasmy level. To unravel the biochemical consequences of the mtDNA 9205delTA microdeletion, we prepared a panel of cybrid cell lines with variable heteroplasmy ranging from 52 % to 100 % and investigated the structure and function of ATP synthase and COX at different heteroplasmy levels.

The first important finding of these studies was that the homoplasmic mtDNA 9205delTA microdeletion leads to down-regulation of the content of both F_o-a and Cox3 subunits to less than 20 % and 10 %, respectively, relative to the control. The

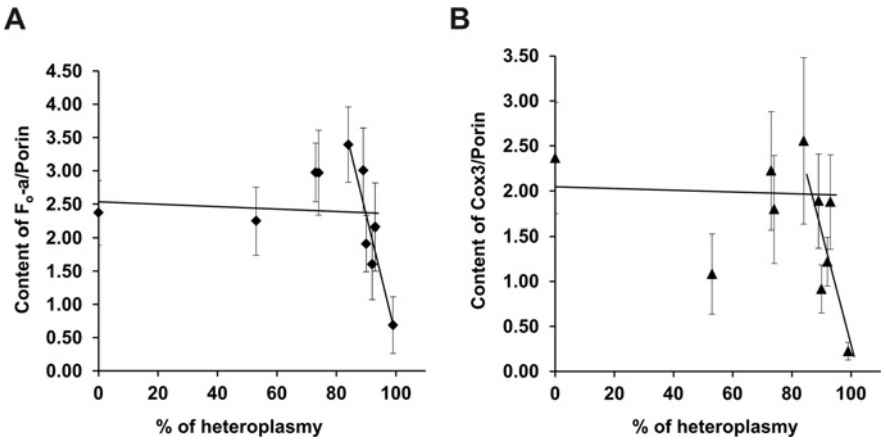

Figure 5 Dependence of subunit F_o-a and Cox3 content on the 9205delTA mutation load

Specific content of (**A**) F_o-a and (**B**) Cox3 subunits was determined in mitochondria of control and 9205delTA cybrid clones by SDS-PAGE and WB, normalized to the content of porin and plotted against the 9205delTA mutation load expressed as a percentage. Data are the means ± S.E.M. for three experiments.

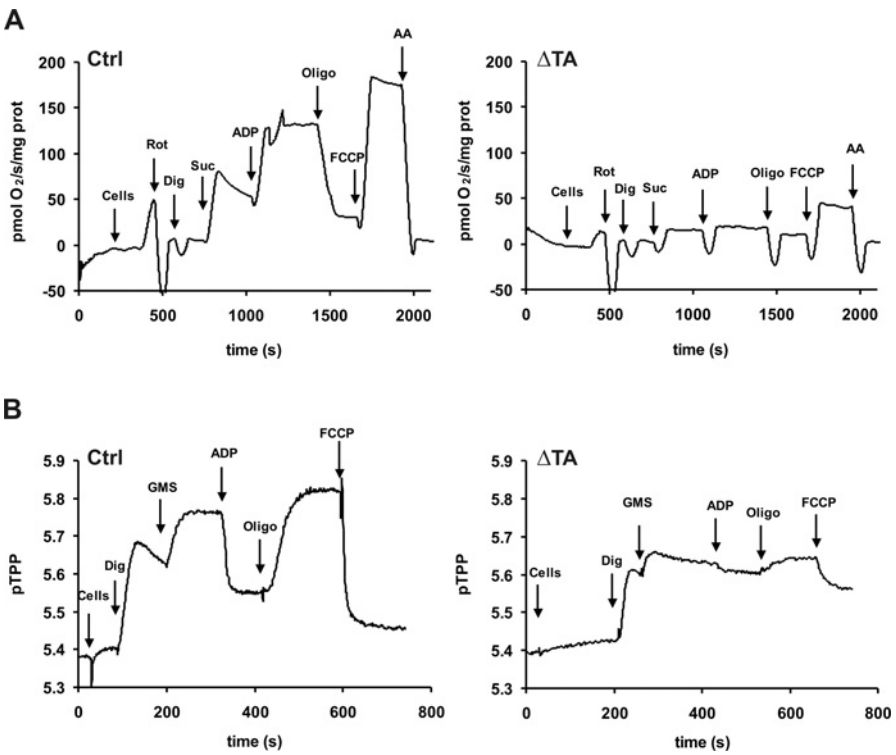

Figure 6 Respiration and mitochondrial membrane potential analysis in control and 9205delTA homoplasmic cybrid mitochondria

(**A**) Respiration and (**B**) TPP^+ measurement of $\Delta\psi_m$ were performed in control (Ctrl) and 9205delTA homoplasmic (ΔTA) cybrids permeabilized with digitonin (Dig) using glutamate (G), malate (M), succinate (Suc, S), ADP, oligomycin (Oligo), FCCP and antimycin A (AA) as indicated.

previously observed insufficient maturation of the *MT-ATP6* and *MT-CO3* mRNAs originating from the polycistronic primary transcript (*MT-ATP8*/*MT-ATP6*/*MT-CO3*) [7] thus decreases the efficacy of their translation to a very low level. Here we show that all the successive changes in the biogenesis and function of OXPHOS complexes cIV and cV are caused by the lack of these two proteins.

The manifestation of the 9205delTA microdeletion in the cybrid cell lines displayed a non-linear dependence on the mutation load and exerted a threshold effect at about 90 % heteroplasmy. This dependence was observed at several levels – the content of subunits F_o-a and Cox3, the content and activity of COX, as well as OXPHOS function measured as coupled respiration and ATP synthesis. Apparently, the non-linear threshold character of the dependence of structural-functional consequences of the 9205delTA mutation originates at the gene–protein level, due to post-transcriptional events affecting the amount of translated subunits F_o-a and Cox3. The 9205delTA microdeletion thus behaves similarly to missense mutations of *MT-ATP6* although the underlying mechanism is mRNA processing and maturation.

From the bioenergetics point of view, it is difficult to conclude which enzyme deficiency is more critical for the disease progression. There was no real difference in threshold effects

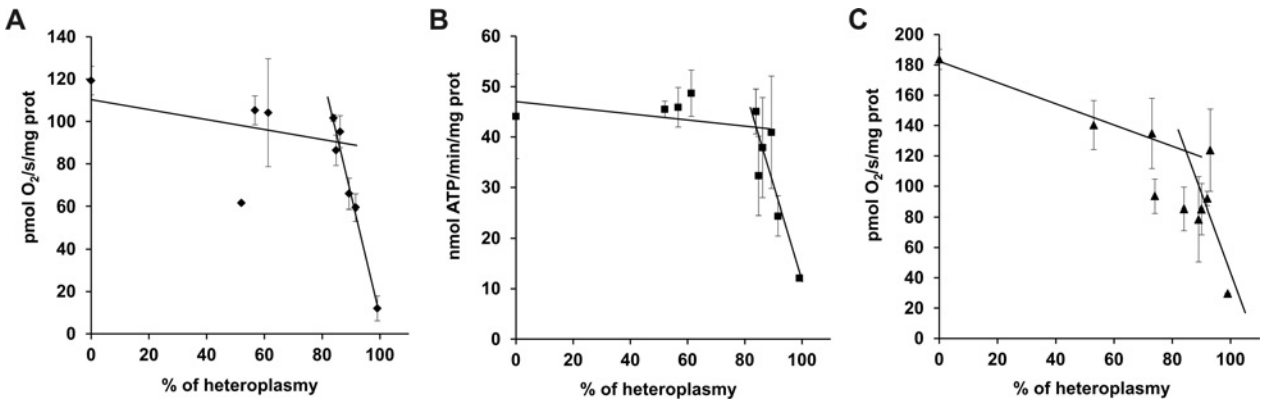

Figure 7 Dependence of ADP-stimulated respiration and ATP synthase and cytochrome *c* oxidase activities on the 9205delTA mutation load

In cybrid cells permeabilized with digitonin, (**A**) ADP-stimulated, oligomycin-sensitive respiration with succinate was measured by oxygraphy, (**B**) ATP production was measured by luciferase assay and (**C**) cytochrome *c* oxidase activity was measured as antimycin A + TMPD + ascorbate oxygen consumption sensitive to KCN. All three parameters were expressed per mg of protein and plotted against the 9205delTA mutation load expressed as a percentage. Data are the means ± S.E.M. for three experiments.

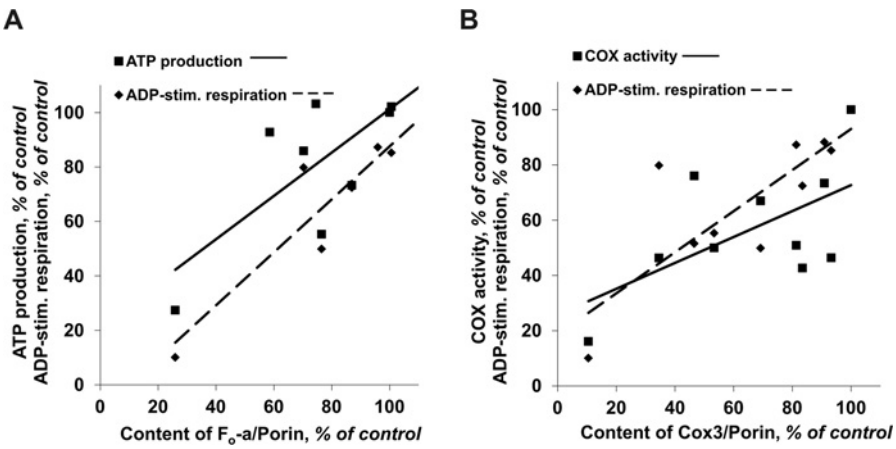

Figure 8 Correlations among 9205delTA-dependent variables

ADP-stimulated respiration, ATP synthesis and cytochrome *c* oxidase activity were plotted against the content of (**A**) F_o-a or (**B**) Cox3 subunits, as indicated, using data from Figures 5 and 7. All values are expressed as a percentage of control.

of COX activity, ADP-stimulated respiration and ATP synthesis. However, the measurements of mitochondrial membrane potential indicated that respiration-dependent proton translocation is severely affected by 9205delTA homoplasmy despite the fact that about 15–20 % of assembled COX and COX activity was preserved. This would imply that the deficiency of COX might be primary and more critical for the overall mitochondrial energy provision.

Our analysis of subunits and assembly forms of cIV and cV revealed, in accordance with our previous studies [7], that for COX, the lack of Cox3 limits the amount of the matured enzyme, but not its structure, while in the case of ATP synthase it is the quality of the enzyme, which is changed – lack of F_o-a results in the production of incomplete, labile and non-functional enzyme.

COX consists of 13 subunits. The three largest mtDNA-encoded Cox1, Cox2 and Cox3 form the catalytic core, the ten small regulatory subunits (Cox4, Cox5a, Cox5b, Cox6a, Cox6b, Cox6c, Cox7a, Cox7b, Cox7c and Cox8) are encoded in the nuclear genome. COX assembly is a stepwise process, which proceeds through several intermediates (S1–S4) [24]. Cox1 represents the first intermediate S1 which progresses to Cox1–Cox4–Cox5a sub-assembly. Subsequently, Cox2 joins this intermediate S2. The process continues with the formation of intermediate S3 after the addition of Cox3 and most of the other remaining subunits. The COX holoenzyme formation (S4) is then completed by the addition of Cox7a/b and Cox6a to S3 [24–27].

At least 14 different heteroplasmic and/or homoplasmic mutations in the *MT-CO3* gene have been reported (www.mitomap.org); and in most cases the decrease in COX activity associates with the defect in COX biogenesis. The clinical outcomes are variable, from optic neuropathies, through Alzheimer's disease, rhabdomyolysis, mitochondrial encephalopathies and myopathies with lactic acidosis, to Leigh or Leigh-like syndromes (LS, LLS). Analysis of affected families in accordance with the studies of the cybrid cell lines revealed that the severity of several *MT-CO3* mutations is heteroplasmy-dependent [28–31]. Interestingly, an improvement in clinical presentation in the case of the 9379G>A mutation was connected with a pronounced decrease in the mutation load [32].

As with many other mtDNA-encoded proteins, most of the *MT-CO3* mutations are single base pair transitions that change highly conserved amino acid residues. Predominantly, they are proposed to affect the interaction of Cox3 with Cox1, or they create a premature stop codon [33,34]. Another type of mutation

is a single base pair insertion or deletion [35,36] leading to the synthesis of truncated Cox3 protein. In addition, a 15-bp deletion, 9480del15, that removes five amino acids (two of them highly conserved) in the third transmembrane region of Cox3 protein was described [29]. This caused pronounced down-regulation of Cox3 steady state levels, similar to the frameshift mutation 9537insC leading to the incomplete Cox3 protein of only 110 amino acids [36]. In 9480del15 cells, Cox3 was translated but was highly unstable. In 9537insC cybrids, the mature *MT-CO3* mRNA was present but was not translated, while in our case of 9205delTA, the low Cox3 content was due to the altered splicing and maturation of the *MT-CO3* transcript. These Cox3-lacking cell lines displayed a pronounced decrease in the content of Cox1 and Cox2 but not of Cox4. No change in Cox5a was found in 9537insC and our 9205delTA cybrids (Figure 2) or in 9952G>A muscle [33] while Cox6c subunit content was significantly reduced in 9205delTA cybrids (Figure 2) and 9952G>A muscle. When Tiranti et al. [36] investigated COX assembly intermediates in 9537insC cybrids, they found the majority of Cox1 in S1 (free Cox1), but significant amounts of Cox1 were also associated with Cox2-containing intermediates depicted as S3 and S2a, both larger than canonical S2. In 9205delTA assembly intermediates (Figure 4), we also found most Cox1 as S1 and little as S3, but there was no indication of S2a, which appears to be specific for 9537insC cells and may reflect the presence of low levels of truncated Cox3. However, we have not observed any accumulated S2 in 9205delTA cells either (Figure 4), which may indicate that these intermediates are quickly degraded, if the COX biogenesis is stalled between S2 and S3. The relative accumulation of free small subunits Cox4 and Cox5a which we observed in our model (Figure 2) was repeatedly described also in other types of COX deficiencies, e.g. *SURF1* or *SCO1* mutations [37], and stems from their relative resistance to degradation.

ATP synthase complex is composed of 16 different subunits organized into membrane-extrinsic F_1 catalytic part (F_1-α, F_1-β, F_1-γ, F_1-δ and F_1-ε subunits) and membrane-embedded F_o part (F_o-a, F_o-c, F_o-e, F_o-f, F_o-g, A6L, F_o-b, F_o-d, F_6 and OSCP) that are connected by two stalks [38]. Small regulatory subunit IF_1 binds to F_1 at low pH and prevents the enzyme from undergoing a switch to hydrolytic mode and ATP hydrolysis. The formation of ATP synthase from individual subunits is a stepwise procedure, expected to proceed via assembly of several modules, starting with an independent formation of F_1 and oligomer of F_o-c subunits [39,40]. Afterwards the F_1 is attached to the membrane-embedded c-ring and the subunits of peripheral arm and of the membranous subcomplex are added. In the last stage the enzyme structure is completed by incorporation of the two mtDNA-encoded subunits, F_o-a and A6L [22].

Over 20 mutations in the mtDNA *MT-ATP6* gene have been reported, all of them single base pair missense mutations. They have been associated with variable brain, heart and muscle disorders, but also with autism, multiple sclerosis, optic neuropathy and diabetes in combination with other mtDNA mutations (www.mitomap.org). The most common are 8993 T>G and T>C mutations manifesting as early-onset maternally inherited Leigh syndrome (MILS) or milder neurogenic muscle weakness, ataxia, and retinitis pigmentosa (NARP) [41–43]. T>G mutations are clinically and biochemically more deleterious, T>C transitions are less frequent and rather late-onset. Similar features were described for the second most common transitions at nt 9176, T>G and T>C associated with LS or familial bilateral striatal necrosis [44,45]. The 9176T>C mutation was also found in the patients with Charcot-Marie-Tooth hereditary neuropathy [46] or the late-onset hereditary spastic paraplegia [47]. Other rare *MT-ATP6* mutations (9185T>C, 9191T>C, 8851T>C, 8989G>C, 8839G>C, 8597T>C) present as LS, LLS, NARP or cardiomyopathy [48–54].

Distinct phenotypes of different *MT-ATP6* mutations are related to the mutation load, but with variable relationships between heteroplasmy and phenotypic presentation. The asymptomatic family members often have a mutation load lower than the affected patients; however, the implicated threshold mutation level for the disease manifestation varies. The best example of phenotypic dependence on the mutation load represents 8993T>G transition – the severity of the disease increases with the mutation load and a milder NARP manifests at lower heteroplasmy (around 70 %) than early-onset devastating MILS (around 90 %). In some cases the severity of symptoms in 8993 patients was found to be heteroplasmy-dependent but without a distinct threshold level for the disease manifestation [55–57] or even with a linear correlation between the mutation load and biochemical parameters [58]. As discussed above, the biochemical defects and the severity of the 9205delTA disease appear to be also heteroplasmy-dependent and point to a steep decline in mitochondrial energy provision above the threshold close to mutation homoplasmy. Interestingly, the healthy mother of the second patient had 85 % heteroplasmy in the blood and 92 % heteroplasmy in fibroblasts [7]. Considering the results obtained in the cybrid cells, the threshold of 9205delTA mutation occurs above 90 % heteroplasmy.

The pathogenicity of *MT-ATP6* mutations is usually given by decreased synthesis of ATP due to defective translocation of the protons across the membrane in 9176T>G mutation [59], or by inefficient coupling between proton translocation and synthesis of ATP in the 8993T>G, 8993T>C, 9035T>C, 9176T>C and 8839G>C mutations [53,57–61]. In the 8993T>C, 9035T>C and 9176T>C mutations, the ATP synthesis is not that severely affected and increased production of ROS (reactive oxygen species) can also contribute to the proposed pathogenic mechanism [47,57,60]. In the 9205delTA mutation, severe reduction in the production of ATP is given by the lack of subunit F_o-a, making the F_o proton channel unable to translocate protons as the reduction in ATP synthesis is accompanied with decreased ADP-stimulated respiration and almost no effect of ADP on mitochondrial membrane potential.

From the structural point of view, the insufficient production of F_o-a subunit resulted in the formation of several BNE-resolved F_1-containing complexes which were smaller than ATP synthase monomer. On the other hand the total amount of various intermediates from F_1 up was normal or even increased. The size of these subcomplexes (460, 380 and 350 kDa), their relative abundance and involvement of F_o subunits closely resembled such complexes found in cells with *MT-ATP6* mutations, ρ° cells, cells upon mtDNA depletion or inhibition of mitochondrial protein synthesis [18,19,21,62–65], where they represent breakdown products of fully assembled ATP synthase complex rather than assembly intermediates. As demonstrated by our hrCNE1 analysis, ATP synthase devoid of subunit F_o-a had a size only ~60 kDa smaller than the control enzyme and was detected as the only form of the 9205delTA enzyme when Coomassie Blue G was omitted. Our data thus provide clear evidence that, in the absence of F_o-a, the almost complete F_1F_o-ATP synthase complex can be quantitatively formed.

F_o-a-deficient cells represent a valuable model for a better understanding of the assembly of mitochondrial ATP synthase structure as well as its function. F_o-a/Atp6 has been implicated as the last subunit incorporating into the enzyme complex during biosynthesis of both the eukaryotic and the prokaryotic enzyme. Our data suggest that ATP synthase lacking F_o-a is assembled and incorporated into the membrane. This is evident from the hrCNE1 experiments, where we could resolve fully assembled (albeit

without F_o-a) enzyme. However, this complex becomes unstable and dissociates when exposed to Coomassie Blue G. After the dye binds to the proteins, it introduces negative charge which apparently breaks down some fragile inter-subunit interactions which keep the F_1c rotor structure connected with the external stalk of the enzyme in the absence of F_o-a. After Coomassie Blue G binding, the major form of F_o-a-deficient enzyme had molecular mass of approximately 460 kDa and contained F_1 subunits and subunit F_o-c, but not subunits F_o-d and OSCP.

The F_o-a-deficient ATP synthase was unable to synthesize ATP but did not leak the protons as both the respiration and mitochondrial membrane potential were affected by FCCP. When an analogous model of bacterial ATP synthase lacking subunit F_o-a was investigated [66], the enzyme complex was found to be rather stable. It could be isolated upon solubilization with Triton X-100 and deoxycholate, incorporated into liposomes and the isolated F_o lacking F_o-a could be reconstituted with F_1. The bacterial enzyme lacking F_o-a was also not proton leaky and, as expected, unable to synthesize ATP as the proton channel was inactive. The absence of F_o-a in the bacterial enzyme further decreased/prevented ATP-hydrolytic activity, indicating that altered F_o structure, possibly the anomalous interaction between c-ring subunits and subunits F_o-b, prevented the rotor rotation. In contrast, the F_o-a-deficient 9205delTA enzyme retained its hydrolytic activity [7], suggesting that c-ring rotation was possible and not hampered, possibly reflecting differences in structure between bacterial and mammalian mitochondrial F_o.

AUTHOR CONTRIBUTION

Josef Houštěk and Kateřina Hejzlarová conceived and designed the experiments. Vilma Kaplanová and Kateřina Hejzlarová prepared cybrid cell lines and analysed mtDNA. Kateřina Hejzlarová and Nikola Kovářová performed electrophoretic experiments, Kateřina Hejzlarová, Pavel Ješina, Hana Nůsková and Zdeněk Drahota performed oxygraphic and spectrophotometric measurements. Kateřina Hejzlarová, Sara Seneca, Tomáš Mráček and Josef Houštěk analysed the data and wrote the paper.

ACKNOWLEDGEMENTS

We acknowledge helpful comments on the manuscript by Professor R.N. Lightowlers and Professor Z.M. Chrzanowska-Lightowlers before submission.

FUNDING

This work was supported by the Grant Agency of the Czech Republic [grant numbers GAP303/11/0970, GAP303/12/1363 and GB14-36804G] and Ministry of Education, Youth and Sports of the Czech Republic [grant number LL1204, RVO:67985823].

REFERENCES

1 DiMauro, S. (2007) Mitochondrial DNA medicine. Biosci. Rep. **27**, 5–9 CrossRef PubMed
2 Ruiz-Pesini, E., Lott, M.T., Procaccio, V., Poole, J.C., Brandon, M.C., Mishmar, D., Yi, C., Kreuziger, J., Baldi, P. and Wallace, D.C. (2007) An enhanced MITOMAP with a global mtDNA mutational phylogeny. Nucleic Acids Res **35**, D823–D828 CrossRef PubMed
3 Seneca, S., Abramowicz, M., Lissens, W., Muller, M.F., Vamos, E. and de Meirleir, L. (1996) A mitochondrial DNA microdeletion in a newborn girl with transient lactic acidosis. J. Inherit. Metab. Dis. **19**, 115–118 CrossRef PubMed
4 Temperley, R.J., Seneca, S.H., Tonska, K., Bartnik, E., Bindoff, L.A., Lightowlers, R.N. and Chrzanowska-Lightowlers, Z.M. (2003) Investigation of a pathogenic mtDNA microdeletion reveals a translation-dependent deadenylation decay pathway in human mitochondria. Hum. Mol. Genet. **12**, 2341–2348 CrossRef PubMed
5 Chrzanowska-Lightowlers, Z.M., Temperley, R.J., Smith, P.M., Seneca, S.H. and Lightowlers, R.N. (2004) Functional polypeptides can be synthesized from human mitochondrial transcripts lacking termination codons. Biochem. J. **377**, 725–731 CrossRef PubMed
6 Fornuskova, D., Tesarova, M., Hansikova, H. and Zeman, J. (2003) New mtDNA mutation 9204delTA in a family with mitochondrial encephalopathy and ATP synthase defect. Cas. Lek. Cesk. **142**, 313
7 Jesina, P., Tesarova, M., Fornuskova, D., Vojtiskova, A., Pecina, P., Kaplanova, V., Hansikova, H., Zeman, J. and Houstek, J. (2004) Diminished synthesis of subunit a (ATP6) and altered function of ATP synthase and cytochrome c oxidase due to the mtDNA 2 bp microdeletion of TA at positions 9205 and 9206. Biochem. J. **383**, 561–571 CrossRef PubMed
8 Rossignol, R., Faustin, B., Rocher, C., Malgat, M., Mazat, J.P. and Letellier, T. (2003) Mitochondrial threshold effects. Biochem. J. **370**, 751–762 CrossRef PubMed
9 Tiranti, V., Munaro, M., Sandona, D., Lamantea, E., Rimoldi, M., DiDonato, S., Bisson, R. and Zeviani, M. (1995) Nuclear DNA origin of cytochrome c oxidase deficiency in Leigh's syndrome: genetic evidence based on patient's-derived rho degrees transformants. Hum. Mol. Genet. **4**, 2017–2023 CrossRef PubMed
10 Bentlage, H.A., Wendel, U., Schagger, H., ter Laak, H.J., Janssen, A.J. and Trijbels, J.M. (1996) Lethal infantile mitochondrial disease with isolated complex I deficiency in fibroblasts but with combined complex I and IV deficiencies in muscle. Neurology **47**, 243–248 CrossRef PubMed
11 Wittig, I., Braun, H.P. and Schagger, H. (2006) Blue native PAGE. Nat. Protoc. **1**, 418–428 CrossRef PubMed
12 Schagger, H. and von Jagow, G. (1987) Tricine-sodium dodecyl sulfate-polyacrylamide gel electrophoresis for the separation of proteins in the range from 1 to 100 kDa. Anal. Biochem. **166**, 368–379 CrossRef PubMed
13 Schagger, H. and von Jagow, G. (1991) Blue native electrophoresis for isolation of membrane protein complexes in enzymatically active form. Anal. Biochem. **199**, 223–231 CrossRef PubMed
14 Wittig, I., Karas, M. and Schagger, H. (2007) High resolution clear native electrophoresis for in-gel functional assays and fluorescence studies of membrane protein complexes. Mol. Cell. Proteomics **6**, 1215–1225 CrossRef PubMed
15 Wittig, I., Carrozzo, R., Santorelli, F.M. and Schagger, H. (2007) Functional assays in high-resolution clear native gels to quantify mitochondrial complexes in human biopsies and cell lines. Electrophoresis **28**, 3811–3820 CrossRef PubMed
16 Havlickova, V., Kaplanova, V., Nuskova, H., Drahota, Z. and Houstek, J. (2010) Knockdown of F1 epsilon subunit decreases mitochondrial content of ATP synthase and leads to accumulation of subunit c. Biochim. Biophys. Acta **1797**, 1124–1129 CrossRef PubMed
17 Ouhabi, R., Boue-Grabot, M. and Mazat, J.P. (1998) Mitochondrial ATP synthesis in permeabilized cells: assessment of the ATP/O values *in situ*. Anal. Biochem. **263**, 169–175 CrossRef PubMed
18 Carrozzo, R., Wittig, I., Santorelli, F.M., Bertini, E., Hofmann, S., Brandt, U. and Schagger, H. (2006) Subcomplexes of human ATP synthase mark mitochondrial biosynthesis disorders. Ann. Neurol. **59**, 265–275 CrossRef PubMed
19 Smet, J., Seneca, S., De Paepe, B., Meulemans, A., Verhelst, H., Leroy, J., De Meirleir, L., Lissens, W. and Van Coster, R. (2009) Subcomplexes of mitochondrial complex V reveal mutations in mitochondrial DNA. Electrophoresis **30**, 3565–3572 CrossRef PubMed
20 Wittig, I., Carrozzo, R., Santorelli, F.M. and Schagger, H. (2006) Supercomplexes and subcomplexes of mitochondrial oxidative phosphorylation. Biochim. Biophys. Acta **1757**, 1066–1072 CrossRef PubMed
21 Houstek, J., Klement, P., Hermanska, J., Houstkova, H., Hansikova, H., Van den Bogert, C. and Zeman, J. (1995) Altered properties of mitochondrial ATP-synthase in patients with a T–>G mutation in the ATPase 6 (subunit a) gene at position 8993 of mtDNA. Biochim. Biophys. Acta **1271**, 349–357 CrossRef PubMed
22 Wittig, I., Meyer, B., Heide, H., Steger, M., Bleier, L., Wumaier, Z., Karas, M. and Schagger, H. (2010) Assembly and oligomerization of human ATP synthase lacking mitochondrial subunits a and A6L. Biochim. Biophys. Acta **1797**, 1004–1011 CrossRef PubMed
23 Kovarova, N., Cizkova Vrbacka, A., Pecina, P., Stranecky, V., Pronicka, E., Kmoch, S. and Houstek, J. (2012) Adaptation of respiratory chain biogenesis to cytochrome c oxidase deficiency caused by SURF1 gene mutations. Biochim. Biophys. Acta **1822**, 1114–1124 CrossRef PubMed
24 Nijtmans, L.G., Taanman, J.W., Muijsers, A.O., Speijer, D. and Van den Bogert, C. (1998) Assembly of cytochrome-c oxidase in cultured human cells. Eur. J. Biochem. **254**, 389–394 CrossRef PubMed
25 Tiranti, V., Galimberti, C., Nijtmans, L., Bovolenta, S., Perini, M.P. and Zeviani, M. (1999) Characterization of SURF-1 expression and Surf-1p function in normal and disease conditions. Hum. Mol. Genet. **8**, 2533–2540 CrossRef PubMed
26 Stiburek, L., Hansikova, H., Tesarova, M., Cerna, L. and Zeman, J. (2006) Biogenesis of eukaryotic cytochrome c oxidase. Physiol. Res. **55** (Suppl 2), S27–S41 PubMed
27 Fornuskova, D., Stiburek, L., Wenchich, L., Vinsova, K., Hansikova, H. and Zeman, J. (2010) Novel insights into the assembly and function of human nuclear-encoded cytochrome c oxidase subunits 4, 5a, 6a, 7a and 7b. Biochem. J. **428**, 363–374 CrossRef PubMed
28 Mkaouar-Rebai, E., Ellouze, E., Chamkha, I., Kammoun, F., Triki, C. and Fakhfakh, F. (2010) Molecular-clinical correlation in a family with a novel heteroplasmic Leigh syndrome missense mutation in the mitochondrial cytochrome c oxidase III gene. J. Child Neurol. **26**, 12–20 CrossRef PubMed

29 Hoffbuhr, K.C., Davidson, E., Filiano, B.A., Davidson, M., Kennaway, N.G. and King, M.P. (2000) A pathogenic 15-base pair deletion in mitochondrial DNA-encoded cytochrome c oxidase subunit III results in the absence of functional cytochrome c oxidase. J. Biol. Chem. **275**, 13994–14003 CrossRef PubMed

30 Manfredi, G., Schon, E.A., Moraes, C.T., Bonilla, E., Berry, G.T., Sladky, J.T. and DiMauro, S. (1995) A new mutation associated with MELAS is located in a mitochondrial DNA polypeptide-coding gene. Neuromuscul. Disord. **5**, 391–398 CrossRef PubMed

31 Bortot, B., Barbi, E., Biffi, S., Angelini, C., Faleschini, E., Severini, G.M. and Carrozzi, M. (2009) Two novel cosegregating mutations in tRNAMet and COX III, in a patient with exercise intolerance and autoimmune polyendocrinopathy. Mitochondrion **9**, 123–129 CrossRef PubMed

32 Horvath, R., Lochmuller, H., Hoeltzenbein, M., Muller-Hocker, J., Schoser, B.G., Pongratz, D. and Jaksch, M. (2004) Spontaneous recovery of a childhood onset mitochondrial myopathy caused by a stop mutation in the mitochondrial cytochrome c oxidase III gene. J. Med. Genet. **41**, e75 CrossRef PubMed

33 Hanna, M.G., Nelson, I.P., Rahman, S., Lane, R.J., Land, J., Heales, S., Cooper, M.J., Schapira, A.H., Morgan-Hughes, J.A. and Wood, N.W. (1998) Cytochrome c oxidase deficiency associated with the first stop-codon point mutation in human mtDNA. Am. J. Hum. Genet. **63**, 29–36 CrossRef PubMed

34 Horvath, R., Scharfe, C., Hoeltzenbein, M., Do, B.H., Schroder, C., Warzok, R., Vogelgesang, S., Lochmuller, H., Muller-Hocker, J., Gerbitz, K.D. et al. (2002) Childhood onset mitochondrial myopathy and lactic acidosis caused by a stop mutation in the mitochondrial cytochrome c oxidase III gene. J. Med. Genet. **39**, 812–816 CrossRef PubMed

35 Marotta, R., Chin, J., Kirby, D.M., Chiotis, M., Cook, M. and Collins, S.J. (2011) Novel single base pair COX III subunit deletion of mitochondrial DNA associated with rhabdomyolysis. J. Clin. Neurosci. **18**, 290–292 CrossRef PubMed

36 Tiranti, V., Corona, P., Greco, M., Taanman, J.W., Carrara, F., Lamantea, E., Nijtmans, L., Uziel, G. and Zeviani, M. (2000) A novel frameshift mutation of the mtDNA COIII gene leads to impaired assembly of cytochrome c oxidase in a patient affected by Leigh-like syndrome. Hum. Mol. Genet. **9**, 2733–2742 CrossRef PubMed

37 Stiburek, L., Vesela, K., Hansikova, H., Pecina, P., Tesarova, M., Cerna, L., Houstek, J. and Zeman, J. (2005) Tissue-specific cytochrome c oxidase assembly defects due to mutations in SCO2 and SURF1. Biochem. J. **392**, 625–632 CrossRef PubMed

38 Walker, J.E. (2013) The ATP synthase: the understood, the uncertain and the unknown. Biochem. Soc. Trans. **41**, 1–16 CrossRef PubMed

39 Ackerman, S.H. and Tzagoloff, A. (2005) Function, structure, and biogenesis of mitochondrial ATP synthase. Prog. Nucleic Acid Res. Mol. Biol. **80**, 95–133 CrossRef PubMed

40 Rak, M., Gokova, S. and Tzagoloff, A. (2011) Modular assembly of yeast mitochondrial ATP synthase. EMBO J. **30**, 920–930 CrossRef PubMed

41 Holt, I.J., Harding, A.E., Petty, R.K. and Morgan-Hughes, J.A. (1990) A new mitochondrial disease associated with mitochondrial DNA heteroplasmy. Am. J. Hum. Genet. **46**, 428–433 PubMed

42 Vazquez-Memije, M.E., Shanske, S., Santorelli, F.M., Kranz-Eble, P., De Vivo, D.C. and DiMauro, S. (1998) Comparative biochemical studies of ATPases in cells from patients with the T8993G or T8993C mitochondrial DNA mutations. J. Inherit. Metab. Dis. **21**, 829–836 CrossRef PubMed

43 Morava, E., Rodenburg, R.J., Hol, F., de Vries, M., Janssen, A., van den Heuvel, L., Nijtmans, L. and Smeitink, J. (2006) Clinical and biochemical characteristics in patients with a high mutant load of the mitochondrial T8993G/C mutations. Am. J. Med. Genet. A **140**, 863–868 CrossRef PubMed

44 Thyagarajan, D., Shanske, S., Vazquez-Memije, M., De Vivo, D. and DiMauro, S. (1995) A novel mitochondrial ATPase 6 point mutation in familial bilateral striatal necrosis. Ann. Neurol. **38**, 468–472 CrossRef PubMed

45 Carrozzo, R., Tessa, A., Vazquez-Memije, M.E., Piemonte, F., Patrono, C., Malandrini, A., Dionisi-Vici, C., Vilarinho, L., Villanova, M., Schagger, H. et al. (2001) The T9176G mtDNA mutation severely affects ATP production and results in Leigh syndrome. Neurology **56**, 687–690 CrossRef PubMed

46 Synofzik, M., Schicks, J., Wilhelm, C., Bornemann, A. and Schols, L. (2012) Charcot-Marie-Tooth hereditary neuropathy due to a mitochondrial ATP6 mutation. Eur. J. Neurol. **19**, e114–e116 CrossRef PubMed

47 Verny, C., Guegen, N., Desquiret, V., Chevrollier, A., Prundean, A., Dubas, F., Cassereau, J., Ferre, M., Amati-Bonneau, P., Bonneau, D. et al. (2011) Hereditary spastic paraplegia-like disorder due to a mitochondrial ATP6 gene point mutation. Mitochondrion **11**, 70–75 CrossRef PubMed

48 Moslemi, A.R., Darin, N., Tulinius, M., Oldfors, A. and Holme, E. (2005) Two new mutations in the MTATP6 gene associated with Leigh syndrome. Neuropediatrics **36**, 314–318 CrossRef PubMed

49 Castagna, A.E., Addis, J., McInnes, R.R., Clarke, J.T., Ashby, P., Blaser, S. and Robinson, B.H. (2007) Late onset Leigh syndrome and ataxia due to a T to C mutation at bp 9,185 of mitochondrial DNA. Am. J. Med. Genet. A **143A**, 808–816 CrossRef PubMed

50 Honzik, T., Tesarova, M., Vinsova, K., Hansikova, H., Magner, M., Kratochvilova, H., Zamecnik, J., Zeman, J. and Jesina, P. (2013) Different laboratory and muscle biopsy findings in a family with an m.8851T>C mutation in the mitochondrial MTATP6 gene. Mol. Genet. Metab. **108**, 102–105 CrossRef PubMed

51 De Meirleir, L., Seneca, S., Lissens, W., Schoentjes, E. and Desprechins, B. (1995) Bilateral striatal necrosis with a novel point mutation in the mitochondrial ATPase 6 gene. Pediatr. Neurol. **13**, 242–246 CrossRef PubMed

52 Duno, M., Wibrand, F., Baggesen, K., Rosenberg, T., Kjaer, N. and Frederiksen, A.L. (2013) A novel mitochondrial mutation m.8989G>C associated with neuropathy, ataxia, retinitis pigmentosa – the NARP syndrome. Gene **515**, 372–375 CrossRef PubMed

53 Blanco-Grau, A., Bonaventura-Ibars, I., Coll-Canti, J., Melia, M.J., Martinez, R., Martinez-Gallo, M., Andreu, A.L., Pinos, T. and Garcia-Arumi, E. (2013) Identification and biochemical characterization of the novel mutation m.8839G>C in the mitochondrial ATP6 gene associated with NARP syndrome. Genes Brain Behav. **12**, 812–820 CrossRef PubMed

54 Tsai, J.D., Liu, C.S., Tsao, T.F. and Sheu, J.N. (2012) A novel mitochondrial DNA 8597T>C mutation of Leigh syndrome: report of one case. Pediatr. Neonatol. **53**, 60–62 CrossRef PubMed

55 Carelli, V., Baracca, A., Barogi, S., Pallotti, F., Valentino, M.L., Montagna, P., Zeviani, M., Pini, A., Lenaz, G., Baruzzi, A. and Solaini, G. (2002) Biochemical-clinical correlation in patients with different loads of the mitochondrial DNA T8993G mutation. Arch. Neurol. **59**, 264–270 CrossRef PubMed

56 Puddu, P., Barboni, P., Mantovani, V., Montagna, P., Cerullo, A., Bragliani, M., Molinotti, C. and Caramazza, R. (1993) Retinitis pigmentosa, ataxia, and mental retardation associated with mitochondrial DNA mutation in an Italian family. Br. J. Ophthalmol. **77**, 84–88 CrossRef PubMed

57 Baracca, A., Sgarbi, G., Mattiazzi, M., Casalena, G., Pagnotta, E., Valentino, M.L., Moggio, M., Lenaz, G., Carelli, V. and Solaini, G. (2007) Biochemical phenotypes associated with the mitochondrial ATP6 gene mutations at nt8993. Biochim. Biophys. Acta **1767**, 913–919 CrossRef PubMed

58 Sgarbi, G., Baracca, A., Lenaz, G., Valentino, L.M., Carelli, V. and Solaini, G. (2006) Inefficient coupling between proton transport and ATP synthesis may be the pathogenic mechanism for NARP and Leigh syndrome resulting from the T8993G mutation in mtDNA. Biochem. J. **395**, 493–500 CrossRef PubMed

59 Vazquez-Memije, M.E., Rizza, T., Meschini, M.C., Nesti, C., Santorelli, F.M. and Carrozzo, R. (2009) Cellular and functional analysis of four mutations located in the mitochondrial ATPase6 gene. J. Cell. Biochem. **106**, 878–886 CrossRef PubMed

60 Sikorska, M., Sandhu, J.K., Simon, D.K., Pathiraja, V., Sodja, C., Li, Y., Ribecco-Lutkiewicz, M., Lanthier, P., Borowy-Borowski, H., Upton, A., Raha, S. et al. (2009) Identification of ataxia-associated mtDNA mutations (m.4052T>C and m.9035T>C) and evaluation of their pathogenicity in transmitochondrial cybrids. Muscle Nerve **40**, 381–394 CrossRef PubMed

61 Pallotti, F., Baracca, A., Hernandez-Rosa, E., Walker, W.F., Solaini, G., Lenaz, G., Melzi D'Eril, G.V., Dimauro, S., Schon, E.A. and Davidson, M.M. (2004) Biochemical analysis of respiratory function in cybrid cell lines harbouring mitochondrial DNA mutations. Biochem. J. **384**, 287–293 CrossRef PubMed

62 Nijtmans, L.G., Klement, P., Houstek, J. and van den Bogert, C. (1995) Assembly of mitochondrial ATP synthase in cultured human cells: implications for mitochondrial diseases. Biochim. Biophys. Acta **1272**, 190–198 CrossRef PubMed

63 Buchet, K. and Godinot, C. (1998) Functional F1-ATPase essential in maintaining growth and membrane potential of human mitochondrial DNA-depleted rho degrees cells. J. Biol. Chem. **273**, 22983–22989 CrossRef PubMed

64 Nijtmans, L.G., Henderson, N.S., Attardi, G. and Holt, I.J. (2001) Impaired ATP synthase assembly associated with a mutation in the human ATP synthase subunit 6 gene. J. Biol. Chem. **276**, 6755–6762 CrossRef PubMed

65 Cortes-Hernandez, P., Vazquez-Memije, M.E. and Garcia, J.J. (2007) ATP6 homoplasmic mutations inhibit and destabilize the human F1F0-ATP synthase without preventing enzyme assembly and oligomerization. J. Biol. Chem. **282**, 1051–1058 CrossRef PubMed

66 Ono, S., Sone, N., Yoshida, M. and Suzuki, T. (2004) ATP synthase that lacks F0a-subunit: isolation, properties, and indication of F0b2-subunits as an anchor rail of a rotating c-ring. J. Biol. Chem. **279**, 33409–33412 CrossRef PubMed

Received 3 December 2014/12 January 2015; accepted 15 January 2015
Published as BJ Immediate Publication 15 January 2015, doi:10.1042/BJ20141462

Biochimica et Biophysica Acta 1817 (2012) 1037–1043

Contents lists available at SciVerse ScienceDirect

Biochimica et Biophysica Acta

journal homepage: www.elsevier.com/locate/bbabio

Compensatory upregulation of respiratory chain complexes III and IV in isolated deficiency of ATP synthase due to *TMEM70* mutation

Vendula Havlíčková Karbanová [a], Alena Čížková Vrbacká [a,b], Kateřina Hejzlarová [a], Hana Nůsková [a], Viktor Stránecký [b], Andrea Potocká [a], Stanislav Kmoch [b], Josef Houštěk [a,*]

[a] Department of Bioenergetics, Institute of Physiology, Academy of Sciences of the Czech Republic
[b] Institute of Inherited Metabolic Disorders, 1st Faculty of Medicine, Charles University in Prague, Czech Republic

ARTICLE INFO

Article history:
Received 6 October 2011
Received in revised form 4 March 2012
Accepted 5 March 2012
Available online 10 March 2012

Keywords:
ATP synthase
TMEM70
Disease
Gene expression profiling
Oxidative phosphorylation
Mitochondrial biogenesis

ABSTRACT

Early onset mitochondrial encephalo-cardiomyopathy due to isolated deficiency of ATP synthase is frequently caused by mutations in *TMEM70* gene encoding enzyme-specific ancillary factor. Diminished ATP synthase results in low ATP production, elevated mitochondrial membrane potential and increased ROS production. To test whether the patient cells may react to metabolic disbalance by changes in oxidative phosphorylation system, we performed a quantitative analysis of respiratory chain complexes and intramitochondrial proteases involved in their turnover. SDS- and BN-PAGE Western blot analysis of fibroblasts from 10 patients with *TMEM70* 317-2A>G homozygous mutation showed a significant 82–89% decrease of ATP synthase and 50–162% increase of respiratory chain complex IV and 22–53% increase of complex III. The content of Lon protease, paraplegin and prohibitins 1 and 2 was not significantly changed. Whole genome expression profiling revealed a generalized upregulation of transcriptional activity, but did not show any consistent changes in mRNA levels of structural subunits, specific assembly factors of respiratory chain complexes, or in regulatory genes of mitochondrial biogenesis which would parallel the protein data. The mtDNA content in patient cells was also not changed. The results indicate involvement of posttranscriptional events in the adaptive regulation of mitochondrial biogenesis that allows for the compensatory increase of respiratory chain complexes III and IV in response to deficiency of ATP synthase.

1. Introduction

Isolated deficiency of ATP synthase belongs to autosomally transmitted mitochondrial diseases that typically affect paediatric population and present with early onset and often fatal outcome [1]. Nuclear genetic origin of ATP synthase deficiency was first demonstrated in 1999 [2] and up to now more than 30 cases have been diagnosed. Within the last few years, mutations in *ATP12* (*ATPAF2*) [3] and *TMEM70* [4] genes, encoding two ATP synthase ancillary factors have been identified as a cause of the disease. Most recently we have found that a mutation in *ATP5E* gene coding for ATP synthase F_1 epsilon subunit can also downregulate enzyme biogenesis resulting in a mitochondrial disease [5]. While *ATP12* and *ATP5E* mutations remain limited to one unique described case, mutations in *TMEM70* were present in numerous patients [4,6–9], thus representing the most frequent cause of ATP synthase deficiency. Up to now at least 8 different pathogenic mutations have been found in *TMEM70* gene [4,8–10]; however, most of the patients are homozygous for *TMEM70* 317-2A>G mutation thus forming a unique cohort of cases with an isolated defect of the key enzyme of mitochondrial ATP production, harboring an identical genetic defect.

TMEM70 is a 21 kDa mitochondrial protein of the inner mitochondrial membrane [11] synthesized as a 29 kDa precursor. It functions as an ancillary factor of mammalian ATP synthase biogenesis [12], and is uniquely specific for higher eukaryotes [4,13]. Its absence caused by the homozygous substitution in *TMEM70* gene (317-2A>G) results in an isolated decrease of the content of fully assembled ATP synthase and reduction of enzyme activity to less than 30% of control values. The clinical presentation of affected patients includes the early onset, lactic acidosis, frequent cardiomyopathy, variable CNS involvement and 3-methylglutaconic aciduria [1,2,4,14].

Diminished phosphorylating capacity of ATP synthase, with respect to respiratory chain capacity, results in low ATP production and insufficient discharge of mitochondrial proton gradient. Elevated levels of mitochondrial membrane potential ($\Delta\Psi_m$) thus stimulate mitochondrial ROS production and the overall metabolic disbalance is characterized by insufficient energy provision and increased oxidative stress in ATP synthase-deficient patient cells [1,15].

Abbreviations: OXPHOS, oxidative phosphorylation; ATP synthase, mitochondrial F_oF_1 ATPase; DDM, dodecyl maltoside; COX, cytochrome *c* oxidase; RT-PCR, real-time PCR; GAPDH, glyceraldehyde-3-phosphate dehydrogenase

* Corresponding author at: Institute of Physiology, Academy of Sciences of the Czech Republic, Vídeňská 1083, 142 20 Prague 4, Czech Republic. Tel.: +420 2 4106 2434; fax: +420 2 4106 2149.
E-mail address: houstek@biomed.cas.cz (J. Houštěk).

0005-2728/$ – see front matter © 2012 Elsevier B.V. All rights reserved.
doi:10.1016/j.bbabio.2012.03.004

Assuming that these metabolic changes may influence the nucleo-mitochondrial signaling, in the present study we tested whether the patient cells may respond to ATP synthase deficiency and consequent metabolic disbalance by changes in biogenesis of mitochondrial OXPHOS system. To investigate possible compensatory/adaptive changes, we performed quantitative analysis of mitochondrial respiratory chain complexes I–V and intramitochondrial proteases (Lon protease, paraplegin, and prohibitins), quantified mtDNA content and compared the protein analysis data with the data from gene expression profiling analyses.

2. Materials and methods

2.1. Patients

Fibroblast cultures from 10 patients with isolated deficiency of ATP synthase (P4–P13 [4]) and 3 controls were used in this study. All the patients showed major clinical symptoms associated with ATP synthase deficiency and harbored a homozygous substitution 317-2A>G in gene *TMEM70* [4]. Relevant clinical, biochemical and molecular data on individual patients included in this study were described previously (see [2,4,6,14,16]).

2.2. Cell culture and isolation of mitochondria

Fibroblast cultures were established from skin biopsies and were grown at 37 °C in 5% (v/v) CO_2 atmosphere in high-glucose Dulbecco's modified Eagle's medium (DMEM, PAA) supplemented with 10% (v/v) fetal calf serum. When indicated, cultivation was also performed in DMEM without glucose (Sigma) that was supplemented with 5.5 mM galactose and 10% dialyzed fetal calf serum. Cells were harvested with 0.05% trypsin and 0.02% EDTA and washed twice with phosphate-buffered saline (PBS, 8 g/l NaCl, 0.2 g/l KCl, 1.15 g/l Na_2HPO_4, 0.2 g/l KH_2PO_4). The protein content was measured by Bio-Rad Protein Assay (Bio-Rad Laboratories), using BSA as standard.

Mitochondria were isolated as in [5] by hypotonic shock cell disruption [17].

2.3. mtDNA quantification

Genomic DNA was isolated by QIAamp DNA Mini kit (Qiagen). To quantify the mtDNA content, we selected two mitochondrial target sequences—16S rRNA and D-loop, and GAPDH as a nuclear target. RT-PCR (LightCycler 480 instrument, Roche Diagnostics) was performed with SYBR Green Master kit (Roche) using the following primers—16S (5′ -3′): F-CCAAACCCACTCCACCTTAC, R-TCATCTTTCCCTTGCGGTA; D-loop: F-CACCATCCTCCGTGAAATCAA, R-GCGAGGAGAGTAGCACTCTTGTG; GAPDH: F-TTCAACAGCGACACCCACT, R-CCAGCCACTACCAGGAAAT [18]. The mtDNA content was calculated from threshold cycle (C_T) ratio of C_{TmtDNA}/C_{TnDNA}.

2.4. Electrophoresis and immunoblot analysis

Tricine SDS polyacrylamide gel electrophoresis (SDS-PAGE) [19] was performed on 10% (w/v) polyacrylamide slab minigels (Mini Protean, Bio-Rad). The samples were incubated for 20 min at 40 °C in 2% (v/v) mercaptoethanol, 4% (w/v) SDS, 10 mM Tris-HCl (pH 7.0) and 10% (v/v) glycerol. Bis-Tris blue-native electrophoresis (BN-PAGE) was performed on 4–13% polyacrylamide minigels [20]. Fibroblasts were solubilized by dodecyl maltoside (DDM, 2 g/1 g of protein) for 15 min at 4 °C in 1.75 mM 6-aminohexanoic acid, 2 mM EDTA, 75 mM Bis-Tris (pH 7). Samples were centrifuged for 20 min at 30000 *g* and 4 °C, Coomassie Brilliant Blue G-250 (8:1, DDM:dye) and 5% glycerol were added to the supernatants and electrophoresis was run for 30 min at 45 V and then at 90 V at 4 °C.

The separated proteins were blotted onto PVDF membranes (Immobilon-P, Millipore) by semi-dry electro transfer for 1 h at 0.8 mA/cm^2. The membranes were blocked with 5% (w/v) non-fat milk in TBS, 0.1% (v/v) Tween-20 and then incubated for 2 h or overnight with subunit specific antibodies. We used monoclonal antibodies from Mitosciences against complex I (NDUFA9-MS111, NDUFS3-MS112), complex II (SDH70-MS204), complex III (Core1-MS303, Core2-MS304), complex IV (Cox1-MS404, Cox2-MS405, Cox4-MS408, Cox5a-MS409), complex V-ATP synthase (F1-β-MS503), and against porin (MSA03). For detection of proteases, the polyclonal antibodies to Lon (kindly provided by Dr. E. Kutejova), paraplegin (kindly provided by Dr. T. Langer), prohibitin 1 (Lab Vision/NeoMarkers) and prohibitin 2 (Bethyl, A300-657A) were used. Quantitative detection was performed using infrared IRDye®-labeled secondary antibodies (goat anti-mouse IgG, Alexa Fluor 680 (A21058) and goat anti-rabbit IgG, Alexa Fluor 680 (A21109), Invitrogen) and Odyssey Infrared Imager (Li-Cor); the signal was quantified by AIDA 3.21 Image Analyzer software (Raytest).

2.5. Gene expression analysis

RNA isolations and RNA quality control were performed as previously described [4]. Total RNA (500 ng) was reverse transcribed, labeled and hybridized onto Agilent 44 k human genome microarray using Two-color Microarray Based Gene Expression Analysis Kit (Agilent). Patient samples and controls (Cy5-labeled) were hybridized against common Cy3-labeled reference RNA isolated from HeLa cell lines. The hybridized slides were scanned with Agilent scanner with PMT gains adjusted to obtain highest intensity unsaturated images. Gene PixPro software (Axon Instruments) was used for image analysis of the TIFF files generated by the scanner. Comparative microarray analysis was performed according to MIAME guidelines [21]. Normalization was performed in R statistic environment (http://www.r-project.org) using Limma package [22], a part of Bioconductor project (http://www.bioconductor.org). Raw data from individual arrays were analyzed as one color data and processed using loess normalization and normexp background correction. Quantile was used for normalization between arrays. Linear model was fitted for each gene given a series of arrays using lmFit function. The empirical Bayes method was used to rank differential expression of genes using eBayes function. Multiple testing correction was performed using the method of Benjamini and Hochberg [23].

2.6. Data accession

Expression data reported in this study are stored and available in Gene Expression Omnibus repository under accessions GPL4133 and GSE10956.

2.7. Protein/transcript correlation

Gene expression signals were background corrected, log2 transformed and normalized using the quantile normalization method. Relative protein levels (ratio to porin) were mean centered, averaged and log2 transformed. For all possible pairs of genes and proteins, we calculated the Pearson correlation coefficient and its significance levels using correlation test function in R statistical language.

2.8. Ethics

This study was carried out in accordance with the Declaration of Helsinki of the World Medical Association and was approved by the Committees of Medical Ethics at both collaborating institutions. The informed consent was obtained from parents.

3. Results

3.1. Changes in the content of mitochondrial OXPHOS complexes and mtDNA

To analyze possible changes in mitochondrial OXPHOS system, we determined by SDS-PAGE and Western blotting the protein content of individual OXPHOS complexes in homogenates of fibroblasts from 10 patients with ATP synthase deficiency caused by *TMEM70* mutation and from 3 healthy controls. We used monoclonal antibodies to selected subunits of ATP synthase (subunit β), complex I (NDUFA9, NDUFS3), complex II (SDH70), complex III (Core1, Core2) and complex IV (Cox1, Cox2, Cox4, and Cox5a). The signal of each subunit was normalized to the signal of porin and expressed as percentage of controls. As shown in Fig. 1, the average content of ATP synthase decreased to 18% of the controls. In contrast, the content of respiratory chain complexes I, II, III, and IV accounted for 115%, 125%, 133%, and 163% of the controls, using antibodies to NDUFA9, SDH70, Core1, and Cox5a, respectively. Analogous differences were observed when the immunodetection data were calculated per mg of protein (102%, 123%, 150%, and 170% of the controls). A similar pattern of changes was found when using antibodies to other subunits of these complexes (Table 1A). The calculation from each subunit signal data thus revealed a significant increase to 124–133% of the control in complex III subunits and to 150–262% in complex IV subunits. Only detection of the subunit Cox4 behaved differently than other complex IV subunits, and the change of its content was small and insignificant.

The changes in complex IV and complex III content revealed by SDS-PAGE were also observed at the level of assembled OXPHOS complexes resolved by BN-PAGE of DDM-solubilized mitochondrial proteins (Fig. 2, Table 1B). Cytochrome *c* oxidase detected with Cox1 antibody was increased to 184% of the control. The bc_1 complex detected with Core 1 antibody was increased to 153% of the control. There was also a tendency of increase in the complex I content but the difference was not significant due to a large variation of values. The content of complex II that accounted for 101% of the control was the least varying one. When the relative ratio of complexes III, IV and V to complex II was calculated and compared to control, the complex V was decreased to 11% and complexes III and IV were increased to 130% and 181%, respectively.

We have also performed cultivation of fibroblasts in galactose medium lacking glucose to increase their dependence on oxidative metabolism. As a result, the growth of patient fibroblasts with *TMEM70* mutation progressively declined and after 2–3 passages they stopped growing. SDS-PAGE and Western blotting did not reveal any significant change in respiratory chain complexes I–IV, due to the change in cultivation conditions, there was also no change in the low content of complex V (not shown).

Table 1
Protein content of OXPHOS subunits (A), OXPHOS complexes (B) and mitochondrial proteases (C) in fibroblasts of patients with *TMEM70* mutation expressed in % of control. Data are mean ± SD and *p*-values are determined by *t*-test (*p*-values <0.05 are in bold).

A

Complex	Subunit	% control ± SD	*p*-value
ATP synthase	$F_1\beta$	18 ± 5.5	**9.4121E−08**
Complex I	NDUFA9	115 ± 29.2	0.4623
Complex I	NDUFS3	110 ± 35.2	0.7369
Complex II	SDH70	125 ± 28.1	0.2747
Complex III	Core 1	133 ± 20.2	**0.0309**
Complex III	Core 2	124 ± 16.6	**0.0477**
Complex IV	Cox1	150 ± 21.1	**0.0084**
Complex IV	Cox2	262 ± 74.0	**0.0052**
Complex IV	Cox4	107 ± 30.0	0.7243
Complex IV	Cox5a	163 ± 21.6	**0.0003**

B

Complex	Antibody to	% control ± SD	*p*-value
ATP synthase	$F_1\beta$	11 ± 4.8	**0.0001**
Complex I	NDUFA9	126 ± 54.4	0.3150
Complex II	SDH70	101 ± 14.9	0.9799
Complex III	Core 1	153 ± 70.6	**0.0463**
Complex IV	Cox1	184 ± 83.6	**0.0207**

C

Protein	% control ± SD	*p*-value
Lon protease	136 ± 61	0.4516
Paraplegin	104 ± 27.6	0.9793
Prohibitin 1	99 ± 36.1	0.2763
Prohibitin 2	90 ± 10.7	0.8514

When determining the content of mtDNA in patient and control fibroblasts, we found that the mtDNA copy number reflected by mtDNA/nDNA ratio is not influenced by the *TMEM70* mutation (Table 2).

3.2. Changes in mitochondrial proteases

When the ATP synthase assembly is impaired due to *TMEM70* mutation, the unused subunits of ATP synthase have to be degraded by mitochondrial quality control system [24]. Therefore, we analyzed the protein content of several components of mitochondrial proteolytic machinery in fibroblast mitochondria by Western blotting using polyclonal antibodies to matrix Lon protease that degrades misfolded, unassembled and oxidatively damaged matrix proteins [25], paraplegin, subunit of the inner membrane mAAA protease that degrades membrane spanning and membrane associated subunits of respiratory chain complexes [26] and prohibitins 1 and 2—regulatory proteins of AAA proteases [27]. As shown in Fig. 3, the changes in the

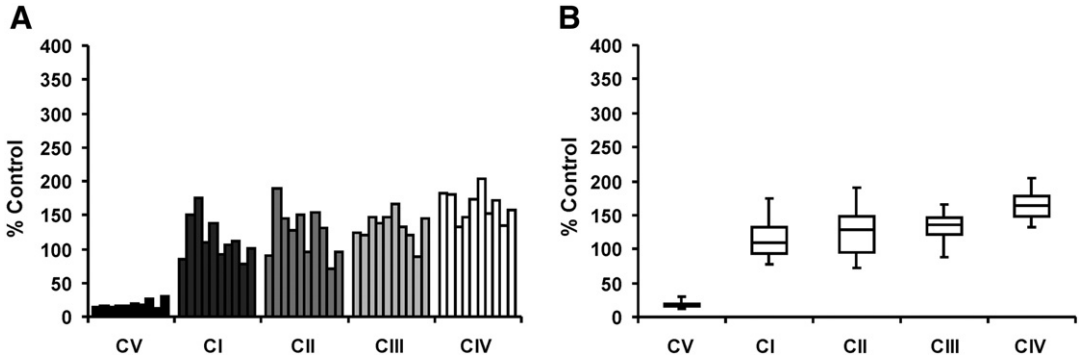

Fig. 1. The protein content of respiratory chain complexes in fibroblasts with *TMEM70* mutation. SDS-PAGE and Western blot analysis of fibroblasts were performed using subunit specific monoclonal antibodies. Detected signals were normalized to mitochondrial marker porin and expressed in % of control values. A—Values for each patient cell line. B—Statistical analysis of 10 patient cell lines, box plot represents maximum, Q3, median, Q1, and minimum.

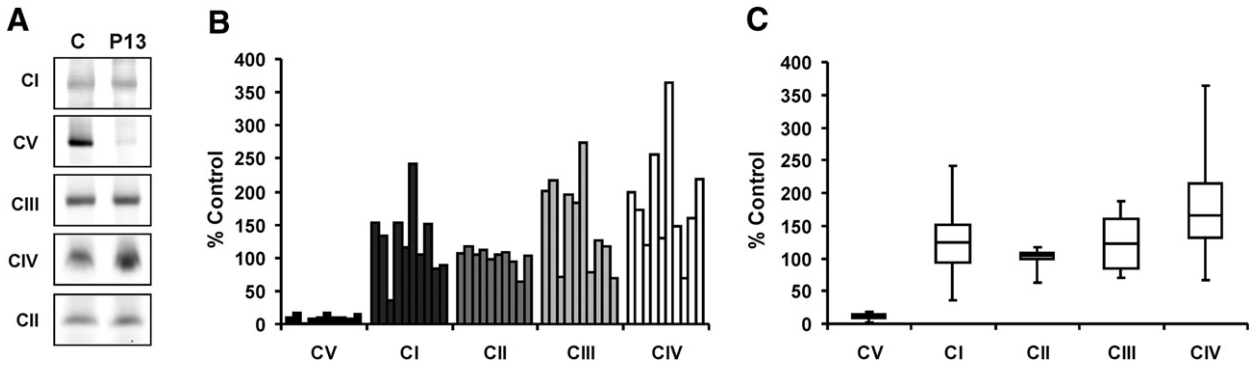

Fig. 2. The content of native respiratory chain complexes in fibroblasts with *TMEM70* mutation. BN-PAGE and Western blot analysis of DDM-solubilized fibroblasts were performed using subunit specific monoclonal antibodies. A—Analysis of control and P13 patient fibroblasts is shown. Detected signals were expressed in % of control values. B—Values for each patient cell line. C—Statistical analysis of 10 patient cell lines, box plot represents maximum, Q3, median, Q1, and minimum.

content of mitochondrial ATP-dependent proteases and prohibitins did not reveal significant differences in patient cells as compared with the controls. In case of Lon protease we observed only a moderate increase of about 30%; however, this difference was also not statistically significant.

3.3. Changes in mRNA expression profiles

To assess putative changes in transcriptional activity of genes involved in mitochondrial biogenesis, we analyzed mRNA expression profiles using whole genome (44 k) array. From the whole dataset, 51% gene spots provided a signal of sufficient quality to be used for microarray analysis. Out of this subset, there were 2700 genes upregulated and 525 downregulated in patient cells as compared to controls at unadjusted $p<0.05$. At adjusted $p<0.01$, 104 and 2 genes were upregulated and downregulated, respectively.

The generalized upregulation of transcriptional activity in patient cells indicates their tendency to increase the levels of majority of transcripts. However, only a small number of the significantly upregulated genes were associated with OXPHOS metabolism. No significant differences in expression levels of the genes encoding ATP synthase subunits and ATP synthase assembly factors were found; the only exception was *TMEM70* gene whose transcript in patient cells was decreased by a factor of 4.6 (adj. $p<0.001$). Furthermore, in case of other genes encoding OXPHOS subunits only the expression of 6 genes differed from the controls (unadjusted $p<0.05$, Table 3). Specifically, 3 subunits of complex I, 1 subunit of complex II, and 2 subunits of complex III, revealed slight (1.2–1.6 fold change) but non-consistent changes, with up- and downregulation observed for genes encoding different subunits of the same complex.

Among differentially expressed genes two pro-mitochondrial regulatory genes, the *TFAM* and *PPRC1* participating in mitochondrial biogenesis were 1.3 fold upregulated, while the COX-specific SCO2 assembly factor was downregulated. The expression profiling did not reveal any changes in mitochondrial proteases or other components of the mitochondrial quality control system.

3.4. Correlation of expression profiling and protein amount

In the investigated group of OXPHOS genes (structural subunits or specific assembly factors) we did not find any correlation between mRNA and protein levels. Even in case of complexes IV and III, with significantly increased protein content, no parallel significant changes in mRNA levels were found in corresponding nuclear or mtDNA encoded genes. The results indicate that ATP synthase deficiency-induced changes in respiratory chain complexes are not related with corresponding changes in the transcriptional activity of the genes involved in OXPHOS biogenetic machinery.

Table 2
The content of mtDNA in patient fibroblasts, determined as a ratio between mtDNA (16S or D-loop) and nDNA (GAPDH), expressed in % of control.

mtDNA gene/nDNA gene	% control ± SD
16S/GAPDH	100.21 ± 1.41
D-loop/GAPDH	101.00 ± 1.95

4. Discussion

The aim of our study was to investigate possible compensatory/adaptive changes of mitochondrial OXPHOS system in a unique group of fibroblast cell lines from 10 patients with an identical mutation in *TMEM70* gene, downregulating specifically the ATP synthase (complex V) content and function. We found a pronounced and significant increase in cellular protein content of the subunits of respiratory chain complex III and complex IV, in accordance with our previous analysis of one of the patients [16]. The increase of complex IV subunits was found in mtDNA encoded subunits Cox1 and Cox2 and in nuclear encoded subunit Cox5a, ranging 150–262% of the control, whereas Cox4 protein showed only a small increase. Complex III was increased in Core1 and Core2 subunits and accounted for 125–133% of the control. BN-PAGE analyses further showed that these changes reflected a corresponding increase to 153% and 184% in assembled respiratory complexes III and IV, respectively.

Changes in the content, morphology, or cellular localization of mitochondria, as well as secondary changes in the content of some of mitochondrial OXPHOS complexes are often observed in mitochondrial disorders. Good examples are ragged-red muscle fibers of MERRF patients with mtDNA 8344A>G mutation in the $tRNA^{Lys}$ gene [28], mitochondrial cardiomyopathies [29] or AZT-induced mtDNA depletion [30]. However, little is known about the underlying adaptive mechanisms.

The pronounced isolated defect in one OXPHOS complex induced by identical homozygous autosomal mutation, such as ATP synthase deficiency studied here, represents an interesting model for investigation of possible adaptive changes. Despite methodical limitations of patient cell culture studies (differences in patients' age, number of passages in cell culture), the upregulation of complex IV and complex III could be demonstrated as an apparent consequence of complex V deficiency in patients with *TMEM70* 317-2A>G homozygous mutation [4], leading to the absence of the TMEM70 protein [11]. Interestingly, when we analyzed fibroblasts with ATP synthase deficiency due to mutation in *ATP5E* gene, we also observed elevated contents of complexes III and IV [5]. On the other hand, in case of ATP synthase deficiency due to *ATP12* mutation, BN-PAGE and in gel enzyme activity staining revealed unchanged content of respiratory chain complexes I, II and IV [3]. However, for each of these two mutations (*ATP5E*,

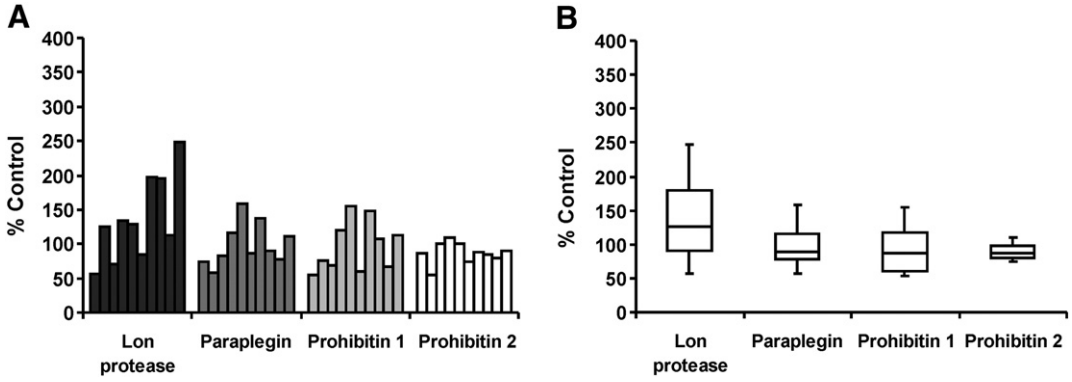

Fig. 3. The protein content of mitochondrial proteases in fibroblasts with *TMEM70* mutation. The content of Lon protease, paraplegin subunit of mAAA protease, prohibitin 1 and prohibitin 2 was analyzed in fibroblasts mitochondria by SDS-PAGE and WB using polyclonal antibodies. Detected signals in patient fibroblasts were normalized to protein content and expressed in % of controls. A—Values for each patient cell line. B—Statistical analysis of 10 patient cell lines, box plot represents maximum, Q3, median, Q1 and minimum.

ATP12) there has been only one case described so far, and, thus, these observations can hardly be generalized.

Mitochondrial OXPHOS complexes are formed independently by biogenetic processes with the help of numerous, complex-specific helper proteins [31,32]. The decreased content of ATP synthase could therefore influence biogenesis and assembly of other respiratory complexes only indirectly, possibly *via* changes in membrane potential ($\Delta\Psi_m$), adenine nucleotides levels or mitochondrial ROS production [1,15]. High values of $\Delta\Psi_m$, increased ROS production as well as low ATP production are also hallmarks of ATP synthase dysfunction due to mtDNA mutations in *ATP6* gene encoding subunit a of ATP synthase. The most pathogenic is T8993G missense mutation resulting in numerous NARP/MILS cases at high mutation load [33,34]. Pathogenic mechanism of T8993G mutation has been intensively studied in different tissues, fibroblasts and derived cybrids and while some authors observed increase of the respiratory chain complexes [35], others found no significant changes [36] or even decrease [34]. It is possible that this variability may reflect varying heteroplasmy of *ATP6* mutation; however, a nuclear genetic background of different patients should also be considered [37]. Our data also showed a pronounced variation of the adaptive responses at the level of complex IV and complex III in individual cell lines with homozygous *TMEM70* mutation, which may reflect differences in nuclear genome of individual cases, determining their potential to respond to underlying ATP synthase deficiency.

The extent of adaptive response could depend on the relative contribution of OXPHOS system to the overall energetics of fibroblasts, which is small as fibroblasts are largely glycolytic cells. However, we were not able to further increase upregulation of respiratory chain complexes in fibroblasts with *TMEM70* mutation by cultivating them in galactose medium in order to increase their oxidative metabolism. In fact, the viability of fibroblasts with *TMEM70* mutation was strongly impaired and they stopped growing in galactose medium. This would indicate that the lack of ATP synthase prevents sufficient ATP production when glycolysis was inhibited and that observed compensatory upregulation of respiratory chain complexes was, as expected, energetically unproductive.

It would be interesting to see whether the variation of data in fibroblast cell lines associates with the *in vivo* impairment of mitochondrial energetics and consequently with the clinical state of individual cases. Nevertheless, it is very problematic to link the changes in respiratory chain complexes in fibroblasts with the clinical presentation of *TMEM70* mutation as previous clinical studies of large number of patients revealed no real differences in the disease onset and severity of clinical symptoms and indicated that management of intensive care after the birth is crucial for patients' survival beyond the neonatal period [6].

Studies in yeast represent efficient strategy to investigate pathogenic mechanisms of human mitochondrial diseases, in particular various types of ATP synthase disorders [38]. Di Rago and colleagues created a yeast model of *ATP6* mutations and recent studies in *Saccharomyces cerevisiae* demonstrated both in ATP synthase-deficient or in oligomycin-inhibited cells that the content of complex IV selectively and rapidly decreases, due possibly to translational downregulation of Cox1 subunit caused by high $\Delta\Psi_m$ [39]. This is in sharp contrast with upregulation of complex IV in patient cells with *TMEM70* mutation. Apparently, the yeast and mammalian/human cells respond differently to dysfunction of ATP synthase and consequent increase of $\Delta\Psi_m$, due to differences in the mechanism and regulation of synthesis and assembly of mtDNA encoded Cox1. While Cox1 is synthesized in a precursor form in *S. cerevisiae* and its translation and processing depend on MSS51 [40], human Cox1 is not processed and its translation is controlled by two factors, TACO1, a specific translational activator that might have evolved in concert with the loss of the mitochondrial mRNA regulatory sequences that occurred with the extreme reduction in the size of

Table 3
OXPHOS genes expressed differently in patient and control cells (unadjusted $p<0.05$).

Gene ID	Gene	Gene name	M	Fold change	*p*-value
NM_004548	*NDUFB10*	NADH dehydrogenase (ubiquinone) 1 beta subcomplex, 10, 22 kDa	−0.32	1.3	0.051
NM_005006	*NDUFS1*	NADH dehydrogenase (ubiquinone) Fe-S protein 1, 75 kDa	0.28	1.2	0.039
NM_015965	*NDUFA13*	NADH dehydrogenase (ubiquinone) 1 alpha subcomplex, 13	−0.31	1.2	0.046
NR_003266	*LOC220729*	Succinate dehydrogenase complex, subunit A	0.64	1.6	0.001
NM_001003684	*UCRC10*	Ubiquinol-cytochrome c reductase, complex III subunit X	−0.45	1.4	0.012
NM_003366	*UQCRC2*	Ubiquinol-cytochrome c reductase core protein II	0.34	1.3	0.025
NM_005138	*SCO2*	SCO cytochrome oxidase deficient homolog 2 (yeast)	−0.26	1.2	0.042
NM_017866	*TMEM70*	Transmembrane protein 70	−2.20	4.6	<0.001
NM_015062	*PPRC1*	Peroxisome proliferator-activated receptor gamma, coactivator-related 1	0.38	1.3	0.005
NM_003201	*TFAM*	Transcription factor A, mitochondrial	0.39	1.3	0.007

the metazoan mitochondrial genome [41] and C12orf62, a vertebrate specific, small transmembrane protein that is required for coordination of the Cox1 synthesis with the early steps of COX assembly [42].

The important finding of our study is that the observed adaptive response of mitochondrial biogenesis is probably enabled by post-transcriptional events that allow for an increased biosynthesis of two respiratory chain complexes without correspondingly increased mRNAs. Our attempts to link protein changes to transcriptional profiles did not show any direct correlation. Besides very low *TMEM70* transcript, only 9 genes encoding OXPHOS biogenesis proteins were differentially expressed, but only with a low significance, including two pro-mitochondrial regulatory genes participating in mitochondrial biogenesis, *viz TFAM* and *PPRC1* (PGC-1 related co-activator) that were 1.3-fold increased. As neither the mRNAs for multiple regulatory and/or assembly factors, nor for structural subunits of complexes III and IV were consistently increased, our data suggest that posttranscriptional, possibly translational regulation may be responsible for the adaptive changes observed. It is tempting to speculate that $\Delta\Psi_m$ and/or ROS may be the signals activating/stimulating this process and that the targets might be the factors such as the transcriptional activator TACO1 [41], metazoan specific LRPPRC protein implicated in regulation of stability and handling of mature mitochondrial mRNAs as part of a ribonucleoprotein complex [43], processing of ribosomal MRPL32 protein by mAAA protease [44] or alike, and that the observed adaptive responses may include increased stability of the mRNA coding for some subunits of upregulated OXPHOS complexes, or a longer half-life of the corresponding protein subunits, or both.

The pronounced isolated deficiency of one key complex of mitochondrial energy provision also represents an interesting model to study the function of mitochondrial biogenesis quality control system that determines the fate of all newly synthesized mitochondrial proteins and directly modulates mitochondrial translation [24,45]. Our analysis of mitochondrial proteases revealed that the elimination of unassembled subunits of ATP synthase is associated neither with the increased mitochondrial content of these proteases nor with upregulation of the respective transcripts. The degradation of excess subunits can be apparently maintained by a normal, steady state level of mitochondrial proteases. A moderate increase was only found in case of Lon protease.

Normal levels of transcripts for ATP synthase subunits observed in patient cells indicate that enzyme subunits are synthesized, whereas Western blot analysis showed that the unused subunits are effectively degraded by mitochondrial surveillance system. ATP synthase is one of the most abundant proteins of mammalian mitochondria and represents several percents of the total mitochondrial protein. However, based on analysis of mitochondrial proteases as well as expression profiling data, it appears that the capacity of mitochondrial quality control system is fully sufficient to degrade the orphan subunits of ATP synthase in cells with *TMEM70* mutation, which has been demonstrated by rapid degradation of newly synthesized beta F_1 subunit observed in patient fibroblasts [2]. This is in accordance with the view that up to 30% of newly synthesized nascent mitochondrial proteins are rapidly degraded owing to folding errors [46,47]. Efficient removal of excess subunits was also described in complex I disorder due to ND1 mutation [48], or in SDH deficiency in yeasts caused by the lack of SDH5 ancillary factor [49]. The efficacy of mitochondrial quality control and protein degradation pathway is also apparent from tissue specific downregulation of ATP synthase in brown fat, where the lack of the subunit c leads to a 10-fold decrease of ATP synthase complex without any accumulation of unassembled subunits, despite the fact that their mRNA levels are the highest among mitochondria-rich mammalian tissues [50]. Under conditions of high excess of unfolded proteins degraded to peptides, increase in the transcription of HSP60 or mtHSP70 can be triggered by upregulation of bZIP transcription factor ZC376.7 [51,52]. However, based on our expression profiling data, this does not seem to be the case in patient cells with *TMEM70* mutation.

Acknowledgements

This work was supported by the Grant Agency of the Ministry of Health of the Czech Republic (NS9759-3), the Grant Agency of the Czech Republic (P303/11/0970, 303/03/H065) and the Grant Agency of the Charles University (370411) and Ministry of Education, Youth and Sports of the Czech Republic (AV0Z 50110509, 1 M6837805002).

References

[1] J. Houstek, A. Pickova, A. Vojtiskova, T. Mracek, P. Pecina, P. Jesina, Mitochondrial diseases and genetic defects of ATP synthase, Biochim. Biophys. Acta 1757 (2006) 1400–1405.
[2] J. Houstek, P. Klement, D. Floryk, H. Antonicka, J. Hermanska, M. Kalous, H. Hansikova, H. Hout'kova, S.K. Chowdhury, T. Rosipal, S. Kmoch, L. Stratilova, J. Zeman, A novel deficiency of mitochondrial ATPase of nuclear origin, Hum. Mol. Genet. 8 (1999) 1967–1974.
[3] L. De Meirleir, S. Seneca, W. Lissens, I. De Clercq, F. Eyskens, E. Gerlo, J. Smet, R. Van Coster, Respiratory chain complex V deficiency due to a mutation in the assembly gene ATP12, J. Med. Genet. 41 (2004) 120–124.
[4] A. Cizkova, V. Stranecky, J.A. Mayr, M. Tesarova, V. Havlickova, J. Paul, R. Ivanek, A.W. Kuss, H. Hansikova, V. Kaplanova, M. Vrbacky, H. Hartmannova, L. Noskova, T. Honzik, Z. Drahota, M. Magner, K. Hejzlarova, W. Sperl, J. Zeman, J. Houstek, S. Kmoch, TMEM70 mutations cause isolated ATP synthase deficiency and neonatal mitochondrial encephalocardiomyopathy, Nat. Genet. 40 (2008) 1288–1290.
[5] J.A. Mayr, V. Havlickova, F. Zimmermann, I. Magler, V. Kaplanova, P. Jesina, A. Pecinova, H. Nuskova, J. Koch, W. Sperl, J. Houstek, Mitochondrial ATP synthase deficiency due to a mutation in the ATP5E gene for the F1 epsilon subunit, Hum. Mol. Genet. 19 (2010) 3430–3439.
[6] T. Honzik, M. Tesarova, J.A. Mayr, H. Hansikova, P. Jesina, O. Bodamer, J. Koch, M. Magner, P. Freisinger, M. Huemer, O. Kostkova, R. van Coster, S. Kmoch, J. Houstek, W. Sperl, J. Zeman, Mitochondrial encephalocardio-myopathy with early neonatal onset due to TMEM70 mutation, Arch. Dis. Child. 95 (2010) 296–301.
[7] J.M. Cameron, V. Levandovskiy, N. Mackay, C. Ackerley, D. Chitayat, J. Raiman, W.H. Halliday, A. Schulze, B.H. Robinson, Complex V TMEM70 deficiency results in mitochondrial nucleoid disorganization, Mitochondrion 11 (2011) 191–199.
[8] O.A. Shchelochkov, F.Y. Li, J. Wang, H. Zhan, J.A. Towbin, J.L. Jefferies, L.J. Wong, F. Scaglia, Milder clinical course of Type IV 3-methylglutaconic aciduria due to a novel mutation in TMEM70, Mol. Genet. Metab. 101 (2010) 282–285.
[9] R. Spiegel, M. Khayat, S.A. Shalev, Y. Horovitz, H. Mandel, E. Hershkovitz, F. Barghuti, A. Shaag, A. Saada, S.H. Korman, O. Elpeleg, I. Yatsiv, TMEM70 mutations are a common cause of nuclear encoded ATP synthase assembly defect: further delineation of a new syndrome, J. Med. Genet. 48 (2011) 177–182.
[10] A.I. Jonckheere, M. Huigsloot, M. Lammens, J. Jansen, L.P. van den Heuvel, U. Spiekerkoetter, J.C. von Kleist-Retzow, M. Forkink, W.J. Koopman, R. Szklarczyk, M.A. Huynen, J.A. Fransen, J.A. Smeitink, R.J. Rodenburg, Restoration of complex V deficiency caused by a novel deletion in the human TMEM70 gene normalizes mitochondrial morphology, Mitochondrion 11 (2011) 954–963.
[11] K. Hejzlarova, M. Tesarova, A. Vrbacka-Cizkova, M. Vrbacky, H. Hartmannova, V. Kaplanova, L. Noskova, H. Kratochvilova, J. Buzkova, V. Havlickova, J. Zeman, S. Kmoch, J. Houstek, Expression and processing of the TMEM70 protein, Biochim. Biophys. Acta 1807 (2011) 144–149.
[12] S. Calvo, M. Jain, X. Xie, S.A. Sheth, B. Chang, O.A. Goldberger, A. Spinazzola, M. Zeviani, S.A. Carr, V.K. Mootha, Systematic identification of human mitochondrial disease genes through integrative genomics, Nat. Genet. 38 (2006) 576–582.
[13] J. Houstek, S. Kmoch, J. Zeman, TMEM70 protein—a novel ancillary factor of mammalian ATP synthase, Biochim. Biophys. Acta 1787 (2009) 529–532.
[14] W. Sperl, P. Jesina, J. Zeman, J.A. Mayr, L. Demeirleir, R. Van Coster, A. Pickova, H. Hansikova, H. Houst'kova, Z. Krejcik, J. Koch, J. Smet, W. Muss, E. Holme, J. Houstek, Deficiency of mitochondrial ATP synthase of nuclear genetic origin, Neuromuscul. Disord. 16 (2006) 821–829.
[15] T. Mracek, P. Pecina, A. Vojtiskova, M. Kalous, O. Sebesta, J. Houstek, Two components in pathogenic mechanism of mitochondrial ATPase deficiency: energy deprivation and ROS production, Exp. Gerontol. 41 (2006) 683–687.
[16] J.A. Mayr, J. Paul, P. Pecina, P. Kurnik, H. Förster, U. Fötschl, W. Sperl, J. Houstek, Reduced respiratory control with ADP and changed pattern of respiratory chain enzymes due to selective deficiency of the mitochondrial ATP synthase, Pediatr. Res. 55 (2004) 1–7.
[17] H.A. Bentlage, U. Wendel, H. Schagger, H.J. ter Laak, A.J. Janssen, J.M. Trijbels, Lethal infantile mitochondrial disease with isolated complex I deficiency in fibroblasts but with combined complex I and IV deficiencies in muscle, Neurology 47 (1996) 243–248.
[18] M. Pejznochova, M. Tesarova, T. Honzik, H. Hansikova, M. Magner, J. Zeman, The developmental changes in mitochondrial DNA content per cell in human cord blood leukocytes during gestation, Physiol. Res. 57 (2008) 947–955.

[19] H. Schagger, G. von Jagow, Tricine-sodium dodecyl sulfate-polyacrylamide gel electrophoresis for the separation of proteins in the range from 1 to 100 kDa, Anal. Biochem. 166 (1987) 368–379.
[20] H. Schagger, G. von Jagow, Blue native electrophoresis for isolation of membrane protein complexes in enzymatically active form, Anal. Biochem. 199 (1991) 223–231.
[21] A. Brazma, P. Hingamp, J. Quackenbush, G. Sherlock, P. Spellman, C. Stoeckert, J. Aach, W. Ansorge, C.A. Ball, H.C. Causton, T. Gaasterland, P. Glenisson, F.C. Holstege, I.F. Kim, V. Markowitz, J.C. Matese, H. Parkinson, A. Robinson, U. Sarkans, S. Schulze-Kremer, J. Stewart, R. Taylor, J. Vilo, M. Vingron, Minimum information about a microarray experiment (MIAME)—toward standards for microarray data, Nat. Genet. 29 (2001) 365–371.
[22] G.K. Smyth, Limma: Linear Models for Microarray Data, Bioinformatics and Computational Biology Solutions using R and Bioconductor, Springer, New York, 2005, pp. 397–420.
[23] Y. Benjamini, Y. Hochberg, Controlling the false discovery rate: a practical and powerful approach to multiple testing, J. R. Stat. Soc. Ser. B (1995) 289–300.
[24] B.M. Baker, C.M. Haynes, Mitochondrial protein quality control during biogenesis and aging, Trends Biochem. Sci. 36 (2011) 254–261.
[25] I. Lee, C.K. Suzuki, Functional mechanics of the ATP-dependent Lon protease—lessons from endogenous protein and synthetic peptide substrates, Biochim. Biophys. Acta 1784 (2008) 727–735.
[26] T. Tatsuta, T. Langer, AAA proteases in mitochondria: diverse functions of membrane-bound proteolytic machines, Res. Microbiol. 160 (2009) 711–717.
[27] G. Steglich, W. Neupert, T. Langer, Prohibitins regulate membrane protein degradation by the m-AAA protease in mitochondria, Mol. Cell. Biol. 19 (1999) 3435–3442.
[28] S. DiMauro, E.A. Schon, Mitochondrial DNA mutations in human disease, Am. J. Med. Genet. 106 (2001) 18–26.
[29] M. Sebastiani, C. Giordano, C. Nediani, C. Travaglini, E. Borchi, M. Zani, M. Feccia, M. Mancini, V. Petrozza, A. Cossarizza, P. Gallo, R.W. Taylor, G. d'Amati, Induction of mitochondrial biogenesis is a maladaptive mechanism in mitochondrial cardiomyopathies, J. Am. Coll. Cardiol. 50 (2007) 1362–1369.
[30] B.H. Kiyomoto, C.H. Tengan, R.O. Godinho, Effects of short-term zidovudine exposure on mitochondrial DNA content and succinate dehydrogenase activity of rat skeletal muscle cells, J. Neurol. Sci. 268 (2008) 33–39.
[31] E.A. Shoubridge, Nuclear genetic defects of oxidative phosphorylation, Hum. Mol. Genet. 10 (2001) 2277–2284.
[32] F. Diaz, H. Kotarsky, V. Fellman, C.T. Moraes, Mitochondrial disorders caused by mutations in respiratory chain assembly factors, Semin. Fetal Neonatal Med. 16 (2011) 197–204.
[33] E.A. Schon, S. Santra, F. Pallotti, M.E. Girvin, Pathogenesis of primary defects in mitochondrial ATP synthesis, Semin. Cell Dev. Biol. 12 (2001) 441–448.
[34] M. Mattiazzi, C. Vijayvergiya, C.D. Gajewski, D.C. DeVivo, G. Lenaz, M. Wiedmann, G. Manfredi, The mtDNA T8993G (NARP) mutation results in an impairment of oxidative phosphorylation that can be improved by antioxidants, Hum. Mol. Genet. 13 (2004) 869–879.
[35] M. D'Aurelio, C. Vives-Bauza, M.M. Davidson, G. Manfredi, Mitochondrial DNA background modifies the bioenergetics of NARP/MILS ATP6 mutant cells, Hum. Mol. Genet. 19 (2010) 374–386.
[36] J. Houstek, P. Klement, J. Hermanska, H. Houstkova, H. Hansikova, C. van den Bogert, J. Zeman, Altered properties of mitochondrial ATP-synthase in patients with a T→G mutation in the ATPase 6 (subunit a) gene at position 8993 of mtDNA, Biochim. Biophys. Acta 1271 (1995) 349–357.
[37] L. Vergani, R. Rossi, C.H. Brierley, M. Hanna, I.J. Holt, Introduction of heteroplasmic mitochondrial DNA (mtDNA) from a patient with NARP into two human rho degrees cell lines is associated either with selection and maintenance of NARP mutant mtDNA or failure to maintain mtDNA, Hum. Mol. Genet. 8 (1999) 1751–1755.
[38] R. Kucharczyk, M. Zick, M. Bietenhader, M. Rak, E. Couplan, M. Blondel, S.D. Caubet, J.P. di Rago, Mitochondrial ATP synthase disorders: molecular mechanisms and the quest for curative therapeutic approaches, Biochim. Biophys. Acta 1793 (2009) 186–199.
[39] I.C. Soto, F. Fontanesi, M. Valledor, D. Horn, R. Singh, A. Barrientos, Synthesis of cytochrome c oxidase subunit 1 is translationally downregulated in the absence of functional F1F0-ATP synthase, Biochim. Biophys. Acta 1793 (2009) 1776–1786.
[40] F. Fontanesi, I.C. Soto, D. Horn, A. Barrientos, Mss51 and Ssc1 facilitate translational regulation of cytochrome c oxidase biogenesis, Mol. Cell. Biol. 30 (2010) 245–259.
[41] W. Weraarpachai, H. Antonicka, F. Sasarman, J. Seeger, B. Schrank, J.E. Kolesar, H. Lochmuller, M. Chevrette, B.A. Kaufman, R. Horvath, E.A. Shoubridge, Mutation in TACO1, encoding a translational activator of COX I, results in cytochrome c oxidase deficiency and late-onset Leigh syndrome, Nat. Genet. 41 (2009) 833–837.
[42] W. Weraarpachai, F. Sasarman, T. Nishimura, H. Antonicka, K. Aure, A. Rotig, A. Lombes, E.A. Shoubridge, Mutations in C12orf62, a factor that couples Cox I synthesis with cytochrome c oxidase assembly, cause fatal neonatal lactic acidosis, Am. J. Hum. Genet. 90 (2012) 142–151.
[43] F. Sasarman, C. Brunel-Guitton, H. Antonicka, T. Wai, E.A. Shoubridge, LRPPRC and SLIRP interact in a ribonucleoprotein complex that regulates posttranscriptional gene expression in mitochondria, Mol. Biol. Cell 21 (2010) 1315–1323.
[44] M. Nolden, S. Ehses, M. Koppen, A. Bernacchia, E.I. Rugarli, T. Langer, The m-AAA protease defective in hereditary spastic paraplegia controls ribosome assembly in mitochondria, Cell 123 (2005) 277–289.
[45] P. Smits, J. Smeitink, L. van den Heuvel, Mitochondrial translation and beyond: processes implicated in combined oxidative phosphorylation deficiencies, J. Biomed. Biotechnol. 2010 (2010) 737385.
[46] U. Schubert, L.C. Anton, J. Gibbs, C.C. Norbury, J.W. Yewdell, J.R. Bennink, Rapid degradation of a large fraction of newly synthesized proteins by proteasomes, Nature 404 (2000) 770–774.
[47] S.B. Qian, M.F. Princiotta, J.R. Bennink, J.W. Yewdell, Characterization of rapidly degraded polypeptides in mammalian cells reveals a novel layer of nascent protein quality control, J. Biol. Chem. 281 (2006) 392–400.
[48] E. Bonora, A.M. Porcelli, G. Gasparre, A. Biondi, A. Ghelli, V. Carelli, A. Baracca, G. Tallini, A. Martinuzzi, G. Lenaz, M. Rugolo, G. Romeo, Defective oxidative phosphorylation in thyroid oncocytic carcinoma is associated with pathogenic mitochondrial DNA mutations affecting complexes I and III, Cancer Res. 66 (2006) 6087–6096.
[49] H.X. Hao, O. Khalimonchuk, M. Schraders, N. Dephoure, J.P. Bayley, H. Kunst, P. Devilee, C.W. Cremers, J.D. Schiffman, B.G. Bentz, S.P. Gygi, D.R. Winge, H. Kremer, J. Rutter, SDH5, a gene required for flavination of succinate dehydrogenase, is mutated in paraganglioma, Science 325 (2009) 1139–1142.
[50] J. Houstek, U. Andersson, P. Tvrdik, J. Nedergaard, B. Cannon, The expression of subunit c correlates with and thus may limit the biosynthesis of the mitochondrial F0F1-ATPase in brown adipose tissue, J. Biol. Chem. 270 (1995) 7689–7694.
[51] C.M. Haynes, K. Petrova, C. Benedetti, Y. Yang, D. Ron, ClpP mediates activation of a mitochondrial unfolded protein response in C. elegans, Dev. Cell 13 (2007) 467–480.
[52] C.M. Haynes, Y. Yang, S.P. Blais, T.A. Neubert, D. Ron, The matrix peptide exporter HAF-1 signals a mitochondrial UPR by activating the transcription factor ZC376.7 in C. elegans, Mol. Cell 37 (2010) 529–540.